2nd International Workshop on

Spine Loading and Deformation

Program and Abstract Book

Berlin 18 - 20 May 2017

JULIUS WOLFF INSTITUT

CHARITÉ
UNIVERSITÄTSMEDIZIN BERLIN

Thursday 18th May	Friday 19th May	Saturday 20th May
	8:00–10:00 **Session 3** Lumbar Spine Kinematics	8:30–10:45 **Session 7** Neuromuscular Response
10:00–12:45 **Registration** Coffee & Snack	10:00–10:30 Coffee Break	10:45–11:15 Coffee Break
12:45–13:00 **Welcome**	10:30–12:30 **Session 4** Spinal Loads – In Vivo Measurements & Modeling	11:15–13:15 **Session 8** Spine Biomechanics
13:00–15:00 **Session 1** Intervertebral Discs	12:30–14:00 Lunch Break	13:15–14:30 Lunch Break
15:00–15:30 Coffee Break	14:00–16:00 **Session 5** Spinal Loads – Computational Models	
15:30–17:30 **Session 2** Motion Segments – Biomechanics	16:00–16:25 Coffee Break	
17:30 **Happy Hour**	16:25–18:15 **Session 6** Instrumentation	
	19:00 **Dinner**	

Venue

Julius Wolff Institut
Charité - Campus Virchow Klinikum
Institutsgebäude Süd
Föhrer Straße 15, 13353 Berlin

Date

18-20 May 2017

Organizers

Hendrik Schmidt
Julius Wolff Institute – Charité
Berlin, Germany

Saeed A. Shirazi-Adl
École Polytechnique
Montréal, Canada

Idsart Kingma
Vrije Universiteit Amsterdam
The Netherlands

Coordinator

Friedmar Graichen ✉ friedmar.graichen@charite.de

Secretary

Barbara Schiller ✉ barbara.schiller@charite.de

Table of Contents

Welcome Note of the Congress Chairs

Dear colleagues and friends,

We are pleased to welcome you to the **2nd International Workshop on Spine Loading and Deformation** which will be held once again in Berlin during 18-20 May 2017.

Mechanical loading and deformation in human spine during diurnal activities are recognized to play a major role in the etiology of back disorders and pain. A comprehensive knowledge of these loading/deformations is a basic prerequisite for effective risk prevention and assessment in workplace, sports and rehabilitation, proper management of various disorders, and realistic preclinical testing of spinal implants.

However despite considerable advancement and numerous investigations, many crucial issues remain yet unresolved. In vivo, in vitro and computational model studies are all necessary for tangible progress in this field.

This workshop on spinal loading/deformations aims to bring world-wide researchers active in this field together in order to share and discuss their recent works on related areas and explore the potentials of their findings. The research topics cover trunk loads and motions (imaging, sensors and video camera) measurements/predictions during sports, occupational tasks, perturbations, etc. with focus on the lumbar and thoracic spines.

We cordially welcome you all to this second workshop on **Spine Loading and Deformation** and wish you an enriching scientific meeting and a pleasant stay in Berlin.

Yours,
Hendrik Schmidt
Idsart Kingma
Saeed A. Shirazi-Adl

10:00-12:45	**Registration / Coffee & Snack**
12:45-13:00 Lecture Hall	**Welcome and Workshop Opening Remarks** Hendrik Schmidt, Saeed A. Shirazi-Adl & Idsart Kingma
13:00-15:00 Lecture Hall	**Session 1: Intervertebral Discs** Moderators: Stephen Ferguson & Pieter P. Vergroesen
13:00	Are long-term axial intervertebral disc biomechanics determined by osmosis? Pieter P. Vergroesen (Amsterdam, The Netherlands)
13:15	The effect of the osmotic gradient on water content and pressure in the intervertebral disc Kaj S. Emanuel (Amsterdam, The Netherlands)
13:30	Computational study of the role of fluid content and flow on the disc response in cyclic compression: On how to replicate in vivo conditions Petra Velísková (Berlin, Germany)
13:45	Comparison of constitutive models for describing the six degree of freedom creep bahaviour of human intervertebral discs John J. Costi (Adelaide, Australia)
14:00	Biomechanical response of intact and degenerated intervertebral discs under impact loading Kinda Khalaf (Abu Dhabi, UAE)
14:15	Integrating collagen fiber orientations derived from diffusion weighted MRI into a finite element model of the intervertebral disc Marc Stadelmann (Bern, Switzerland)
14:30	Closing Discussions & Remarks
15:00-15:30	**Coffee Break**
15:30-17:30 Lecture Hall	**Session 2: Motion Segments - Biomechanics** Moderators: Thomas Zander & J Paige Little
15:30	Effect of inter-individual disc geometry variation on load-bearing of the lumbar unit L4-L5 Marwan El-Rich (Edmonton, Canada)
15:45	Effects of eight different spine ligament property datasets on biomechanics of an L4-L5 finite element model Sadegh Naserkhaki (Tehran, Iran)

16:00	Load-sharing in the lumbosacral spine in neutral standing & flexed postures - A combined finite element and inverse dynamic study Tao Liu (Edmonton, Canada)
16:15	The effect of posterior element removal on coupled motions in human and porcine thoracic and lumbar spines Idsart Kingma (Amsterdam, The Netherlands)
16:30	Dynamic stiffening of lumbar spinal specimens Gerd Huber (Hamburg, Germany)
16:45	Spine system equivalence: A new protocol for standardized multi-axis comparison tests Timothy Holsgrove (Exeter, UK)
17:00	Closing Discussions & Remarks
17:30	**Happy Hour** Beer, pretzel and live jazz music

Scientific Program · Friday, May 19th

08:00-10:00 Lecture Hall	**Session 3: Lumbar Spine Kinematics** Moderators: Idsart Kingma & Andre Plamondon
08:00	How do we stand? Variations during repeated standing phases of asymptomatic subjects and low back pain patients Jeronimo Weerts (Berlin, Germany)
08:15	Are there characteristic motion patterns in the lumbar spine during flexion? Thomas Zander (Berlin, Germany)

08:30	Kinetic control of lumbar spine flexion-extension movement using proportional derivative (PD) controller, feedback linearization method and their combinations Mohamad Parnianpour (Tehran, Iran)
08:45	Model-based estimation of changes in lumbar spine kinematics with alterations in trunk neuromuscular strategy Babak Bazrgari (Lexington, United States)
09:00	Variations in lumbar facet kinematics across segments during in vivo extension movement Ameet Aiyangar (Duebendorf, Switzerland)
09:15	Estimation of spinal joint centers from external spinal profile and anatomical landmarks Agathe Nérot (Paris, France)
09:30	Closing Discussions & Remarks
10:00-10:30	**Coffee Break**
10:30-12:30 Lecture Hall	**Session 4: Spinal Loads – In Vivo Measurements & Modeling** Moderators: Theodoor Smit & Marwan El-Rich
10:30	Subject-specific regression equations to estimate spinal loads in symmetric lifting Farshid Ghezelbash (Montréal, Canada)
10:45	Obesity and spinal loads, a combined MR imaging and subject-specific modeling investigation Navid Arjmand (Tehran, Iran)
11:00	Vertebral loading predictions are influenced by incorporation of CT-based measurements of trunk anatomy into subject-specific musculoskeletal models of the thoracolumbar spine Hossein Mokhtarzadeh (Boston, United States)
11:15	Spinal loads and trunk muscles forces during level walking - A combined in vivo and in silico study on six subjects Rizwan Arshad (Berlin, Germany)
11:30	Subject - Specific validation of a trunk musculoskeletal model in maximum voluntary exertions Andre Plamondon (Montréal, Canada)
11:45	Estimation of in vivo inter-vertebral loading during motion using fluoroscopic and magnetic resonance image informed finite element models Judith Meakin (Exeter, UK)
12:00	Closing Discussions & Remarks

12:30-14:00	**Lunch Break**
14:00-16:00 Lecture Hall	**Session 5: Spinal Loads – Computational Models** Moderators: Judith Meakin & Navid Arjmand
14:00	Sensitivity of intervertebral joint forces to center of rotation location and trends along its migration path Marco Senteler (Zurich, Switzerland)
14:15	Effects of joint positioning and stiffness on spinal loads and kinematics in trunk musculoskeletal models Saeed Shirazi-Adl (Montréal, Canada)
14:30	A combined passive and active musculoskeletal model study to estimate L4-L5 load sharing Navid Arjmand (Tehran, Iran)
14:45	Effects of hand-held loads at various orientations, heights and magnitudes on spine biomechanics in upright posture Zakaria El Ouaaid (Montréal, Canada)
15:00	Thoracolumbar spine loading during activities of daily living performed by the young and the elderly Dominika Ignasiak (Zurich, Switzerland)
15:15	Effect of arm swinging on lumbar spine and hip joint forces Lorenza Angelini (Berlin, Germany)
15:30	Closing Discussions & Remarks
16:00-16:25	**Coffee Break**
16:25-18:15 Lecture Hall	**Session 6: Instrumentation** Moderators: Werner Schmoelz & Fabio Galbusera
16:25	Live demonstration of telemetry hip implant measurements Phillip Damm (Berlin, Germany)
16:45	Functional in vitro testing of pedicle screw anchorage Werner Schmoelz (Innsbruck, Austria)
17:00	An under-sized pedicle screw reaches a similar biomechanical performance as an over-sized screw after fatigue loading – an in-vitro human cadaveric study Jaw-Lin Wang (Taipei, Taiwan)
17:15	Development and validation of a µFEA model for the investigation of the pedicle-screw-bone-interface under different loading conditions Yan Chevalier (Munich, Germany)

17:30 On the clinical relevance of international standards for preclinical evaluation of posterior stabilization devices
Luigi La Barbera (Milano, Italy)

17:45 Closing Discussions & Remarks

19:00 Departure of the Bus to the Restaurant

19:30 Social Event: Dinner

Scientific Program · Saturday, May 20th

08:30-10:45 Session 7: Neuromuscular Response
Lecture Hall Moderators: Jaap H. van Dieën & Mohamad Parnianpour

08:30 Superimposed eccentric sudden trunk loading: Effect on trunk peak torque and muscle activity
Steffen Mueller (Potsdam, Germany)

08:45 Effect of high-intensity perturbations during core-specific sensorimotor exercises on trunk muscle activation pattern
Juliane Mueller (Berlin, Germany)

09:00 Systems identification of trunk stabilization suggest acceleration sensitivity of muscle spindle feedback
Jaap H. van Dieën (Amsterdam, The Netherlands)

09:15 Muscle strength and neuromuscular control in low back pain: elite athletes vs. general population
Maria Moreno Catalá (Berlin, Germany)

09:30	Generating desired optimal trajectory of trunk for rhythmic and discrete sagittal movement by central pattern generators Mohamad Parnianpour (Tehran, Iran)
09:45	Subject specific proprioceptive control model for spine disorders analysis Wafa Skalli (Paris, France)
10:00	Does multifidus muscle disruption cause intervertebral discs degeneration in the lumbar spine of rat? Huub Maas (Amsterdam, The Netherlands)
10:15	Closing Discussions & Remarks
10:45-11:15	**Coffee Break**
11:15-13:15 Lecture Hall	**Session 8: Spine Biomechanics** Moderators: Babak Bazrgari & Dennis E. Anderson
11:15	Ambulatory hand force estimation during manual lifting using an inertial sensor suit and instrumented force shoes Gert Faber (Amsterdam, The Netherlands)
11:30	Estimating the L5S1 moment using a simplified ambulatory measurement setup Axel S. Koopman (Amsterdam, The Netherlands)
11:45	Mechanical demands of a lowering and lifting task on the lower back of patients with acute low back pain Babak Bazrgari (Lexington, United States)
12:00	Faster walking speeds differentially alter spinal loads in persons with traumatic lower limb amputations Brad Hendershot (Bethesda, United States)
12:15	The rib cage affects intervertebral disc pressures in dynamic tests of cadaveric thoracic spines Dennis E. Anderson (Boston, United States)
12:30	The contribution of the ribcage to thoracolumbar spine biomechanics in a sheep model: progress towards a validated computational representation of ribcage biomechanics J Paige Little (Brisbane, Australia)
12:45	Closing Discussions & Remarks
13:15-14:30	**Lunch Break**

Abstracts

Are Long-Term Axial Intervertebral Disc Biomechanics Determined by Osmosis?

Vergroesen PPA[a], Emanuel KS[a], Peeters M[a], Kingma I[b], Smit TH[a]

[a]*Department of Orthopedic Surgery, VU University Medical Center, Amsterdam, The Netherlands*

[b]*Faculty of Behavioral and Movement Sciences, VU University, Amsterdam, The Netherlands*

The intervertebral disc faces high compressive forces during daily activities. Axial compression induces creeping fluid loss and reduction in disc height. With degeneration, disc fluids and height are progressively lost, altering biomechanics. It is assumed that this loss of fluids is caused by a drop in osmolality in the disc due to proteoglycan depletion. Here we investigate the isolated effect of a reduction in osmosis on long-term axial biomechanics of the disc. Continuous diurnal loading was applied to healthy caprine intervertebral discs in a loaded disc culture system for a total of 6 days. We increased medium osmolality with two doses of polyethylene-glycol (PEG 13.3% and 26.6%), reducing the osmotic gradient between the disc and the medium. Thereby we could study the isolated effect of reduced osmosis on axial creep, without damaging the disc. We evaluated: daily creep and recovery, recovery time-constants and compressive stiffness. Additionally, we investigated water content and biochemical composition. There was a strong dose-dependent effect of PEG concentration on water content and long-term axial creep behaviour (Figure 1): disc height, amplitude and rate of creep and recovery were all significantly reduced. Axial compressive stiffness of the disc was not affected. No biochemical changes were observed. Reduction of water content and amplitude of creep and recovery is similar to degenerative disc biomechanics. However, the time-constants increased, indicating that the hydraulic permeability was reduced, in contrast to what happens with degeneration. This suggests that besides the osmotic gradient, the permeability of the tissues is important for healthy intervertebral disc biomechanics.

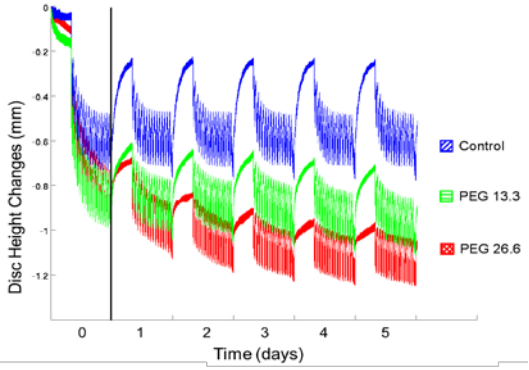

Fig. 1: Typical examples of the displacement data over the days of the experiment. PEG groups show an increased overall loss of disc height over the experiment with increasing osmotic value of the culture medium.

The Effect of the Osmotic Gradient on Water Content and Pressure in the Intervertebral Disc

Emanuel KS[a,b], van der Veen AJ[b,c], Smit TH[a,b], Kingma I[b,d]

[a]*Department of Orthopedic Surgery, VU University Medical Center, Amsterdam,The Netherlands*

[b]*Amsterdam Movement Sciences, Amsterdam,The Netherlands*

[c]*Department of Physics and Medical Technology, VU University Medical Center, Amsterdam, The Netherlands*

[d]*Department of Human Movement Sciences, Faculty of Behavioural and Movement Sciences, Vrije Universiteit Amsterdam,The Netherlands*

The mechanical behaviour of the intervertebral disc is highly dependent on the content and transport of interstitial fluid. It is unclear, however, how these depend on the osmotic gradient between the high-osmolar intervertebral disc and the surrounding fluid. Here we explicitly investigate water content, nucleus pressure and disc height changes as a function of both mechanical and osmotic loading.

Six goat IVDs, immersed in physiological saline, were subjected to a static compressive force with a pressure needle inserted in the nucleus. The loading protocol was: 10N (6 hours); 150N (42 hours); 10N (48 hours). Half-way the 150N-phase, 26% poly-ethylene glycol was added to the saline to reduce the osmotic gradient. Half-way the final 10N-phase the osmotic gradient was restored to its original value. For sixty-six additional discs, the water content of the nucleus and annulus was determined after 6, 24, 48, 72 or 96 hours (see Fig. 1).

t=6-24h: The increased compressive load is initially counterbalanced by the hydrostatic pressure in the nucleus. The high pressure forced 4.3% of the water out of the nucleus through the annulus, which caused a reduction of nucleus pressure of 52(±6) %. t=24-48h: The equilibrium disc height was disturbed by the reduction of the osmotic gradient, and a significant loss of annulus water content was found. However, nucleus pressure and water content remained unchanged. t=48-72h: After unloading, 43(±6) % of the disc height restored without a change in water content. However, the nucleus pressure remained close to zero. t=72-96h: With normalisation of the osmotic gradient, the nucleus pressure, disc height and water content in both annulus and nucleus were restored.

Remarkably, after t=24h, the reduced osmotic gradient affected equilibrium disc height through annulus water content without changes in nucleus water content or pressure. Furthermore, in the absence of an osmotic gradient, the disc height showed substantial viscoelastic recovery after unloading. However, for restoration of the nucleus pressure, and for full restoration of disc height, an osmotic gradient is needed.

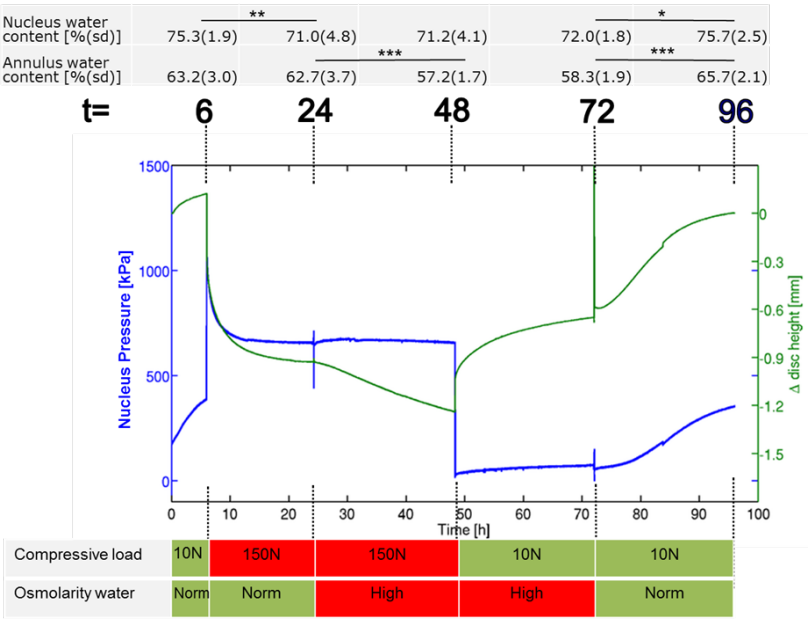

Fig. 1: Typical example of the nucleus pressure (blue) and changes in disc height (green) over time. Bottom: the protocol. Top: water content at five time points. Statistical significant differences between sequential time points are marked with *p<0.05, **p<0.01, ***p<0.001.

Computational Study of the Role of Fuid Content and Flow on the Disc Response in Cyclic Compression: On how to Replicate *In Vivo* Conditions

Velísková P[a], Shirazi-Adl A[b], Bashkuev M[a], Schmidt H[a,]

[a]*Julius Wolff Institute, Charité – Universitätsmedizin Berlin, Germany*
[b]*École Polytechnique, Montréal, Canada*

The intervertebral disc viscoelastic response is due primarily to its fluid content and flow. *In vivo* changes in spinal height and disc fluid content/pressure via stadiometry, magnetic resonance imaging and intradiscal pressure measurements demonstrate that the disc volume, fluid content, height and nucleus pressure completely recover during resting even after diurnal loading with twice longer duration (16 vs. 8 hours). In view of much longer periods required for the recovery of disc height and pressure *in vitro*, concerns have been raised on the fluid inflow through the endplates that might be hampered by clogged blood vessels post mortem. This *in silico* study aimed to identify fluid-flow dependent response of discs and conditions essential to replicate *in vivo* observations.

A 3D nonlinear osmo-poroelastic finite element model of the human lumbar L4-L5 intervertebral disc-bone unit was developed. Simulating earlier *in vitro* experiments on bovine discs (J Biomech. 11;49(6):846-56), the loading protocol started with 8 hours preload at 0.06 MPa followed by 30 high/low compression loading cycles each lasting 7.5 minutes at 0.5/0.06 MPa, respectively. Three different endplate configurations were investigated: (i) free flow with permeable endplates in both directions, (ii) no inflow with a direction-dependent permeability and (iii) closed endplates with no flow. To gain further insight and based on *in vitro* studies, (iv) the preload magnitude was increased from 0.06 MPa to 0.28 MPa and 0.50 MPa, or (v) the initial nucleus hydration was reduced from 80% to 66% and 50%.

For 0.06 MPa preload, the model with no inflow (ii) best matched *in vitro* data. The FE model with free inflow (i) increased segment height (Fig.) and nucleus pressure while the model with no fluid inflow (ii) resulted in a relatively small recovery in segment height and a rather constant nucleus pressure during unloading periods. Larger preloads (Fig. 1) or lower disc hydration levels further increased the consistency between *in silico* and *in vitro* results.

Results highlight an excessive mobile fluid content as well as a restricted fluid inflow through endplates as likely causes of the discrepancies between *in vivo* and *in vitro* studies. To replicate *in vivo* conditions *in vitro*, disc hydration (i.e., mobile fluid) and/or fluid transport should diminish.

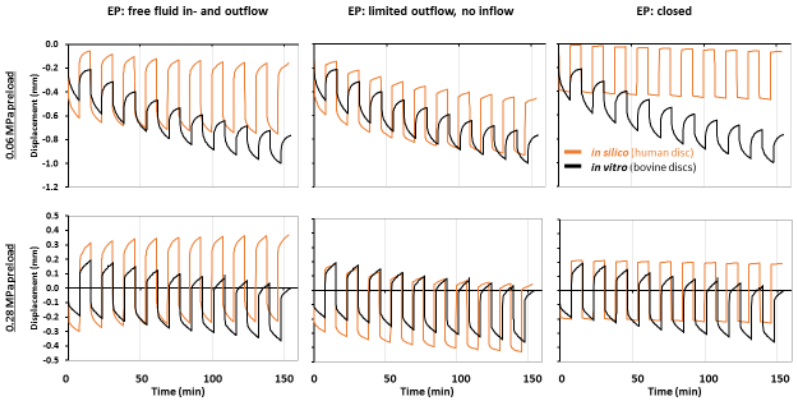

Fig. 1:
(i) In silico simulations: “Free flow” within left figures,
(ii) “No inflow” within middle figures and
(iii) “No flow” within right ones in comparison with in vitro data.

Comparison of Constitutive Models for Describing the Six Degree of Freedom Creep Bahaviour of Human Intervertebral Discs

Costi JJ, Warneford M

Biomechanics and Implants Laboratory, Medical Device Research Institute, Flinders University, Adelaide, Australia

The intervertebral disc exhibits complex, nonlinear, anisotropic, multiphasic behavior that is superimposed on the intrinsic viscoelastic behavior of the solid phase. The time dependent creep behavior of the disc plays a major role in fluid redistribution and equilibration during sustained compressive loading and various constitutive models have been used to describe this behavior. However, little is known about the creep behavior in six degrees of freedom (6DOF), and whether these constitutive models can accurately describe these responses, particularly in those directions that do not promote fluid flow where intrinsic viscoelasticity dominates (shear loading). The aim of this study was to compare the coefficient of multiple determination (R^2) between four constitutive models: (Voigt (VT), Standard Linear Solid (SLS), Four Parameter Double-Voigt (DV), and Stretched Exponential (STR)), between each of 6DOF loading directions, and those DOFs that are dominated by fluid-flow dependent behavior, compared to those dominated by intrinsic viscoelastic behavior of the solid phase.

Fifteen intact human lumbar functional spinal units (FSU - without posterior elements) were dissected from human spines (mean (SD) age 76 (11) years). Each FSU was subjected to a 12 hr axial compressive preload equivalent to a nucleus pressure of 0.1MPa in a 37 °C saline bath to reach hydration equilibrium in a hexapod robot. FSUs were then subjected to a sweep of dynamic 6DOF tests at four loading frequencies (0.001 Hz, 0.01 Hz, 0.1 Hz and 1 Hz), followed by creep, stress relaxation and creep recovery tests in each DOF, under a physiological preload (0.5 MPa). Amplitudes of applied creep in each DOF were: 1.1 MPa for axial compression, 300 N for all translational shear directions, 10 Nm for axial rotation, 20 Nm for lateral bending, and 10 Nm for flexion and extension. The duration of the creep tests were 30 min for compression and 5 min for all other DOFs. The experimental creep displacements (excluding the ramp phase) in each DOF were fitted to the four constitutive models (Matlab: lsqcurvefit) and R^2 was calculated for each fit. DOFs were then divided into two groups: the poroelastic (poro) group expected to favor fluid flow during loading (compression, lateral bending, flexion/extension), and the viscoelastic (visco) group expected to exhibit primarily intrinsic (solid phase) viscoelastic behavior (shears and axial rotation). Separate repeated measures ANOVAs were performed on the within-subjects effect of R^2 for each of the four models, and between-subjects effects of the poro and visco groups (poro-visco).

The mean (SD) R^2 across all DOFs and specimens for each model were VT: 0.623 (0.452), SLS: 0.765 (0.349), DV: 0.921 (0.133) and STR: 0.845 (0.394). The overall effect of R^2 across all four models was significant for all DOFs ($p<0.02$) apart for flexion ($p=0.215$). Pairwise comparisons of those significant DOFs found that overall

the VT model had a significantly lower R^2 fit compared to the other models ($p<0.05$), followed by the SLS model, which was significantly lower than the DV and STR models ($p<0.41$). There were no significant differences between the DV and STR models for all DOFs ($p>0.05$). When comparing the R^2 across the poro and visco groups, the visco groups had significantly larger R^2 fits for each of the four models ($p<0.01$, Fig. 1).

The R^2 value varied between different commonly used constitutive models, with the Voigt model having the worst fit, followed by the SLS model. While no significant differences in model fit were found between the DV and STR models, the constants of the STR models do not have physical relevance compared to the spring and damping constants from the DV model. The DV model is therefore recommended for fitting creep curves in all DOFs. The comparison in R^2 values between the poro and visco groups revealed that more accurate model fits were obtained for the visco groups, which is expected since the models were derived from the behavior of the solid phase. The lower R^2 values for the poro groups suggests that other parameters should be included in the creep models to account for fluid flow through the porous-permeable matrix.

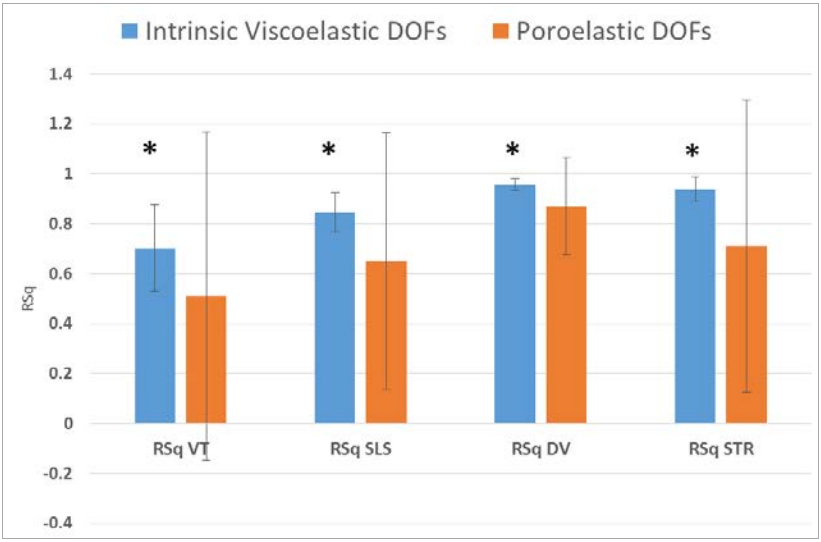

Fig. 1: Comparison of mean (SD) R2 values for each fitted viscoelastic models between intrinsic viscoelastic DOFs and poroelastic DOFs. VT = Voigt model, SLS = Standard Linear Solid model, DV = Double Voigt Model, STR = Stretched Exponential model. * denotes significant difference between the Intrinsic Viscoelastic and Poroelastic DOFs.

Biomechanical Response of Intact and Degenerated Intervertebral Discs under Impact Loading

Khalaf K[a], Nikkhoo M[b], Wang JL[c], Parnianpour M[d]

[a]*Department of Biomedical Engineering, Khalifa University of Science, Technology and Research, Abu Dhabi, UAE*

[b]*Department of Biomedical Engineering, Science and Research Branch, Islamic Azad University, Tehran, Iran*

[c]*Institute of Biomedical Engineering, National Taiwan University, Taipei, Taiwan*

[d]*School of Mechanical Engineering, Sharif University of Technology, Tehran, Iran*

Recent work reveals that degenerative changes in the spine affect the distribution of its structural properties under impact loading [1]. Assessment of the effect of disc degeneration on the viscoelastic stiffness and damping characteristics (shock absorption mechanism) under impact loading is indeed critical, as these parameters play an important role in the risk of endplate and vertebral fracture. While some studies have investigated the biomechanical effects of degeneration under impact loading using in-vitro experiments [1], there remains a gap of knowledge in the detailed response of the intact and degenerated disc under impact loading. The objective of this study was twofold: first to develop a specimen-specific finite element model of the intervertebral disc using ex-vivo experiments, and second, to characterize the detailed mechanical response of the intact and degenerated disc under impact loading with different durations.

A total of 16 porcine intervertebral discs were dissected from 6-month-old juvenile pigs within 4 hours after death. Upon the removal of the posterior elements and muscle tissue, the discs were incubated for 7 days in a whole disc culture system. Specimens were equally assigned to 2 groups: intact and degenerated discs. Disc degeneration was simulated by injecting 0.5 ml Trypsin solution (0.25 %) into nucleus pulposus (NP) on the first day, followed by applying 4hr fatigue loading (F_{RMS}=420N, 2.5 Hz) 1-day after the trypsin injection. At the end of the incubation period, a custom-made drop-tower type testing apparatus was used for impulse testing [2]. The averaged peak loading during impulse was 1200 N, and the shock absorbers were designed to give the contact periods at a level of 20 milliseconds. A validated inverse poroelastic FE methodology developed by the authors [3], in conjunction with the results of the impulse tests, was used to find the material properties of each specimen. A UMAT code was developed to consider the strain-dependent permeability for the poroelastic FE model. Furthermore, specimen-specific models were used to calculate the axial stress and intradiscal pore pressure under a 400 N preload in order to simulate body weight subjected to a sequence of impact loading during five different impact durations (i.e. 10, 20, 30, 40, and 50 milliseconds). Each impact test was simulated as a triangular waveform with a displacement of 1 mm.

The results of the reverse poroelastic FE models were well comparable with the results of impulse tests, with an average error of 6.69 (±1.79) %, and 8.34 (±1.52) % for intact and degenerated discs, respectively. The highest axial stress values were

observed in the Annulus Fibrosus (AF) (averages of 1.68 (±0.25), and 1.93 (±0.18) MPa in intact and degenerated disc, respectively). The calculated intradiscal pore pressure values in the Nucleus Pulposus (NP) were 1.96 (±0.29), and 1.42 (±0.23) MPa in the intact and degenerated disc, respectively. The differences in the axial stress response were not significant among the different range of impact events for both groups. However, the intradiscal pressure significantly decreased from 10 to 50 ms for the degenerated group (P=0.012).

This study provides a validated specimen-specific FE model to estimate the biomechanical responses of intact and degenerated discs subject to impact loading during various durations. The results confirm that disc degeneration leads to the collapse of the extracellular matrix, thereby disturbing its porous structure and substantially decreasing the water content. Hence, while the axial stress increases, the intradiscal pore pressure decreases as compared with the intact disc. The condensed collagen fibers of the annulus intensively interfere with the fluid flow, which is reflected in a much lower hydraulic permeability. The variation of intradiscal pore pressure was found significant for various impact durations in degenerated discs. It is therefore concluded that degeneration can alter the IVD damping coefficient but does not change its stiffness. The main contribution of this work lies in providing a validated methodology for investigating spinal impact trauma while shedding light on IVD etiology and injury mechanisms under different types of loading.

[1] Colloca et al., Spine, 2007 (32)

[2] Wang et al., Spine, 2008 (33)

[3] Nikkhoo, Khalaf et al., Proc. Inst. Mech. Eng. H., 2013 (227)

Integrating Collagen Fiber Orientations derived from Diffusion Weighted MRI into a Finite Element Model of the Intervertebral Disc

Stadelmann M[a], Maquer G[a], Grant A[b], Alkalay R[b], Zysset PK[a]

[a]*Institute for Surgical Technology and Biomechanics, University of Bern, Switzerland*
[b]*Center for Advanced Orthopedic Studies, Beth Israel Deaconess Medical Center, Harvard University, Boston, USA*

Intervertebral disc (IVD) degeneration is a common disease starting early in life and can lead to chronic back pain. This degeneration also induces changes in the mechanical behavior of the IVD. Previous studies proposed to capture those alterations using MRI-based finite element analysis (FEA) [1, 2]. In these studies one main contributor to the discs mechanics, the collagen fibers, are defined based on knowledge from histological studies. The real fiber density and orientation distributions are hardly accounted for. Our hypothesis is that diffusion weighted MRI (DWI) can capture the fibrous structure of the disc and therefore improve the realism of the FE models.

To maximize the heterogeneity of our dataset, human, porcine and bovine discs (three each) were imaged in a High Field MRI (Bruker BioSpec, 9.4T) using a diffusion weighted echo planar imaging protocol. A constrained least-squares tensor estimation was used to compute the diffusion tensor images (DTI) [3]. This avoided negative, unrealistic diffusion values as often obtained with the standard DTI estimation procedure. Local mean diffusions were calculated as the trace of the diffusion tensors. This information was used as a weighting factor for the local fiber density (Fig. 1 A). The disc's geometry was then segmented and meshed. Using our experience on homogenization of the trabecular bone structure [4], the element size was defined to cover several alternating annular fiber layers (representative volume element). Two fiber directions were thus assigned to each element to represent the underlying fiber structure (Fig. 1 B). To do so, all principal eigenvectors corresponding to the main diffusion directions were first computed within a spherical sub-volume located at the center of each finite element. The two main fiber orientations were then estimated via a clustering technique.

For all species, the mean diffusion increased from the annulus fibrosus (AF) towards the nucleus pulposus (NP). A clear interface was observed between those regions for the porcine samples, but smooth transitions occurred in human and bovine discs. A random pattern of diffusion directions was observed in the NP whereas principal diffusion direction in the AF followed the circumferential contour of the disc.

Histology reveals that the AF is composed of densely packed collagen fibre organized in layers. This probably enforces the anisotropic diffusion along the fibre layers. A more disorganized and loose collagen content is found in the NP. This is consistent with our observations of a higher mean diffusion without privileged directions. Next, the fibre information will be interpreted in a material model and validated against in vitro biomechanical tests.

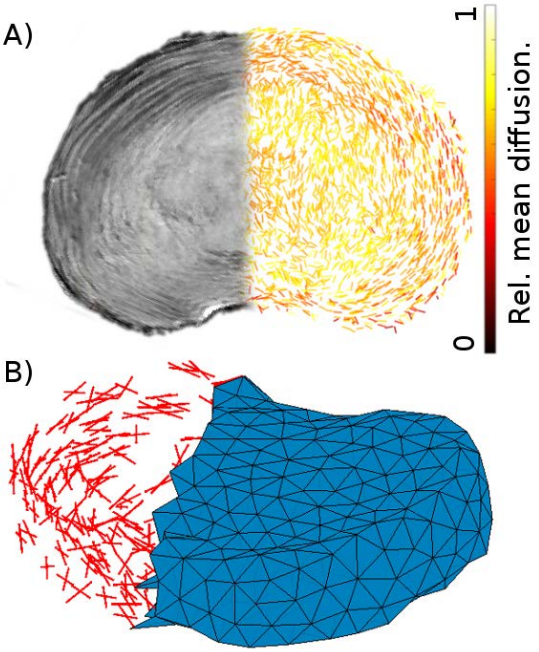

Fig. 1: A) T1-weighted image of a human IVD and its principal diffusion direction. The color represents a normalized local mean diffusion. B) Corresponding mesh and computed fiber orientations.

[1] Maquer, G. et al. J Mech Behav Biomed Mater, 42 (2015), 54-66.

[2] Schmidt, H. et al. J Biomech, 46 (2013), 2342-55.

[3] Niethammer, M. et al. Conf Proc IEEE Eng Med Biol Soc (2006), 2622-25.

[4] Pahr, DH and Zysset, PK. Comput Methods Biomech Biomed Engin, 12 (2009), 45-57.

Acknowledgements: This project is supported by SNF grant no. 147153

Effect of Inter-Individual Disc Geometry Variation on Load-Bearing of the Lumbar Unit L4-L5

Arezodar FF[a], Naserkhaki S[b], El-Rich M[a,c]

[a]*Department of Civil and Environmental Engineering, University of Alberta, Edmonton, Canada*
[b]*Department of Mechanical Engineering, Sharif University of Technology, Tehran, Iran*
[c]*Department of Mechanical Engineering, Khalifa University, Abu Dhabi, United Arab Emirates*

Most of the numerical studies of the lumbar spine used the proportion 44% nucleus and 56% annulus with the nucleus center being located 3.5mm posteriorly with respect to the annulus center according to histological findings. However, these parameters might vary along the spine of the same individual or among individuals, which might in turn affect the spinal load bearing. The objective of this study are: 1- to determine the nucleus size and position in the lumbar L4-L5 discs of 15 patients using their MRI data and 2- to investigate effects of variation on the segment response to mechanical load using finite element method.

With ethics approval, MR images of lumbar spines of 15 male subjects were collected. Geometry of the discs L4-L5 was constructed using the software Mimics. Cross-sectional area of the nucleus pulposus and whole disc as well as position of the nucleus centroid with respect to centroid of the whole disc were determined using the software GeoMagic. Six distinct proportion size and position of the nucleus to the whole disc were selected from the patients data to conduct the FE analysis. A previously developed and validated FE model of the spinal unit L4-L5 [1] was used. It included the vertebrae L4 and L5, the disc including the nucleus pulposus and annulus fibrosus, and the surrounding ligaments. Size and position of the nucleus in the FE model were modified to match the selected dimensions while the remaining spinal structures remained unchanged. The vertebra L4 was subjected to 10 Nm moment in the three anatomical planes to simulate flexion, extension, right and left lateral bending, and right and left axial rotation while L5 was fixed.

The proportion of nucleus's cross section area to the whole disc for all subjects varied between 25% and 57%. Location of the nucleus centroid varied between 0.85 mm anteriorly to 3.26 mm posteriorly with respect to centroid of the whole disc. Rotation of L4 with respect to L5 was 5.46°, 2.9°, 5.7°, 6.4°, 1.85° and 1.55°, in flexion, extension, left and right lateral bending, left and right axial rotation, respectively. The discs with high nucleus to disc size ratio (discs with bigger nucleus) experienced lower intradiscal pressure (IDP) but high strain in annular fibers in case of lateral bending (Fig. 1). Discs with nucleus located posteriorly withstood lower IDP in all cases except extension but higher strain in the annular fibers in lateral bending cases (Fig. 1).

These preliminary results demonstrated that, for the loading scenarios applied, size and position of the nucleus only affected the IDP and annular fibers strain while rotation of L4 thus response of the ligaments and facet joints remained unchanged. Further cases with various combination of nucleus size and position will be

investigated under complex loading including combined compressive load and bending moments.

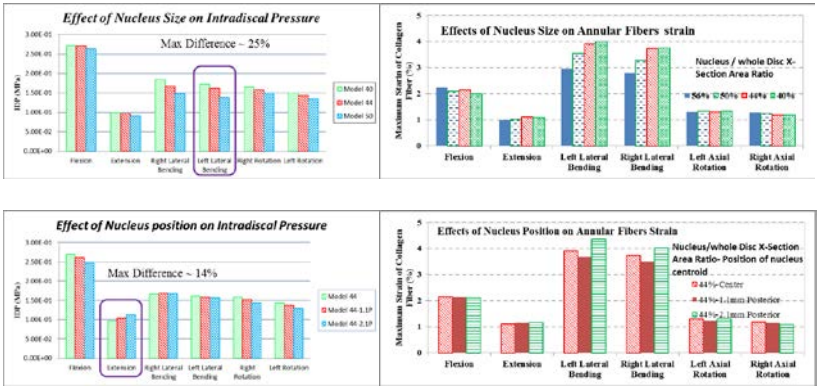

Fig. 1: effects of nucleus size and location on L4-L5 response to bending moments (ratio of nucleus cross section area to the whole disc (%), difference between nucleus centroid and disc centroid in anterior-posterior direction (mm)).

[1] Naserkhaki S, Jaremko JL, Adeeb S, El-Rich M., 2016. On the load-sharing along the ligamentous lumbosacral spine in flexed and extended postures: Finite element study. J Biomech. 49:974-82.

Effects of Eight Different Spine Ligament Property Datasets on Biomechanics of an L4-L5 Finite Element Model

Naserkhaki S[a], Arjmand N[a], Shirazi-Adl A[b], Farahmand F[a], El-Rich M[c]

[a]*Department of Mechanical Engineering, Sharif University of Technology, Tehran, Iran*
[b]*Division of Applied Mechanics, Department of Mechanical Engineering, Ecole Polytechnique, Montréal, Canada*
[c]*Department of Civil and Environmental Engineering, University of Alberta, Edmonton, Canada*

Finite element (FE) modeling of the passive spine often involves making assumptions in loading, geometry and material properties of the discs/ligaments/facets. Modeling of the ligaments, whose role is crucial in spine kinematics and load sharing, is a challenge due to their nonlinear large-deformation behaviour. Different material properties have been considered for ligaments with likely effects on predictions. The present study aims to investigate the influence of eight different ligament property datasets reported in earlier model studies on responses of an L4-L5 FE model when compared to in vitro-in vivo results. Attention is focused on the changes in the range of motion (RoM), load sharing and instantaneous center of rotation (ICoR) of the segment under pure moments ± compression follower force.

A L4-L5 FE model [1] with a disc (annulus ground substance reinforced with collagen fibers and the nucleus pulposus as an incompressible material), facet contact joints, and uniaxial anterior (ALL) and posterior (PLL) longitudinal, capsular (CL), ligamentum flavum (LF), interspinous (ISL), and supraspinous (SSL) ligaments was used. Eight different ligament property datasets (from literature) were incorporated in the model to develop 8 distinct models. Each model was loaded (15 Nm at the L4) in different planes while fixing the inferior L5 endplate/facet joints. The models were first loaded with no ligaments/facets (disc alone) and then with all components (intact model) while sequentially removing the ligaments/facets and comparing predicted RoMs and ICoR with available data.

RoMs of the disc-alone model matched well in vitro data. The 8 intact models predicted diverse RoMs at 10 Nm in flexion (~3-7.1°) and extension (~3.8-5.8°) with 4 being out of the in vitro range (available up to 10 Nm). Ligament properties significantly affected RoMs only in the sagittal plane. Sequential removal of ligaments influenced sagittal RoMs compared to reported in vitro ranges. A stiffer SSL caused smaller RoM and more posterior CoR in flexion while a stiffer ALL yielded smaller RoM and more anterior CoR in extension (Fig. 1 where results are also compared to in vivo data of Pearcy and Bogduk, 1988, recorded under constrained pelvis). In 2 models under 15 Nm load, ISL and SSL forces exceeded their failure forces. Alterations in ligament properties in between models considerably affected the load sharing of disc/facets. Only few models with softer posterior ligaments resulted in overall agreement with measurements. In continuation, we will consider compression follower load and alterations in facet gap distance (simulating also extreme cases ± facets) in a single ligament model and analyze the effects on RoMs and ICoRs.

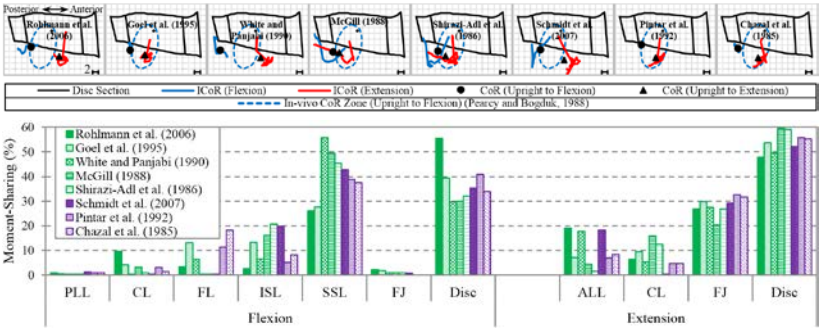

Fig. 1: Instantaneous and average CoR of the 8 intact models and moment-sharing in flexion/extension (15 Nm).

[1] Naserkhaki et al., 2016. J Biomechanics 49: 974-82.

Acknowledgements: Iran National Elites Foundation.

Load-Sharing in the Lumbosacral Spine in Neutral Standing & Flexed Postures - A combined Finite Element and Inverse Dynamic Study

Liu T[a], *Naserkhaki S*[b], *El-Rich M*[a,c]

[a]*Department of Civil and Environmental Engineering, University of Alberta, Edmonton, Alberta, Canada*

[b]*Department of Mechanical Engineering, Sharif University of Technology, Tehran, Iran*

[c]*Department of Mechanical Engineering, Khalifa University, Abu Dhabi, UAE*

Knowledge of load-sharing in the lumbar spine in *in-vivo* conditions is necessary in spinal implant design and testing as well as in injury prevention and treatment programs. Previous *in-vitro* and numerical studies of load-sharing that considered real geometry of the spinal components applied compressive follower load combined or not with bending moment to account for muscle forces effects. Studies that used musculoskeletal models which include muscle forces used simple beam or spherical joint to simulate the intervertebral disc and did not consider the articular facet joints.

This study investigates spinal load-sharing in the lumbosacral spine in upright and flexed posture using a detailed and geometrically realistic Finite Element (FE) of a passive lumbosacral spine that is fed with muscle forces and intra-abdominal pressure predicted by the AnyBody musculoskeletal model of the upper body.

Geometry of the spine of the musculoskeletal model including size and orientation of the vertebrae (lordosis) is used to build the FE model. Flexural stiffness of the spherical joints used to simulate the discs in the musculoskeletal model is modified to match the nonlinear stiffness measured experimentally [1]. The muscle forces and abdominal pressure in upright and 30º flexed postures subjected to gravity load with no load in hands are predicted by the musculoskeletal model. Quadratic muscle recruitment criterion is used in muscle force optimization. The loads, in addition to the upper body weight are applied to the FE model while the lower sacrum is completely fixed. The intradiscal pressure, strain in the annular fibers, contact force in the facet joints and forces in the ligaments are predicted. The internal forces and moments in the discs are calculated using the equilibrium equations which consider the applied load including muscle forces and intra-abdominal pressure and the forces in the ligaments and facet joints predicted by the FE model. Load-sharing is calculated as the portion of total spinal load that each spinal structures carries along the spine [2].

A FE model for the segment L5-Sacrum only is created and tested so far while the muscle forces and the abdominal pressure along the whole spine in both postures are predicted by the musculoskeletal model. The FE model predicts IDP in good agreement with *in-vivo* value measured at L4-L5 level; 0.5MPa in upright posture and 1.3MPa in 30º flexed posture.

The preliminary results are promising and confirm the feasibility of the approach proposed in this study. The FE model of the whole spine will be validated and

subjected to the loading scenario predicted by the musculoskeletal model to determine the spinal load-sharing.

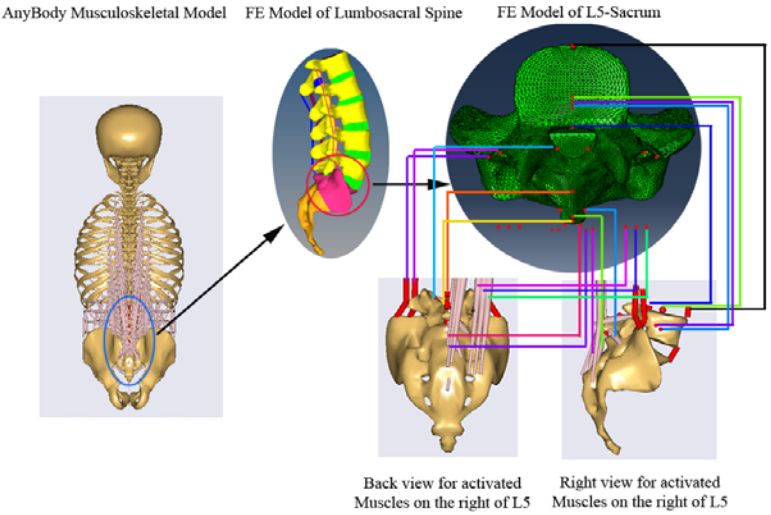

Load scenarios for L5. The order is from left to right: 1,2: Intertransverse Ligament, 3: Ligamentum Flavium, 4: Supra-spinous Ligament, 5: Interspinous Ligament,6-13: Erector Spinae,14: Posterior Longitudinal Ligament, 15:Center of Gravity for L5 ,16:Intra-abdominal pressure, 17:Joint between L4 and L5, 18:Anterior Longitudinal Ligament.

[1] Schmidt, T.A. et al. 1998. The stiffness of lumbar spinal motion segments with a high-intensity zone in the anulus fibrosus. Spine 23:2167-73.

[2] Naserkhaki, S et al. 2016. On the load-sharing along the ligamentous lumbosacral spine in flexed and extended postures: Finite element study. J Biomech, 49:974-82.

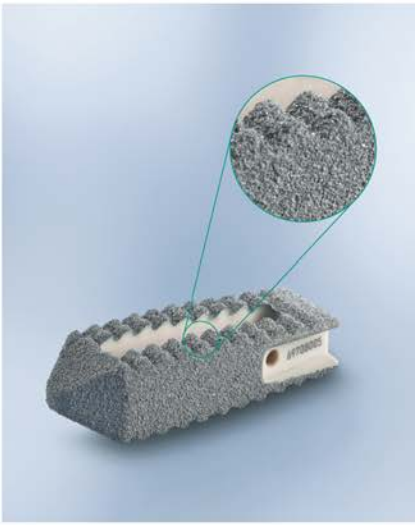

A-SP14001

Redefining Fusion.

Plasmapore[XP®]

Stability starts on the surface:
Osteoconductive[1] porous titanium coating on PEEK-OPTIMA®

CeSPACE®XP

Cervical Interbody Fusion System with Plasmapore[XP®] coating

PROSPACE®XP

PLIF Interbody Fusion System with Plasmapore[XP®] coating

Arcadius[XP] L®

Plasmapore[XP®] coated Lumbar Stand-Alone Interbody Device

[1] Boyle C. Cheng, PhD, Biomechanical Pullout Strength and Histology of Plasmapore[XP®] Coated Implants: Ovine Multi Time Point Survival Study, Aesculap ART129 12/13

B|BRAUN
SHARING EXPERTISE

Aesculap AG | Am Aesculap-Platz | 78532 Tuttlingen | Germany
Phone +49 7461 95-0 | Fax +49 7461 95-2600 | www.aesculap.com

Aesculap – a B. Braun company

The Effect of Posterior Element Removal on Coupled Motions in Human and Porcine Thoracic and Lumbar Spines

Kingma I[a], Busscher I[b], van der Veen AJ[c], Verkerke GJ[b,d], Veldhuizen AG[b], Homminga J[d], van Dieën JH[a]

[a]*Dept. of Human Movement Sciences, Vrije Universiteit Amsterdam, The Netherlands*
[b]*University Medical Center Groningen, Groningen, The Netherlands*
[c]*VU University Medical Center, Amsterdam, The Netherlands*
[d]*University of Twente, Enschede, The Netherlands*

Coupled spine motions, i.e. motions along axes other than the loaded axis, have been reported to occur in the human spine, but results have been contradicting. Furthermore, the role of facet joints in such motions is as yet unclear. In the present in vitro study, 6 elderly human and 6 young porcine spines were sectioned in four segments, each consisting of four vertebrae and three intervertebral discs. Segments were loaded along each of the three axes, and three-dimensional rotations of the middle intervertebral disc were quantified. Subsequently, posterior elements were removed and the protocol was repeated. In contrast to other studies, local axes at the vertebrae were defined as aligned with the global axes prior to each applied load. This approach was taken to avoid complications in interpretation due to mixed loading between Axial Rotation (AR) and Lateral Bending (LB) which occurs when vertebrae are inclined due to lordosis or kyphosis.

Expressed as a percentage of motion in the loaded direction, coupled motions were larger in human spine (Fig. 1) than in porcine spines (medians 20.9% and 12.8%, respectively). Largest coupled motions were obtained in axial loading of the lumbar spine segments, with median values of 48.6% and 23.9% for human L2L3 and porcine L3L4 joints, respectively. Surprisingly, removal of posterior elements had no substantial effects on coupled motions, with exception of axial rotation loading of the human lumbar spine segment, where posterior element removal decreased coupled motion from 48.6% to 30.7%. Neither the porcine nor the human spines showed consistency in direction of coupled motions across spines, neither before nor after removal of posterior elements.

The present results indicate that coupled motions are not consistent when axes are aligned with the actual loading of the spine. Furthermore, posterior elements only had a minor contribution to coupled motions.

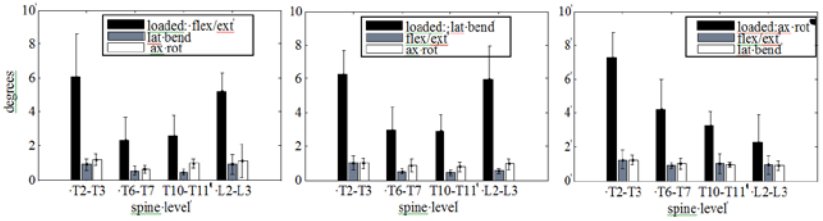

Fig. 1: Three dimensional human spine motions of the middle intervertebral joint in four sections of four vertebrae at 4 Nm loads prior to removal of posterior element.

Dynamic Stiffening of Lumbar Spinal Specimens

Huber G[a], Klein A[b], Püschel K[b], Morlock MM[a], Nagel K[a,c]

[a]*Institute of Biomechanics, TUHH Hamburg University of Technology, Germany*
[b]*Dept. of Legal Medicine, University Medical Centre Hamburg-Eppendorf, Germany*
[c]*Syntellix AG, Hannover, Germany*

Whole body vibrations are considered a major cause of lumbar spinal injury at the workplace. The detailed pathway between mechanical cyclic loading and biological degeneration remains unclear. Numerical whole-body models are promising tools to fill this gap and might help in deciding which loads are acceptable and which should be avoided. Model complexity is a limiting factor for the usability of these tools, but more importantly, there is a huge lack of suitable basis functions and parameters describing the essential dynamic behaviour of the functional spinal unit.

This study aims to provide the dynamic stiffness of lumbar functional spinal units in a frequency range that is relevant for occupational health issues.

Lumbar spinal specimens (L2-L3, n = 17 and L4-L5, n = 16) of three groups were collected: young male (n = 11, 25 - 44 a), midlife male (n = 10; 45 - 65 a) and midlife female (n = 12; 45 – 65 a). Specimens were stored frozen and CT scanned (Mx8000 IDT 16, Philips Healthcare, Best, The Netherlands). The scan included a phantom (dipotassium phosphate; K_2HPO_4) to determine equivalents of bone mineral density. After thawing on the day of testing, the muscles and the transverse ligaments were removed and both vertebrae were embedded in metal holders.

A servo-hydraulic test machine (MTS Bionix, Eden Prairie, MN) was complemented with a second hydraulic axis perpendicular to the original. The two axes were connected via beams with elastic bending joints so that the loading-platform could move independently in horizontal and vertical axes. This construct enabled high dynamic two-dimensional loading and avoided friction and slip-stick effects that are common for joint and slider based setups.

The cranial vertebra was connected to the moving loading-platform while the caudal vertebra was connected to a six-component load-cell (Huppert, Herrenberg, Germany). During testing the specimens were immersed in ringer solution at 37°C, that contained 10 ml/l antibiotics (Penicillin/Streptomycin, PAA, Austria) to inhibit biological degeneration.

The specimens underwent several sets of consecutive non-destructive force-controlled cyclic parameter measurements with different amplitudes (axial: 200 N to 1000 N; shear: 50 N to 200 N) for frequencies of 0.005 Hz to 12 Hz. The cyclic loading was overlaid by an offset load so that the peak axial compression reached -2000 N and the anterior-posterior shear -300 N.

Load hystereses exhibited commonly-observed progressive nonlinearity with increasing slopes for increasing deformation. Consequently, the overall stiffness significantly increased with increasing offset load and decreased when larger contents of the low deformation range were incorporated because of higher

amplitudes. Axial stiffness exhibited a 10-fold higher stiffness compared to shear. The apparent axial stiffness exhibited an increase of about 20 % between frequencies of 0.02 Hz and 10 Hz ($p < 0.001$) while shear stiffness increase by as much as 30 % within this range (Fig. 1).

Dynamic effects caused by the viscoelastic and poroelastic nature of spinal specimens are generally discussed with regard to loading with little dynamic content, e.g. creep initiated by constant loading. However, this study demonstrates that dynamic stiffening occurs for frequencies that are relevant to passive cyclic loading during everyday activities. Axial cyclic compression of the spine may be considered as the principle loading direction during sitting on vibrating chairs of various vehicles. However, due to different seating postures coupled multiaxial loading is to be expected, and presumably this will further accelerate damage to the structure. In vitro testing can be used to determine values for particular clearly defined loading regimes while detailed numerical modelling, based on data for dynamic loading will be needed to interpolate between these discrete measurements..

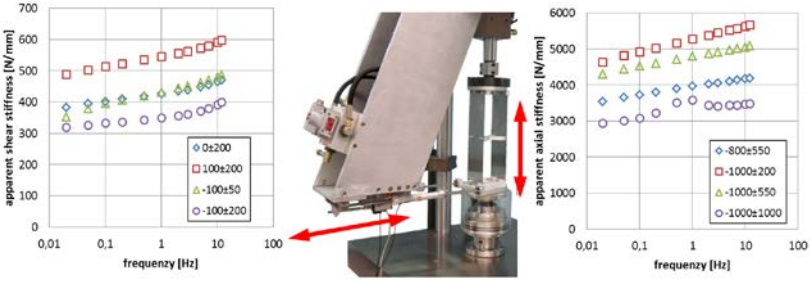

Fig. 1: Apparent shear and axial stiffness with respect to the frequency of the cyclic loading. Shear was applied via the complementary second hydraulic actuator, while axial compression was generated by the actuator of the standard servo-hydraulic test machine.

Acknowledgement: This study was funded by FIOSH, Germany, projects F2059 and F2069. All authors disclose having no financial or personal relationships with other people or organizations that could inappropriately influence this work.

Spine System Equivalence: A New Protocol for Standardized Multi-Axis Comparison Tests

Holsgrove TP[a,b], Amin D[c], Ramos Pascual S[a], Ding B[d], Welch WC[e], Gheduzzi S[a], Miles AW[a], Winkelstein BA[e,f], Costi JJ[c]

[a]*Centre for Orthopaedic Biomechanics, Department of Mechanical Engineering, University of Bath, Bath, UK*
[b]*College of Engineering, Mathematics & Physical Sciences, University of Exeter, Exeter, UK*
[c]*Biomechanics & Implants Research Group, The Medical Device Research Institute, Flinders University, Adelaide, SA, Australia*
[d]*School of Mechanical Engineering, The University of Adelaide, Adelaide, SA, Australia*
[e]*Department of Neurosurgery, University of Pennsylvania, PA, USA*
[f]*Department of Bioengineering, School of Engineering & Applied Science, University of Pennsylvania, PA, USA*

Accurately replicating the in-vivo loads of the spine is a critical aspect of in-vitro spine testing, but the complexity of this structure renders this challenging. The design and control capabilities of multi-axis spine systems vary considerably, and though recommendations have been made [1, 2], standardized in-vitro methods have not yet been established. As such, it is often difficult to compare different biomechanical studies [3]. The aim of this study was to use international standards [4, 5], and spine testing recommendations [1-3] to develop a standardized protocol for the evaluation of different multi-axis spinal test systems. The protocol was implemented on three six-axis spine systems, and the data used to establish stiffness and phase angle limits.

Synthetic lumbar motion segments (n=5) were produced, each comprising three heavy-duty, die-cast springs embedded in polymer [4, 5]. Specimens were tested on each system using pure moments of ±8 Nm at 0.1 Hz in flexion-extension (FE), lateral bending (LB), and axial rotation (AR). Tests were completed using sine and triangle waves, and with axial preloads of 0 and 500 N. Five cycles were applied for each test, with the last three used to calculate the stiffness, phase angle, and R^2 value at the geometric center of each specimen. Stiffness and phase angle limits were calculated based on the 95% confidence intervals of the data from all three systems for each test (Table 1).

All test systems demonstrated similar stiffness across all tests, though there were small (<10%) but significant differences in FE ($p<0.002$) and LB ($p<0.003$) with a 500 N preload, and in AR ($p<0.046$) without a preload. There were significant differences ($p<0.032$) in 15 of 36 comparisons of phase angle, though the mean angle was <4º in all tests.

This test protocol can be adopted to evaluate and ensure equivalence of different multi-axis spine systems, providing a better way to compare in-vitro spine studies.

Table 1. Stiffness and phase angle limits for pure moment tests with synthetic specimens.

Parameter	0 N preload					
	FE		LB		AR	
	Sin	Tri	Sin	Tri	Sin	Tri
Stiffness upper limit (Nm/°)	3.50	3.48	4.12	4.11	7.73	7.82
Stiffness lower limit (Nm/°)	2.72	2.73	2.98	2.96	5.29	5.23
Phase angle limit (°)	6.12	6.43	3.03	3.63	3.17	4.19
	500 N axial preload					
	FE		LB		AR	
	Sin	Tri	Sin	Tri	Sin	Tri
Stiffness upper limit (Nm/°)	4.07	4.08	5.05	5.07	10.27	10.41
Stiffness lower limit (Nm/°)	3.23	3.24	4.01	4.01	6.79	6.74
Phase angle limit (°)	5.90	6.51	2.18	2.64	3.10	4.33

[1] Goel et al, 2006. J Bone Joint Surg Am, 88 Suppl 2, 103-109.

[2] Wilke et al, 1998. Eur Spine J, 7(2), 148-154.

[3] Holsgrove et al, 2015. Int J Spine Surg, 9, 34.

[4] BS ISO 12189:2008.

[5] BS ISO 10243:2010+A1:2011.

Acknowledgement: This research was supported by the Catherine Sharpe Foundation, the Enid Linder Foundation, the Higher Education Innovation Fund, and the University of Bath Alumni Fund.

How Do We Stand? Variations during Repeated Standing Phases of Asymptomatic Subjects and Low Back Pain Patients

Schmidt H[a], Bashkuev M[a], Weerts J[a], Graichen F[a], Altenscheidt J[b], Maier C[b], Reitmaier S[a]

[a]*Julius Wolff Institute, Charité – Universitätsmedizin Berlin, Germany*
[b]*Department of Pain Management, BG-University Hospital Bergmannsheil, Bochum, Germany*

An irreproducible standing posture can lead to misinterpretation of radiological measurements, wrong diagnoses and possibly unnecessary treatment. This study aimed to evaluate the differences in lumbar lordosis and sacrum orientation in six repetitive upright standing postures of 353 asymptomatic subjects (including 332 non-athletes and 21 athletes) and 83 low back pain (LBP) patients using a non-invasive back-shape measurement device.

In the standing position, all investigated cohorts displayed a large inter-subject variability in sacrum orientation (~40°) and lumbar lordosis (~53°). Asymptomatic athletes and non-athletes showed a strong positive and significant correlation between both parameters ($R^2 \leq 0.71$, $p<0.001$). In LBP patients, the correlation between lumbar lordosis and sacrum orientation substantially decreased ($0.38 \leq R^2 \leq 0.49$, $p<0.001$). In the asymptomatic cohort (non-athletes), 51% showed variations in lumbar lordosis of 10–20% after six repeated standing phases, 29% of the subjects showed variations of even more than 20%. In the sacrum orientation, 53% of all asymptomatic subjects revealed variations of >20% and 31% of even more than 30%.

It can be concluded that standing is highly individual and poorly reproducible. The reproducibility was independent of age, gender, height and weight. Variability in standing showed no difference between back pain patients and asymptomatic subjects. The number of standing phases performed showed no positive effect on the reproducibility. Therefore, it should be considered that X-ray or other physical examinations of standing can greatly differ on subsequent analyses.

Are there Characteristic Motion Patterns in the Lumbar Spine during Flexion?

Zander T, Bashkuev M, Schmidt H

Julius Wolff Institute, Charité – Universitätsmedizin Berlin, Germany

Flexion is the main motion of the lumbar spine. While *in vitro* tests with pure moments suggest larger intra-segmental rotations for the more caudal segments [1–4] *in vivo* results partly show an oppositional motion distribution [5, 6]. The present study analysed the motion distribution *in vivo* on 319 asymptomatic subjects (BMI <26, age 20-75 years).

The change of the back shape between standing and upper body flexion was determined using the back shape measuring device Epionics SPINE [7] which is based on strain gauge technology. Linear, bilinear, trilinear, quadratic, and cubic regression models were fit to each of the segmental motion distributions over the length of lordosis. Simplicity (degree of freedom of the model) and approximation quality (adjusted coefficient of determination, aCoD) were used to assign the motion distributions to the regression models. Statistical analyses were performed with R [8].

78% of the motion distributions could best be explained by a bilinear model (Fig. 1). Further 10% and 11% could be represented by a linear and trilinear model, respectively. Mean aCoD of these models was 0.97. About 1% of the distributions could not be represented by the models (aCoD <0.7). Quadratic and cubic were always inferior to bi- and trilinear regressions and were thus excluded. All of the bilinear models showed maximum flexion in the middle of lordosis (41% from caudal, SD 11%). All linear models showed a decreasing rotation from caudal to cranial. Most of the trilinear models (76%) showed a distribution similar to the bilinear but with another increase cranial. Neither the length of lordosis nor the number of regression pieces (linear, bi-, trilinear) was correlated to the body height.

The results provide a potent description of the healthy population and may serve to identify spinal motion abnormalities. They can further be used in computational models and to create more realistic *in vitro* load protocols. For the workshop as well as for the special issue we will additionally provide data on age, sex, and body height effects.

[1] Guan et al.: J Biomech 2007, 1975–80
[2] Panjabi et al.: J Bone Joint Surg Am 1994, 413–424
[3] Wilke et al.: J Orthop Res 1996, 500–3
[4] Yamamoto et al.: Spine 1989, 1256–60
[5] Pearcy et al.: Acta Orthop Scand Suppl 1985, 1–45
[6] Wong et al.: Spine 2006, 414–9
[7] Consmüller et al.: Eur Spine J 2012, 2170–80
[8] R Development Core Team (2008): ISBN 3-900051-07-0

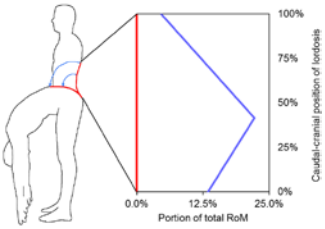

Fig. 1: Characteristic bilinear motion distribution of the lordotic segments during upper body flexion

Kinetic Control of Lumbar Spine Flexion-Extension Movement Using Proportional Derivative (PD) Controller, Feedback Linearization Method and Their Combinations

Abedi M[a], Vossughi GR[a], Parnianpour M[a], Khalaf K[b]

[a]*Department of Mechanical Engineering, Sharif University of Technologies, Tehran, Iran*
[b]*Department of Biomedical Eng. Khalifa University of Science and Research, Abu Dhabi, UAE*

The role of motor control in development of low back pain is subject of many researches both in theoretical and experimental fields. In this work flexion-extension movement of lumbar spine have been controlled by three different methods, including feedback linearization (FBL), PD control and their combinations. The model involves 7 links: 1 link for pelvis, 5 links for lumbar vertebrae and 1 link for thorax. Torque actuators have been used on each joint to make them follow desired sagittal trajectory. In linear control method, equations of motion have been linearized with respect to upright position and then control signals have been applied in the direction of eigenvectors. Desired trajectory of each joint has been produced by Central Pattern Generators (CPGs), which was the subject of our previous work. The ill-posed nature of equations of motion results in divergence of desired and simulated motion if the torques from inverse dynamics is fed to drive the multi-body system in the forward dynamics (Fig. 1). Hence, we need both feedback and feedforward controls and internal model of system to stabilize (regulate) the system performance. Robustness of each method against actuator noise or external perturbation, sensory delay and parameters uncertainty have been investigated.

There is sensory delay, in the information coming from the periphery (afferent signals from muscles, ligaments and joint capsules containing data about the joints angular position and velocity) to the central nervous system which limits the feedback gains due to stability constraints. Inverse models often do not have precise estimation of each model parameters such as mass, length, moment of inertia of each link. The control scheme must remain effective in presence of these parameters uncertainties besides any un-modeled dynamics. Neural noise can affect the actuators and sensors performance that should be considered when designing the performance of the robust controllers. There are many studies on motor control, suggesting different methods that central nervous system (CNS) uses to control body position in different tasks. Feedback Linearization (FBL) Method, have been used by eliminating nonlinear terms so the movement can be controlled by linear methods. Linear control methods usually fail in the problems with many degrees of freedom, because there are many unknowns (gains) for example for proportional and derivative matrices and stability calculation is very complicated process. We linearized equations of motion and calculated eigen-movement directions along which the controls are applied by reducing the number gains while identifying emerging synergies. In the second part FBL method have been used and in last part combination of these two methods have been applied.

The results show that PD controller in comparison with feedback linearization method is more robust in presence of noise and parameters uncertainty, but FBL controller is better when we have sensory delay. Combination of these methods leads to better control in all three simulations. By linearization, equations of motion have been decoupled and torques can be calculated for each eigen-direction independently. The biological idea behind this method is that central nervous system does not control each link independently. Using of FBL controller is advantageous by eliminating nonlinear terms that can reduce the problem to a simple linear one. Therefore linear control methods can be applied more readily. FBL method calculates the exact amount of torque without any linearization or ignoring any parameter. Although this high accuracy is an advantage for FBL method but the output torques are very sensitive to system parameters and system loses its stability with parameter uncertainty. This instability can be compensated by addition of a PD controller (Fig. 2). In this study equations of motion were linearized with respect to only one point (upright position). Division of motion into different sectors and performing linearization for each part separately can lead to better results. Another subject for our future studies is to develop this method to control a system with force actuators.

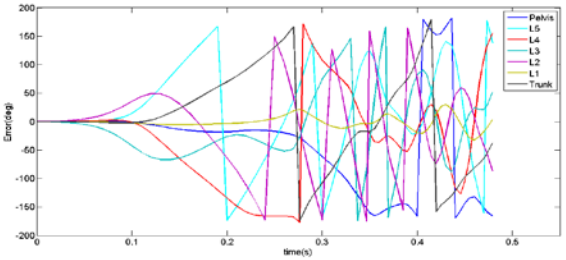

Fig. 1: The ill-posed nature of equations of motion is illustrated by the divergence of the motion without any feedback in less than 60 ms.

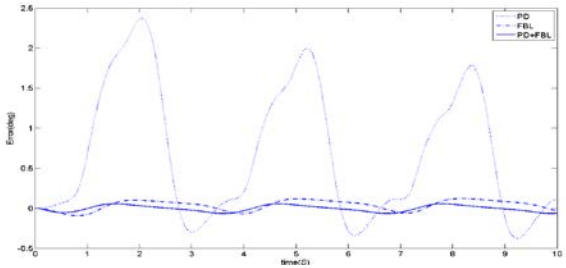

Fig. 2: The performance of the combined FBL and PD controller have significantly improved pelvis error between the desired and simulated motion during 10 s of rhythmic 65 degrees sagittal movement.

[1] A. Seth And M. G. Pandy, "A Neuromusculoskeletal Tracking Method For Estimating Individual Muscle Forces In Human Movement," Journal of Biomechanics, Vol. 40, pp. 356-366, 2007.
[2] A. V. Alexandrov, A. A. Frolov, And J. Massion, "Biomechanical Analysis of Movement Strategies in Human Forward Trunk Bending. I .Modeling," Biological Cybernetics, Vol. 84, pp. 425-434, 2001.

Model-Based Estimation of Changes in Lumbar Spine Kinematics with Alterations in Trunk Neuromuscular Strategy

Shojaei I[a], Arjmand N[b], Meakin J[c], Bazrgari B[a]

[a]*University of Kentucky, Lexington, KY, USA*
[b]*Sharif University of Technology, Tehran, Iran*
[c]*University of Exeter, Exeter, UK*

With regard to the low back pain problem, imaging is used to detect potential structural and geometrical abnormalities in the lumbar spine. Geometrical information from imaging, if combined with proper mechanical models, may provide insight related to potential neuromuscular abnormalities in the lower back. As a first step toward subject-specific characterizations of trunk neuromuscular behavior, the objective of this feasibility study is to investigate whether changes in lumbar spine kinematics due to alterations in trunk neuromuscular strategy are within the reported precision of current imaging techniques.

Five different neuromuscular strategies were investigated, each included a set of muscle forces that minimized a cost function while satisfying equilibrium requirements across the lumbar spine. The cost functions were selected to either represent the suggested trunk neuromuscular strategy of asymptomatic persons (i.e., sum of squared muscle stress) or a neuromuscular strategy minimizing a specific aspect of spinal load (e.g., muscle forces, compression, shear force, or passive moment). For each neuromuscular strategy, kinematics of the lumbar spine (i.e., axial and angular deformation of each motion segment) were obtained under a static flexed trunk posture involving respectively 40 and 10° of thoracic and pelvic rotations in the sagittal plane. This was done using a nonlinear kinematics-driven finite element musculoskeletal model of the spine [1] within a heuristic optimization procedure as described in our earlier work [2].

Minimum (maximum) changes in angular and axial deformations of lumbar motion segments with alterations in neuromuscular strategy ranged from 0 (2.4) to 0.5 (7.5)° and 0 (0.16) to 0.04 (0.48) mm, respectively (Table 1). The differences in kinematics of at least five spine segments between each two neuromuscular strategies are detectable by current imaging techniques whose precision is reported to be ~ 0.1 mm and ~ 0.1° [3]. Particularly, the differences in kinematics of spine segments (6 segments) between each combination of two neuromuscular strategies (10 possible combinations) are detectable in 97% of cases for angular deformation and 55% of cases for axial deformation. Therefore, combined imaging and computational modeling appears capable of predicting neuromuscular strategies/abnormalities. Specifically, a geometrically and materially subject-specified model of the spine can be used in future to obtain the neuromuscular strategy that generates the closest spine kinematics to those measured from imaging. The accuracy of such assessment strategy can further be improved by implementing dynamic rather than static assessment tasks.

Table 1: Estimation of sagittal angular (deg) and axial (mm) deformations of lumbar spine motion segments using different neuromuscular strategies that minimize 1) sum of squared muscle stresses, 2) sum of squared muscles forces, 3 and 4) L5-S1 compression or anterior-posterior shear forces, 5) L5-S1 passive moment.

	T12-L1	L1-2	L2-3	L3-4	L4-5	L5-S1	δT12-L1	δL1-L2	δL2-L3	δL3-L4	δL4-L5	δL5-S1
$\sum Stress^2$	3.0	5.1	4.8	3.6	5.7	7.5	0.70	1.10	1.22	1.24	1.48	0.75
$\sum Force^2$	7.8	7.5	4.8	1.5	2.4	5.7	0.97	1.19	1.22	1.09	1.20	0.70
Compression	7.9	6.8	6	2.1	1.9	5.6	0.97	1.10	1.24	1.07	1.15	0.69
Shearing	5.7	3.3	5.1	7.5	7.8	0.9	0.89	0.96	1.21	1.37	1.52	0.81
L5-S1 passive moment	4.2	6.6	7.2	7.8	4.2	0.0	0.87	1.18	1.32	1.46	1.44	0.86
Minimum change	0.1	0.2	0	0.3	0.5	0.1	0.02	0	0	0.02	0.04	0.01
Maximum change	4.9	4.2	2.4	6.3	5.9	7.5	0.27	0.23	0.11	0.39	0.37	0.17

[1] Bazrgari et al., 2007. *European Spine Journal*, 16: 687-699.
[2] Shojaei et al., 2015 *Int J of Num Methods in Biomedical Engineering,* 31
[3] Ochia et al., 2006. *Spine*, 31: 2073-2078.

Acknowledgements: This work was supported, in part, by an award (5R03HD086512-02) from the National Center for Medical Rehabilitation Research (NIH-NICHD) and the Office of the Assistant Secretary of Defense for Health Affairs, through the Peer Reviewed Orthopaedic Research Program (award #W81XWH-14-2-0144).

Variations in Lumbar Facet Kinematics Across Segments During In Vivo Extension Movement

Byrne R[a], Zheng L[b], Zhou Y[a], Aiyangar A[c], Zhang X[a]

[a]*Department of Mechanical Engineering and Materials Science, University of Pittsburgh, USA*
[b]*Health Effects Lab Division, National Institute for Occupational Safety and Health, Atlanta, USA*
[c]*Mechanical Systems Engineering, EMPA (Swiss Federal Laboratories for Materials Science and Technology), Dübendorf, Switzerland*

Facet joints form an important component of the spinal joint complex, but facet motion, as currently obtained from *in vitro*-based cadaveric studies or static imaging modes such as CT and MRI in supine, non-functional poses, remains inadequately understood. The present study reports on the translation motion of lumbar facet joints between L2-sacrum at each intervertebral level in young, healthy subjects performing a continuous lifting task using a state-of-the-art dynamic stereo X-ray (DSX) imaging system.

Ten asymptomatic participants (24±3 years; 7M, 3F) lifted a known weight (3 levels: 4.5kg, 9.1kg and 13.6 kg) from trunk-flexed (~75° flexion) position to upright position without knee-bending while their lumbar regions were continuously imaged by a DSX system (30frames/s, 2s). Bilateral, 3D facet joint kinematics at each segment (L2L3, L3L4, L4L5, L5S1) were characterized by displacement vectors (green vectors in Figure 1) connecting centroids of the superior facet surfaces (left and right, separately) of the inferior vertebra to the corresponding inferior surfaces of the superior vertebra and expressed in the superior facet's LCS. Repeated measures analysis with data compiled as a mixed model followed by Tukey post-hoc comparison-of-means tests was employed to investigate segment (4 levels)- and loading (3 levels)-specific differences in facet translation.

Overall translation was lowest in L5S1 *{Median (Md) = 3.8mm, p<0.0001}* compared to L2L3, L3L4 and L4L5 segments *(Md = 6.3mm, 6.4mm and 6.7mm respectively)*. No significant differences between the other segments were detected (p>0.5). No significant effect of magnitude of weight lifted (p>0.7) was detected. Although coupled translation was observed, translation in the superior-inferior (SI, local y-axis) direction was dominant contributor. L4L5 and L5S1 had larger translations along the local x- *(Md=0.4mm and 0.5mm respectively)* and z-axes *(Md=1.56mm and 1.03mm respectively)* compared to L2L3 and L3L4 *((x-axis Md = 0.1 mm and 0.3 mm respectively; z-axis Md = 0.7mm and 0.6 mm respectively)*. Following differences were significant along x- (L5S1>L3L4, p=0.01; L4L5>L3L4, p=0.04) and z-axes (L4L5>L2L3, p =0.02). The dynamic dataset describing facet translation patterns contributes to generating a comprehensive, baseline 3D dataset of lumbar spinal kinematics during functional activities.

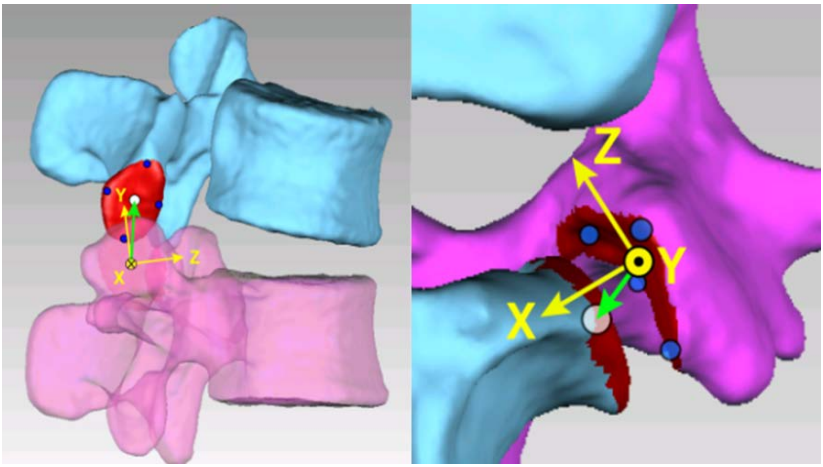

Fig. 1: Local coordinate system shown on the superior facet of the inferior vertebra. Green arrow from parent (superior facet of inferior vertebra) CS origin to child CS (inferior facet of superior vertebra) origin represents the displacement vector. (a) Sagittal view. (b) Top view.

Acknowledgements: Funding sources: (R21OH00996, R01OH0105801) Center for Disease Control and Prevention/National Institute for Occupational Safety and Health (CDC/NIOSH); (PZ00P2_154855/1) Swiss National Science Foundation (SNSF) Ambizione Career Grant Award.

Disclosures: An abstract based on a subset of these data (4.5 kg weight level) was submitted to ORS 2017 Annual Meeting, San Diego, CA, USA, March 19-22, 2017.

Estimation of Spinal Joint Centers from External Spinal Profile and Anatomical Landmarks

Nérot A[a,b], Skalli W[b], Wang X[a]

[a]*Univ Lyon, Université Claude Bernard Lyon 1, IFSTTAR, UMR_T9406, LBMC, Lyon, France*
[b]*Institut de Biomécanique Humaine Georges Charpak, Arts et Métiers ParisTech, Paris, France*

Defining a subject-specific model of the human body is required for motion analysis in many fields, such as in ergonomics and clinical applications, to fully understand the interaction of the body with the environment and its impacts on the musculo-skeletal system. However, locating internal joint centers from external characteristics of the body (e.g. bony landmarks, skin envelope) still remains a challenging issue, mainly due to the lack of data containing both the characteristics from the external body envelope and the internal skeleton. This is particularly true for the spine and pelvis. Recently, biplanar X-rays methods were developed to reconstruct both the bones and the skin envelope in three dimensional space (3D) from a standing posture based on two radiographic views [1]. A database containing both surface envelope and skeleton of 80 asymptomatic subjects has been created. A principal component analysis was performed allowing the prediction of the joint centers of the spine and the pelvis directly from the skin envelope [2]. However, the full 3D trunk surface is not always available because 3D body scanning device may not be a part of motion analysis lab equipment or some body parts may be obstructed by other objects. Therefore, there is a need to provide an alternative way to estimate joint centers only using a limited number of easily palpable landmarks and the external spinal profile.

Two methods were proposed to predict the spinal joint centers: one only using 8 anatomical landmarks (ALs) (2 ASIS, 2 PSIS, T8, C7, IJ and PX) and one using both 8 ALs and the external spinal profile.

A spine local coordinate system (LCS) (**o, d, t**) in the sagittal plane was defined with the origin **o** at C7 spinous process, **t** the axis directing from C7 spinous process to the mid of the two PSIS. **d** was the perpendicular axis to **t** directed forward. For a t_i along **t**, the coordinates at the internal and external spine profiles can be expressed as (t_i, d_i^{int}) and (t_i, d_i^{ext}). In the present work, 11 points the internal and external spine profiles were defined along **t**. Statistical regressions were proposed using the existing database of 80 subjects to predict d_i^{int} and the distance between internal and external spinal profiles D_i (= d_i^{int} - d_i^{ext}). Best predictors were searched among anthropometric dimensions (e.g. stature, weight, waist circumference etc.) and distances between ALs. From either d_i^{int} or D_i (external profile needed), the internal spinal profile can be predicted in the spine LCS. The relative positions (curvilinear abscises normalized by the curvature length) of joint centers along the internal spinal profile were observed quite invariant among the subjects. By applying the normalized curvilinear abscises, the joint centers on the spinal profile can be located.

The predicted location of joint centers showed an average error in 2D distance of

9.7 mm (±5.0) for all joints when using the external spinal profile. Similar results were obtained without use of external spinal profile, 9.5 mm (±5.0).

Though 8 ALs were used in the present work, only C7 and the two PSIS were required to be accurately palpated. Other ALs were used to calculate anthropometrical dimensions used as predictors. Compared to other existing methods, the proposed methods offered a more accurate prediction with smaller number of palpated points. Like all data based methods, the regression equations are data dependent and can only be applied in a standing posture. Methods have to be developed to change the standing position to a desired posture such as seated one.

[1] Dubousset J., G. Charpak, W. Skalli, J. Deguise, G. Kalifa (2010) "EOS: a New Imaging System With Low Dose Radiation in Standing Position for Spine and Bone & Joint Disorders". J Musculoskelet Res, 13(01):1-12

[2] Nérot, A., W. Skalli, X. Wang. (2016) "A Principal Component Analysis of the Relationship between the External Body Shape and Internal Skeleton for the Upper Body." J.Biomech. 49(14): 3415–22

Subject-Specific Regression Equations to Estimate Spinal Loads in Symmetric Lifting

Ghezelbash F[a], El Ouaaid Z[b], Shirazi-Adl A[a], Plamondon A[b], Arjmand N[c]

[a]*Department of Mechanical Engineering, Ecole Polytechnique, Montréal, Canada*
[b]*Institut de recherche Robert Sauvé en santé et en sécurité du travail, Montréal, Canada*
[c]*Department of Mechanical Engineering, Sharif University of Technology, Tehran, Iran*

Excessive loads on the lumbar spine are recognized as a major cause of the back pain. There is no direct way of measuring spinal loads, and due to the invasive nature and limitations of existing indirect methods (i.e., intradiscal pressure measurement, instrumented vertebral replacement), musculoskeletal (MS) biomechanical models are recognized as viable and robust tools. A number of MS models with different degrees of complexity and accuracy have been developed and applied to estimate spinal loads. To simplify the application of these models to various activities of daily living, regression equations have also been developed [1]. Nonetheless, and as a major limitation, existing models do not account for personal factors (e.g., body weight, body height, sex). Thus, we aim here to record spinal kinematics in male/female subjects in various symmetric lifting activities and apply them to drive our MS model [2] towards the development of robust subject-specific regression equations to estimate spinal loads.

Experiments: After signing the informed consent form approved by the institutional ethics committee, 9 female (height=163.4±3.7 cm; weight=61±4.5 kg; age=24.1±4.3 years) and 10 male (height=174.6±4.2 cm; weight=72.2± 8.7 kg; age=30.6±6.5 years) asymptomatic participants held in hands four weights (1, 5, 10 and 15 kg) at four different heights (mid-shank, knee, mid-thigh and navel levels) in stoop positions. We collected spinal kinematics at the S1, T11, C7, head, arms and legs using Optotrak motion capture system and recorded EMG signals of 14 superficial muscles (longissimus, iliocostalis pars thorasis and lumbarum, multifidus, external oblique, internal oblique and rectus abdominis). Kinematics data and EMG signals were low-pass filtered at 10 Hz and band-pass filtered at 30 to 450 Hz, respectively. EMGs were normalized to their maximal root mean square values during maximum voluntary exertions (flexion, extension, lateral and axial directions).

MS modeling: The in vivo experiments on each subject were simulated in the subject-specific model and estimated muscle activities were compared with recorded EMGs. To develop regression equations, we simulated various sagittally symmetric lifting tasks from standing to 90^{o} flexion with different weight locations by applying a sex-specific lumbopelvic rhythm [3] while considering four body heights (155-190 cm), four BMI (18-30 kg/m^2) and two sex (female and male) levels to cover a vast portion of population.

Predictive equations: Quadratic regression equations were fitted to the computed compression and shear forces at the L4-L5 and L5-S1 discs while body height, body weight, sex, hand-held weight, weight position and trunk flexion angle were considered as independent variables.

Model estimations of muscle activities agreed with the measured EMG signals. Input independent variables substantially affected spinal loads, Fig.1. High coefficient of determination (~0.95) combined with low error (~9%) demonstrate the accuracy of regression equations as reliable alternatives to complex MS models; for instance, the L4-L5 shear regression equation at a fixed weight position is expressed as follows (coefficient of determination=0.97; root mean square error=14 N):

$$\begin{aligned}\mathrm{Shear}_{\mathrm{L4-L5}} = {} & -107.12 + 25.03\mathrm{Sex} + 0.739\mathrm{BH} + 0.02\mathrm{BW} + 2.86\mathrm{W} + 0.57\theta \\ & - 0.16\mathrm{Sex.BH} + 0.03\mathrm{Sex.BW} - 0.06\mathrm{Sex.W} + 0.32\mathrm{Sex}.\theta \\ & + 1.82\mathrm{E}^{-3}\mathrm{BH.BW} + 1.19\mathrm{E}^{-3}\mathrm{BH.W} + 0.01\mathrm{BH}.\theta \\ & + 0.01\mathrm{BW.W} + 0.05\mathrm{BW}.\theta + 0.11\mathrm{W}.\theta - 2.29\mathrm{E}^{-3}\mathrm{BH}^2 \\ & + 2.14\mathrm{E}^{-3}\mathrm{BW}^2 - 0.02\mathrm{W}^2 - 0.03\theta^2, \qquad \text{(Eq. 1)}\end{aligned}$$

where sex (female=1 and male=0), body height (BH), body weight (BW), hand-load weight (W) and flexion angle (θ) are inputs. Providing workplace safety professionals and ergonomists with such equations is crucial in order to assist them in reducing the risk of lifting tasks and increasing occupational safety. In the next step, the foregoing regression equations will be updated based on our own *in vivo* measurements of lumbopelvic rhythr

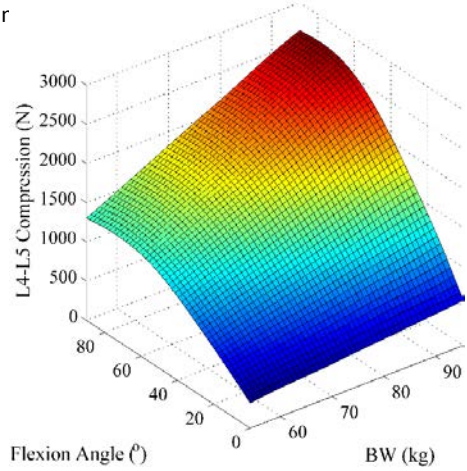

Fig. 1: L4-L5 compression versus body weight (BW) and flexion angle without a hand-load. Sex and body height were set as male and 178.3 cm.

[1] Arjmand et al. (2011), J Biomech 44: 84-91.

[2] Ghezelbash et al. (2015) CMBBE 18: 1760-67.

[3] Pries et al. (2015), J Biomech 48: 3080-87.

Acknowledgements: IRSST & FRQNT-Quebec

Obesity and Spinal Loads, a Combined MR Imaging and Subject-Specific Modeling Investigation

Kazemi H, Akhavanfar MH, Arjmand N

Department of Mechanical Engineering, Sharif University of Technology, Tehran, Iran

Obesity is a worldwide growing health challenge affecting ~30% of the world's population. Increased rate of disc degeneration, low back pain and surgery are reported in obese individuals [1]. Although obesity-related low back diseases have multifactorial etiology, likely greater mechanical loads on the spine of heavier individuals may play a role. However, likely larger trunk muscle moment arms and intervertebral disc sizes (thus larger passive stiffness) in heavier individuals may partly or fully offset the adverse effect of their larger body weight (BW) on the spine loads. Previous musculoskeletal (MS) models have used numerical approximations to scale muscle and disc parameters with BW and have found considerably larger spine loads in obese individuals as compared to normal-weighted ones [2-3]. The present study aims to: (1) use MR images to measure physiological cross-sectional area (PCSA), anterior-posterior (AP) and medio-lateral (ML) moment arms of trunk muscles at all lumbar levels (T12-L5), mass and center of masse (CoM) of all trunk T1-L5 segments, CSAs and height of the lumbar discs (T12-L5) of ten obese (BMI>30 kg/m^2 and waist circumstance≥ 105 cm) and ten normal (20<BMI<25 kg/m^2) individuals to build a comprehensive database for biomechanical models and (2) develop a subject-specific MS model for each of the 20 individuals to quantify their spinal loads during static activities.

A 3.0 Tesla MR machine was used to obtain transverse images from the supine T1-S1 spine of 5 healthy young male obese (mean BMI≈35 kg/m^2) and 5 age-sex-height matched normal (mean BMI≈23 kg/m^2) subjects (ongoing measurements on 10 more subjects). PCSA, AP and ML moment arms of the erector spinae (ES), quadratus lumborum (QL), iliopsoas (IP), rectus abdominus (RA), and oblique abdominal muscles at all lumbar disc levels (T12-L1 through L5-S1), mass and CoM of all T1-L5 segments and CSAs of the T12-L5 discs were determined from the images. For each individual, a subject-specific T1-S1 MS model was developed based on the foregoing measured parameters. Muscle forces and L4-S1 spine loads were estimated in various loaded and unloaded static upright/flexed tasks using an optimization approach.

PCSAs of all muscles were larger in obese individuals as compared to normal ones ($p<0.05$ except for RA and IP). T12-L5 AP moment arms of abdominal muscles were larger in obese individuals ($p<0.05$) while those of their back muscles (ES, MF, and QL) were almost equal to those of normal ones ($p>0.05$). Mass of T1-L5 segments was significantly larger (by ~75% at L1-L5 levels) in obese individuals ($p<0.05$). AP moment arm of CoMs of T1-L5 segments were larger in obese individuals (up to 1.5 cm in some levels) but with no statistical significance in most segments. This was despite the fact that mean waist circumference of obese individuals was larger than that of normal subjects by ~48 cm. T12-L5 disc CSAs were larger in obese

individuals by <10% in average ($p>0.05$). For obese individuals, disc mid-heights were slightly larger at the T12-L3 ($p>0.05$) and smaller at the L3-L5 ($p>0.05$). The MS model predicted considerably larger L4-S1 compression and AP shear loads for obese individuals (Fig. 1). This was because segmental masses and anterior moment arms of CoMs were larger in obese individuals while their moment arms of back muscles and disc sizes (and thus joint passive stiffness) were almost identical to those of normal subjects. For two subjects with identical BW and height muscle parameters and thus spinal loads could be different.

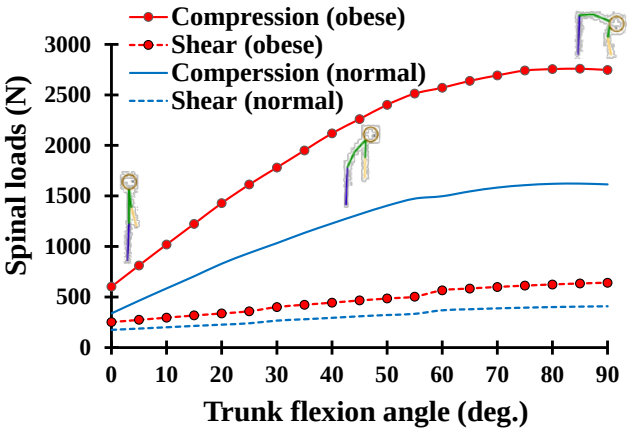

Fig. 1: Mean L5-S1 compression and shear loads in upright and forward flexed postures (without hand load) for obese and normal subjects (results for L4-L5 loads and for tasks with hand load are not depicted).

[1] Shiri et al 2010. Am J Epidemiology 171: 135-154.

[2] Hajihosseinali et al., 2015. J Biomechanics 48: 276-282.

[3] Ghezelbash et al., 2016. J Biomechanics 49: 3492-3501.

Acknowledgements: INSF and Sharif University of Technology (Iran, Tehran).

Vertebral Loading Predictions are Influenced by Incorporation of CT-based Measurements of Trunk Anatomy into Subject-Specific Musculoskeletal Models of the Thoracolumbar Spine

Mokhtarzadeh H[a,b], Bruno AG[c], Allaire BT[b], Velie KR[b], De Paolis Kaluza M[b], Anderson DE[a,b], Bouxsein ML[a,b]

[a]*Department of Orthopedic Surgery, Harvard Medical School, MA, USA*
[b]*Center for Advanced Orthopaedic Studies, Beth Israel Deaconess Medical Center, MA, USA*
[c]*Harvard-MIT Division of Health Sciences and Technology, MA, USA*

Musculoskeletal modeling studies of the spine usually utilize generic models which do not incorporate subject-specific variations in musculoskeletal anatomy, such as spinal curvature and muscle morphology. To determine the degree to which vertebral compressive loading estimates are sensitive to variations in trunk anatomy, we created subject-specific musculoskeletal models by incorporating spine curvature and muscle morphology measurements from 3D computed tomography (CT) scans. We hypothesized that vertebral loading estimates derived from spine musculoskeletal models that incorporate subject-specific anatomy would differ from those derived from models that are simply adjusted for subject height and weight.

We measured spine curvature and trunk muscle morphology from T6-L5 using spine CT scans of 125 men (64.7±14.0yrs, 174.0±7.2cm, 85.4±14.3kg) from the Framingham Heart Study CT cohort. We scaled our previously developed thoracolumbar spine model [1] to subject-specific height and weight for each person (Ht/Wt models), and further incorporated subject-specific spine curvature and trunk morphology to generate three additional models for each person: 1) spine curvature adjusted (+C); 2) muscle morphology adjusted (+M); and 3) spine curvature, and muscle morphology adjusted (+CM). We estimated vertebral compressive loading at T8, T12 and L3 for four different activities using OpenSim, and employed repeated measures analysis of variance to compare vertebral loading estimates from the three curvature and/or muscle adjusted models to those from Ht/Wt models.

The influence of subject-specific morphology on vertebral loading varied by activity and spinal level ($p<0.05$ Fig. 1). The compressive loads predicted with subject-specific musculoskeletal adjustments were between 54% lower to 45% higher than those estimated using Ht/Wt models. Vertebral load estimates were more sensitive to inclusion of subject-specific spine curvature than to trunk muscle morphology ($p<0.05$). Incorporation of subject-specific morphology had a greater influence on vertebral loading predictions for trunk flexion with weights than the other activities ($p<0.05$).

Musculoskeletal models of the spine that incorporate subject-specific trunk anatomy can predict substantially different vertebral compressive loads than musculoskeletal models that do not, indicating that individual variation in spine curvature and trunk muscle morphology has an important effect on *in vivo* spine

loading predictions. A major novelty of this study was using clinical CT-scans to make highly reliable measurements of spine curvature and muscle morphology and then employing automated algorithms to incorporate these measures into a validated musculoskeletal model of the thoracolumbar spine. Our findings indicate that subject-specific spine models that account for individual variations in trunk anatomy may be helpful to improve understanding of spine loading in individuals, with implications for spine injury, back pain, and rehabilitation.

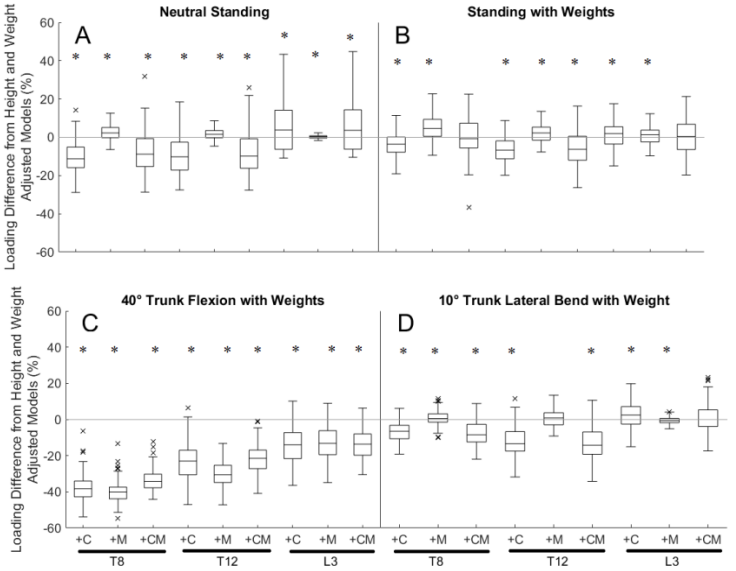

Fig. 1: Differences in vertebral compressive loading between models adjusted for height and weight only (Ht/Wt), and those adjusted for subject-specific trunk morphology measurements. A) neutral standing, B) standing while holding a weight (elbows flexed 90° with 10 kg in each hand), C) 40° trunk flexion while holding 5 kg in each hand, and D) 10° trunk lateral bending to the right, with 5 kg in the right hand. Subject specific models include those adjusted for: 1) height, weight and spine curvature (+C), 2) height, weight, and muscle morphology (+M), and 3) height, weight, spine curvature, and muscle morphology (+CM). Loading differences are reported as percent difference from the Ht/Wt-adjusted models. In the box plot, the central line indicates the median, and the top and bottom edges of the box shows the 25th and 75th percentiles, respectively. The whisker lines represent 95% confidence interval. The outliers are indicated by an 'x' symbol. *p<0.05 vs Ht/Wt-adjusted model.

Bruno et al, J Biomech Eng, 2015; 137(8): 081003.

Acknowledgements: This work was supported by grants from the National Institutes of Health (R01AR053986, F31AG041629, and K99AG042458), by the National Heart, Lung, and Blood Institute (NHLBI) Framingham Heart Study (NIH/NHLBI Contract N01-HC-25195), and by the National Space Biomedical Research Institute through NASA NCC 9-58. The contents are solely the responsibility of the authors, and do not necessarily represent the views of the NIH.

EPIONICS
Monitoring

Form and Function Measurement of the Back

- Dynamic
- Objective
- Lightweight
- High resolution
- Suitable for seated measurements
- Suitable for sporting activity
- Maximum measurement time 24h
- Certified as medical device

Contact:
Epionics Medical GmbH
Phone: +49 331 2373 05 - 21
Email: info@epionics.com
Web: www.epionics.com

Spinal Loads and Trunk Muscles Forces During Level Walking - A Combined *In Vivo* and *In Silico* Study on Six Subjects

Arshad R[a], Angelini L[a,b], Zander T[a], Di Puccio F[b], El-Rich M[c], Schmidt H[a]

[a]*Julius Wolff Institute, Charité – Universitätsmedizin Berlin, Berlin, Germany*
[b]*Department of Civil and Industrial Engineering, University of Pisa, Italy*
[c]*Department of Civil and Environmental Engineering, University of Alberta, Canada*

During level walking the lumbar spine is subjected to 3D cyclic movements leading to an intricate loading of the intervertebral discs and trunk musculature. The normal gait kinematics and kinetics must be well understood to make proper diagnosis of musculoskeletal diseases and to devise viable treatment options. Therefore, this study aimed to estimate spinal loads and trunk muscles forces during level walking.

Six male participants, aged between 24 and 33 years, were requested to walk barefoot on a walkway at 4-5 km/hr. The 3D kinematics and ground reaction forces were recorded using 3D motion capturing system and two force plates. Data were subsequently implemented into a musculoskeletal inverse dynamic model to predict spinal loads and trunk muscles forces. Additionally, the sensitivity of the intra-abdominal pressure (IAP) and lumbar segment rotational stiffness (SRS) was investigated.

Predicted peak spinal loads and trunk muscle forces mostly occurred in between the gait instances of heel strike and toe off. Sensitivity analysis showed that in L4–L5 disc the average peak compressive, anterior-posterior and medio-lateral shear forces were in between 130 to 174%, 2 to 15% and 1 to 7%, with maximum standard deviation (±STD) of 40%, 6% and 3% of the body weight (BW) among six subjects. The average peak global muscles forces were 24 to 55% (longissimus pars thoracic), 11 to 23% (iliocostalis pars thoracic), 12 to 16% (external oblique), 17 to 25% (internal oblique) and 0 to 8% (rectus abdominus) with max. ±STD of 10%, 4%, 8%, 13% and 6% of BW. Also, the average peak local muscles forces were 11 to 19 % (longissimus pars lumborum), 14 to 31% (iliocostalis pars lumborum) and 12 to 17%. (multifidus), with max. ±STD of 8%, 6% and 4% of the BW.

Predicted spinal loads and trunk muscles forces in subjects without low back pain were phasic and well-coordinated. However, large inter-individual differences were found in peak compressive spinal loads and trunk muscles forces whereas the sensitivity analysis also showed the significant variation due to IAP and SRS.

Subject-Specific Validation of a Trunk Musculoskeletal Model in Maximum Voluntary Exertions

Ghezelbash F[a], El Ouaaid Z[b], Shirazi-Adl A[a], Plamondon A[b], Arjmand N[c]

[a]*Department of Mechanical Engineering, Ecole Polytechnique, Montréal, Canada*
[b]*Institut de recherche Robert Sauvé en santé et en sécurité du travail, Montréal, Canada*
[c]*Department of Mechanical Engineering, Sharif University of Technology, Tehran, Iran*

Maximum voluntary exertion (MVE) tasks aim to quantify individual's trunk (and muscle) strength in various planes with both clinical and biomechanical applications (e.g., injury prevention, functional diagnosis, rehabilitation). Simulation of MVE tasks in musculoskeletal (MS) models and comparison of estimated strength and muscle activities with measurements are also appropriate means to verify relative validity of MS models as well as their neuromuscular algorithms for muscle force estimation and personalization (or scaling) scheme. This appears as a more suitable and sensitive approach compared to the validation against very limited and invasive in vivo intradiscal pressure measurements. In the current study, we aim to carry out isometric MVE experiments in flexion, extension, axial and lateral directions on asymptomatic male and female subjects while recording EMGs of superficial muscles. We subsequently simulate the tasks for each subject separately to validate our subject-specific MS model [1].

Experiments: With approval from our review board and consent from participants, healthy subjects (9 females: height=163.4±3.7 cm, weight=61±4.5 kg, age=24.1±4.3 years and 10 males: height=174.6±4.2 cm, weight=72.2±8.7 kg, age=30.6±6.5 years) performed two trials of flexion, extension, axial and lateral isometric MVEs (lasting ~8 s each) in a dynamometer at a semi-seated posture. Dynamometer signals (3 forces and 3 moments) and EMG of 14 superficial muscles (longissimus, iliocostalis pars thorasis and pars lumbarum, multifidus, external oblique, internal oblique and rectus abdominis) were recorded at 128 Hz and 1024 Hz, respectively. The effects of noises and artifacts were reduced by using a band-pass filter (30 and 450 Hz), and subsequently, EMG signals were normalized to their recorded maximum root mean squared values.

MS modeling: We applied moments via forces directly to the thorax and adjusted the posture to simulate the semi-seated positions [1, 2]. Muscle forces were computed through a kinematics-driven optimization algorithm and then compared with measured EMG signals.

Statistical analysis: Analysis of variance was used to compare moments and muscle activities between females and males.

Female (male) participants generated 181±47 Nm (218±49 Nm) in extension, 121±13 Nm (130±33 Nm) in flexion, 122±17 Nm (143±24 Nm) in right lateral, 122±17 Nm (163±25 Nm) in left lateral, 61±13 Nm (93±24 Nm) in right axial and 73±12 Nm (97±19 Nm) in left axial directions. Males exerted greater moments, with significant differences in the left lateral ($p = 0.0014$), right ($p = 0.0382$), left axial ($p = 0.005$) and right axial ($p = 0.0029$). The MS model predicted large spinal

loads reaching ~5500 N in compression and ~2100 N in shear. With the models individualized with each subject's personal parameters, and with a satisfactory agreement between estimated muscle activities (taking a 10 Nm antagonistic moment) and measured EMGs (Fig. 1) while simulating MVEs, the relative validity and accuracy of the scaling (personalization) and muscle force estimation algorithms are confirmed.

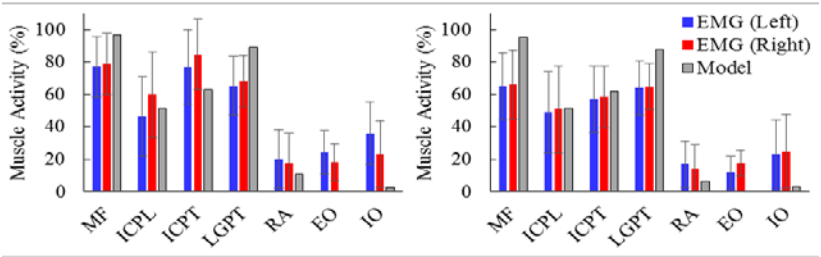

Fig. 1: Normalized EMG signals and estimated muscle activities of female (left) and male (right) subjects in MVE in extension. MF: Multifidus; ICPL: Iliocostalis pars labarum; ICPT: Iliocostalis pars thoracis; LGPT: Longissimus pars thoracis; RA: Rectus abdominis; EO: External oblique; IO: Internal oblique.

[1] Ghezelbash et al. (2016) BMMB 15:1699-1712.

[2] El Ouaaid et al. (2013) J Biomech 46:2228-35.

Acknowledgement: IRSST & FQRNT-Quebec

Estimation of In Vivo Inter-Vertebral Loading During Motion Using Fluoroscopic and Magnetic Resonance Image Informed Finite Element Models

Zanjani-pour S[a], Meakin J[a], Breen Alex[b], Breen Alan[c]

[a]*University of Exeter, UK*
[b]*Anglo-European College of Chiropractic, UK*
[c]*Bournemouth University, UK*

Determining the loads on the spine in vivo is challenging but essential to understand normal spinal biomechanics and to assess patients with functional impairments. Image driven finite element (FE) models allow measurements of vertebral displacement in vivo to be applied to a finite element model to predict the disc stresses. The aim of this study was to combine magnetic resonance (MR) imaging and quantitative fluoroscopy (QF) in a participant-specific finite element (FE) model to predict spinal loading in upright, flexed and extended postures.

Images of the lumbar spine were acquired from healthy participants in the supine posture using a 0.5 T open bore MR scanner (Paramed Srl., Italy). A volumetric scanning sequence provided images with voxels of dimension 0.98 x 0.98 x 1.1 mm (Figure 1c). Participant-specific 3D FE models of the spine from L3 to L5 (Figure 1d) were created from the MR data using ScanIP and FE+ (Simpleware Ltd., UK), and Abaqus (Dassault Systèmes Simulia Corp.). The models comprised vertebrae, nucleus and annulus and a softened contact interaction between the facet joints. QF data was acquired from the same participants who performed trunk flexion from upright standing (Figure 1a) to 60^{o} (Figure 1b) and trunk extension to 20^{o}. The location and orientation of the vertebral bodies was defined by their corners and tracked during motion. The displacements and rotations required to map the position of the vertebra in the MR images to that in the fluoroscopy images were calculated and applied to the FE model. The resulting stresses in the centre of the nucleus were determined.

Results from seven participants gave a compressive stress (perpendicular to the disc mid-plane, averaged for L3L4 and L4L5) of 0.49 ± 0.39 MPa (mean ± standard deviation) in upright standing and 1.35 ± 0.68 MPa in 60^{o} flexion, and 0.84 ± 0.26 MPa in 20^{o} extension. Disc stress was predicted to increase with changes in disc wedging and orientation (angle with respect to the vertical); a significant correlation (Pearson's $R = 0.87$, $p = 0.01$) was found between compressive stress and disc orientation at 60^{o} flexion.

The results demonstrate that MR and QF data can be combined in a participant-specific FE model to investigate spinal loading. Predicted stresses were within expected ranges reported in the literature and demonstrate the relationships between motion parameters and disc stresses in vivo.

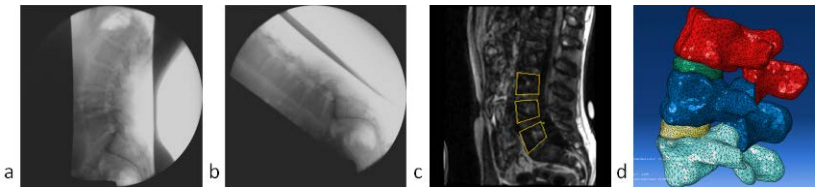

Fig. 1: QF image in (a) standing and (b) 60o flexion. (c) MR image and (d) 3D FE model.

Sensitivity of Intervertebral Joint Forces to Center of Rotation Location and Trends along its Migration Path

Senteler M[a,b,c], Aiyangar A[c], Weisse B[c], Farshad M[a], Snedeker JG[a,b]

[a]*Department of Orthopaedics, Balgrist Hospital, University of Zurich, Switzerland*
[b]*Institute for Biomechanics, ETH Zürich, Switzerland*
[c]*Empa, Swiss Federal Laboratories for Materials Science and Technology, Dübendorf, Switzerland*

Presence of translational vertebral motion during functional tasks manifests itself in dynamic loci for center of rotation (COR). A shift of COR affects moment arms of muscles and ligaments; consequently, muscle and joint forces may be altered. Based on published posture- and level-specific trends of COR migration, we hypothesized the following: (1) In flexion, an anteriorly located COR results in the lowest magnitude joint reaction force, while in an upright position, it occurs at a posteriorly located COR, and (2) lower lumbar levels benefit from a more superiorly located COR compared to the upper segments.

A recently improved and validated OpenSim®-based rigid body musculoskeletal model of the upper body (from head to femur) was employed to test the above hypotheses. The COR in the model was varied up to ±6 mm in steps of 2 mm in posterior-anterior and inferior-superior direction, resulting in a total of 49 (7x7) configurations (Fig. 1).

Torso extension movement from 45° forward flexion to upright standing was simulated for each configuration. Joint reaction forces (resolved into compressive and shear components) were computed at levels L2L3 to L5S1. Note that, for each simulation, the COR remained fixed at the prescribed grid location.

An anterior COR (+6 mm) in the upright position increased compression forces at all levels by 66 N (+15 %) on average as compared to the most posterior COR location (-6 mm). At levels L3 to S1 shear forces also increased by +33 N (+31 %) on average. In contrast, in 30° flexion, more anterior CORs (+6 mm vs. -6 mm) decreased compression and shear forces at all levels on average by -250 N (-26 %) and -60 N (-25 %), respectively. Compression force gradients (change in force per mm shift in COR location) in superior direction differed substantially between upper and lower levels, particularly in forward flexed postures (30°, 45°): A superior COR location at L4L5 and L5S1 reduced the resulting compression forces almost twice as much (-182 N or -16 %) than at upper levels (-96 N or -9 %) for the same amount of COR displacement. Results clearly confirmed the first hypothesis and provided evidence for the validity of the second hypothesis. Therefore they offer a biomechanical explanation for the migration paths of CORs observed during functional flexion/extension movement. Reported sensitivity of shear and compression forces to COR location furthermore fill a gap in the current literature and provide a possible explanation for the biomechanical implications of COR migration. Findings are considered relevant for the interpretation of COR migration data, the development of numerical models, and could have an implication on clinical diagnosis and treatment or the development of spinal implants.

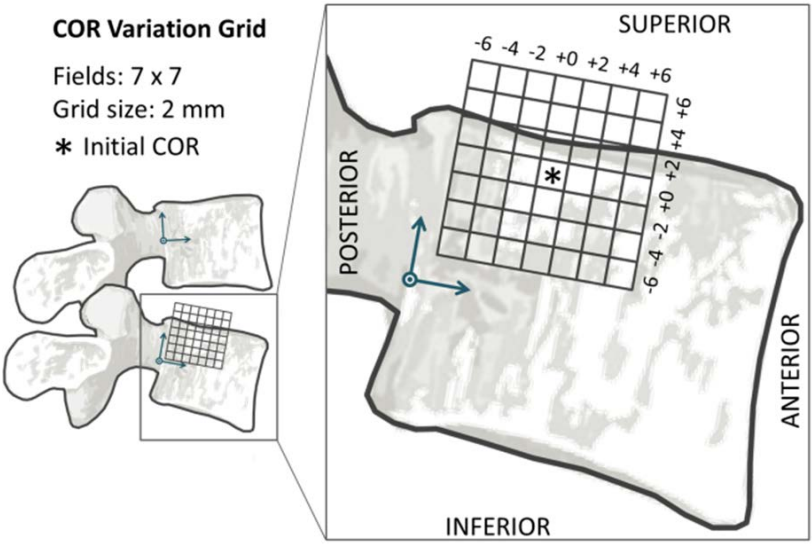

Fig. 1: Motion segment with COR variation grid projected on right sagittal section view.

Effects of Joint Positioning and Stiffness on Spinal Loads and Kinematics in Trunk Musculoskeletal Models

Ghezelbash F[a], Eskandari AH[b], Shirazi-Adl A[a], Arjmand N[b], El Ouaaid Z[c], Plamondon A[c]

[a]*Department of Mechanical Engineering, Ecole Polytechnique, Montréal, Canada*
[b]*Department of Mechanical Engineering, Sharif University of Technology, Tehran, Iran*
[c]*Institut de recherche Robert Sauvé en santé et en sécurité du travail, Montréal, Canada*

In musculoskeletal (MS) model studies, the moment equilibrium equations are commonly enforced at the origin of the joint coordinate system placed often at the joint geometrical center or center of rotation. It is also assumed that this point coincides with the joint center of reaction where the passive joint reaction moments disappear. The estimated muscle forces and internal joint loads are hence markedly dependent on the positioning of this origin of coordinate system and changes therein as demonstrated by earlier investigations [1]. Trunk MS studies routinely model spinal motion segments at different levels by spherical joints with/without rotational springs or by beam elements with linear/nonlinear properties. We aim to investigate the role of positioning and representation of motion segments when predicting trunk muscle forces, kinematics and spinal loads.

We initially compared displacements- and rotation-moment responses and instantaneous center of rotation (ICoR) of a detailed passive lumbar spine finite element (FE) model [2] with those of the simplified models (using either beams or spherical joints with equivalent moment-rotation springs) under 20 Nm flexion moment and 2.7 kN follower compression load. Then, using a validated nonlinear subject-specific FE MS model of the trunk [3], shear deformable beam elements and spherical joints with/without equivalent rotational springs (representing entire motion segments) are shifted in the anterior-posterior direction from the reference point located at the joint geometrical center (i.e., offset=0 mm) and muscle forces as well as spinal kinematics/loads are computed. Spinal loads at the L4-L5 are subsequently compared versus reported in vivo intradiscal pressures (IDPs) [4].

The beam model with the offset at -2 to 4 mm (+: posterior) demonstrated satisfactory performance in predicting kinematics of the detailed FE model whereas the spherical joint model with springs showed deviations in cranial-caudal translation (~33% for the 0 mm offset) and ICoR estimations (~5% for the 0 mm offset) due to overlooking shear and axial compliances. Neglecting passive responses of the ligamentous spine (in spherical joints without springs) increased spinal loads by ~52% in compression and 74% in shear. Offsetting discs (beams or spherical joints) posteriorly yielded larger local spinal loads (~11% in compression and ~15% in shear for +4 mm offset in the beam model), Fig. 1. Shifting joints (except in the spherical joint without equivalent springs) in the range of -2 to +4 mm generated IDP in satisfactory agreement with in vivo measurements [4]. Although neglecting translational degrees of freedom and compression-induced stiffening may be acceptable in smaller flexion angles and lighter tasks, the effects

on spinal loads in larger flexions and more demanding tasks are substantial. In contrast, passive moment-carrying capacity of joints should not be overlooked even in smaller flexion angles.

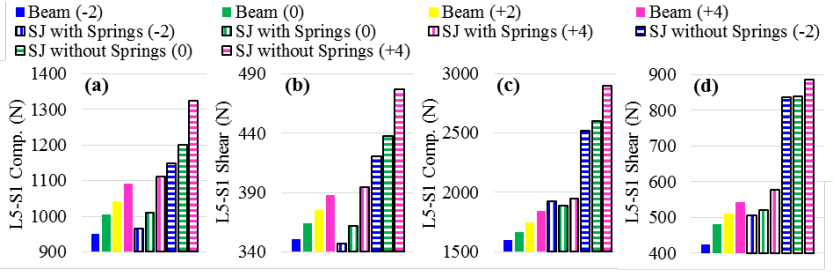

Fig. 1: L5-S1 compression (a,c) and shear (b,d) forces for different joint offsets (to the reference position) at 20o (a,b) and 80o (c,d) trunk flexion. Values in brackets denote joint offset to the joint reference center (in mm). SJ: spherical joint.

[1] Ghezelbash et al. (2015) CMBBE 18: 1760-67.

[2] Shirazi-Adl (1994) Spine 19:2407-14.

[3] Ghezelbash et al. (2016) BMMB 1-14.

[4] Wilke et al. (2001) Clin Biomech 16:S111-26.

Acknowledgements: IRSST & FQRNT-Quebec

A Combined Passive and Active Musculoskeletal Model Study to Estimate L4-L5 Load Sharing

Azari F[a], Arjmand N[a], Shirazi-Adl A[b], Rahimi-Moghaddam T[a]

[a]*Department of Mechanical Engineering, Sharif University of Technology, Tehran, Iran*
[b]*Division of Applied Mechanics, Department of Mechanical Engineering, Ecole Polytechnique, Montréal, Canada*

Musculoskeletal (MS) models of the spine are routinely used to estimate muscle forces and spinal loads (compression/shear forces) during *in vivo* activities. In accordance with their objectives, a detailed architecture for the trunk muscles but very simplified models for the complex intervertebral joints (e.g., pivots or beams) are considered. They overlook, hence, the detailed load sharing among joint structures (discs, facets, and ligaments). On the contrary, passive finite element (PFE) models incorporate detailed geometry of the intervertebral joints thus allowing estimation of joint load sharing. They are, however, devoid of muscles and as such should be analyzed under assumed external loads and/or displacements. The present study aims to prescribe muscle forces predicted by a MS model of the spine [1] during 12 static activities into a matched (geometry and passive property) PFE model of the L4-L5 segment to estimate joint load sharing (intradiscal pressure (IDP), facet joint forces (FJFs), and ligament forces).

A previously validated MS model [1] was used to estimate trunk muscle forces in 12 static tasks in upright/flexed postures. Forces estimated in all trunk muscles with proximal insertions at or above the L4 vertebra along with gravity loads (head, arms, and trunk) were considered in the PFE model. The L4 and L5 vertebrae were rigidly rotated in the PFE model (developed and validated here) so that their orientations matched those in the MS model (initially determined from video-camera motion analysis) for the task under consideration. The foregoing resultant forces from the MS model were then applied to the center of the L4 vertebral body in the PFE model to estimate *in vivo* load sharing among the joint structures. Finally, the equivalent compression follower load was estimated in PFE model for each task simulated in a manner to yield identical IDP value as those obtained under muscle forces (analyses are currently underway).

The moment-rotation behaviour of the PFE model and that of the L4-L5 motion segment of the MS model were similar (e.g., *RMSE* < 0.25° in flexion/extension moments from 0 to 10 Nm). The predicted and measured [2] L4-L5 IDPs under *in vivo* tasks were in agreement (R^2 = 0.98 and *RMSE* = 0.18 MPa) (Fig 1). The body weight/height (68.4 kg/174.5 cm) considered in the MS model were similar to those of the male subject (70 kg and 168 cm) that participated in the IDP measurement study. Such comparisons should however be performed qualitatively as disc cross-sectional area was quite different between the subject of *in vivo* measurement study (~1800 mm^2) and that of the PFE model (~1200 mm^2). Compared to the upright posture, forces in posterior ligaments increased with trunk forward flexion angle but decreased in symmetric and asymmetric tasks

under hand load. FJFs were small in the neutral upright standing (~6% of the subject's body weight in the MS model) and flexed tasks but considerably increased under symmetric holding of loads. FJFs increased also with the trunk or load asymmetry as. In clinical applications and design of implants, considering *in vivo* loading conditions in PFE models under simulated muscle exertions is essential.

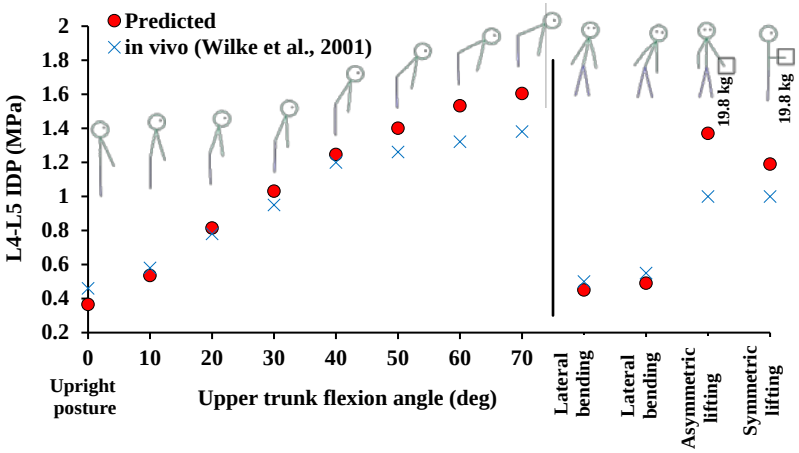

Fig. 1: Predicted (by the PFE model) versus measured IDP for 12 tasks.

[1] Arjmand et al., 2010. J of Biomechanics 43: 485-91.
[2] Wilke et al., 2001. Clinical Biomechanics 16: S111-26.

Acknowledgements: Sharif University of Techology (Iran, Tehran).

Effects of Hand-Held Loads at Various Orientations, Heights and Magnitudes on Spine Biomechanics in Upright Posture

El Ouaaid Z[a], Shirazi-Adl A[b], Plamondon A[a]

[a]*Institut de recherche Robert Sauvé en santé et en sécurité du travail, Montréal, Canada*
[b]*Department of Mechanical Engineering, Ecole Polytechnique, Montréal, Canada*

Substantial changes occur in spinal compression/shear forces and trunk stability as the external load elevation and orientation alter while pulling/pushing carts and objects where loads remain no more in the gravity direction [1, 2]. As a consequence of marked alterations in spinal loads, the risk of back injury and pain could potentially increase. The objective of this work is to estimate compression/shear forces on the spine (L5-S1 level), trunk muscle forces and trunk stability for symmetric tasks in the upright standing under different static hand-held load magnitudes, elevations and orientations covering all pull and push configurations.

An iterative kinematics-driven finite element model with nonlinear ligamentous proprieties and trunk musculature [2, 3] was used to simulate the pull/push tasks of one of 12 participants (body height 181.5 cm and body weight 68.3 kg) in a previous study [3]. Trunk muscle forces, spinal loads at the L5-S1 as well as stability margin were calculated in the upright standing under measured trunk rotations, body weight and three external forces (80, 120 and 160 N in both hands) acting in the sagittal plane at 4 elevations (0, 20, 40 and 60 cm to the L5-S1) and 24 different orientations (0^o to 360^o) covering all push and pull possibilities. Coactivity moments (5 and 10 Nm) to generate activity in antagonistic muscles and intra-abdominal pressure (<12 kPa) were also considered in some cases.

At all elevations and under identical posture and external load magnitude, predicted trunk muscle forces, spinal loads and stability margin were markedly influenced by the force orientation (Fig. 1). In all force orientations and elevations, as expected, an increase in the load magnitude and/or coactivity moment increased spine loads and muscle forces. With changes in force orientation, the spinal forces reached their maximum under inclined downward pulls (0^o to 90^o, Fig.1A). In contrast, minimal spinal forces were found, in general, under upward pulls or horizontal/inclined upward pushes (180^o to 270^o, Fig. 1A). At lifting (90º), global extensor muscles were more active than lumbar and abdominal muscles while in pulls, local lumbar muscles were the most active. In agreement with previous studies [1, 4], compression forces at the L5-S1 are generally larger during pulling ($0\text{-}90^o$) versus pushing ($180\text{-}270^o$). Under identical load magnitude and orientation, spinal and muscle forces were altered as load elevation increased from 0 to 60 cm with respect to L5-S1.At all elevations, the maximum spinal load was observed in inclined downward pulls ($\sim 60^o$). No effect of elevation was noted at upward and downward pulls (90^o and 270^o). Under identical upright standing posture and load magnitude/elevations, the trunk stability margin significantly increased when the external force pulled upward (270º to 360º, Fig. 1B) and

reached its maximum at 315º. The minimum stability margin was found in lifting (90°) and downward push orientations. In conclusion, minimum spinal forces are computed at all elevations under loads in the upward pull and upward/downward push directions. Trunk stability is maximum under horizontal to upward pulling force directions.

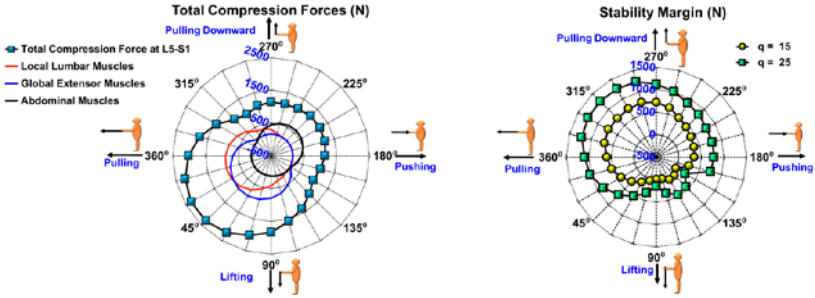

Fig. 1: Effect of hand-held load orientation on compression force at the L5-S1 (muscle contributions are also shown separately) and trunk stability at 2 different muscle stiffness coefficients q (External force F=120 N held at 40 cm elevation with 5 Nm antagonistic moment).

[1] Hoozemans et al. (2004) Ergonomics, 47, 1–18.

[2] El Ouaaid et al. (2013) Comp Meth Biomech Biomed Eng. 16, 54-65.

[3] El Ouaaid et al. (2014) J Biomech 47, 3035-3042.

[4] Knapik and Marras (2009) Ergonomics.

Acknowledgements: IRSST (Quebec)

Thoracolumbar Spine Loading During Activities of Daily Living Performed by the Young and the Elderly

Ignasiak D[a], Rüeger A[b], Sperr R[a], Ferguson SJ[a]

[a]*Institute for Biomechanics, ETH Zurich, Zurich, Switzerland*
[b]*Schulthess Clinic, Zurich, Switzerland*

Excessive mechanical loading of the spine is a critical factor in vertebral fracture initiation. Most vertebral fractures develop spontaneously or due to mild trauma [1], as physiological loads during activities of daily living might exceed the failure load of osteoporotic vertebra [2]. Spinal loading patterns are affected by vertebral kinematics [3], which differ between elderly and young individuals [4]. In this study, the effects of age-related changes in spine kinematics on thoracolumbar segmental loading during dynamic activities of daily living were investigated using combined experimental and modeling approach.

Forty-four healthy volunteers were recruited into two age groups: young (N=23, age=27.1±3.8) and elderly (N=21, age=70.1±3.9). The spinal curvature was assessed with a skin-surface device and the kinematics of the spine and lower extremities were recorded during daily living tasks (flexion-extension and stand-sit-stand) with a motion capture system. The obtained data provided input for a previously developed and validated musculoskeletal model of the fully articulated thoracolumbar spine [5], which was used stand-alone or incorporated in a full-body model of a seated human [6]. Inverse dynamics simulations were performed in the AnyBody Modeling System (Fig. 1) to estimate corresponding spinal loads.

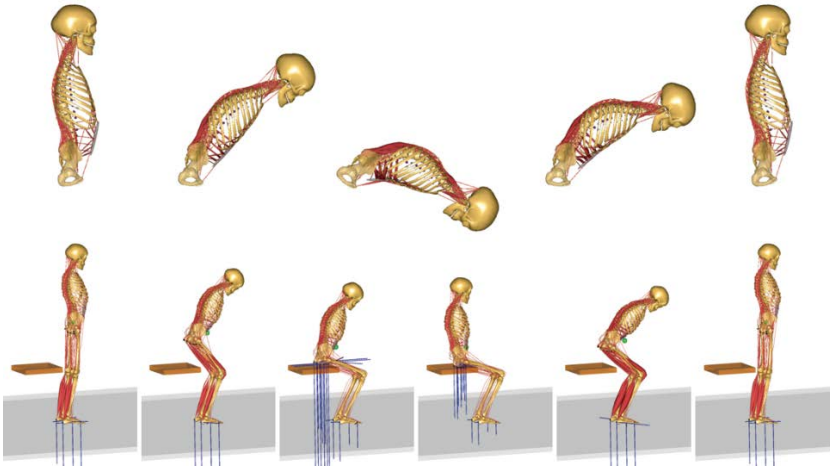

Fig. 1: Illustration of the simulated tasks: full range flexion-extension and stand-sit-stand transitions.

The maximum compressive loads predicted for the elderly motion patterns were lower than those of the young for T4T5 and most lumbar levels during flexion and for upper thoracic levels during stand-to-sit (T1T2-T7T8) and sit-to-stand (T1T2-T6T7). However, the maximum loads predicted for the lower thoracic levels (T8T9-T12L1), a common site of vertebral fractures, were similar compared to the young. Nevertheless, these loads acting on the vertebrae of compromised bone quality might contribute to a higher fracture risk for the elderly.

[1] Cooper et al., JBMR 7(2), 1992.

[2] Myers & Wilson, Spine 22(S), 1997.

[3] Davis & Marras, Clin Biomech 15, 2000.

[4] Ignasiak et al., ESB, Prague, Czech Republic, 2015.

[5] Ignasiak et al., J Biomech 49(6), 2016.

[6] Rasmussen et al., Int J Ind Ergonom 39(1), 2009.

Effect of Arm Swinging on Lumbar Spine and Hip Joint Forces

Angelini L[a,b], Damm P[a], Zander T[a], Arshad R[a], Di Puccio F[b], Schmidt H[a]

[a]*Julius Wolff Institut, Charité – Universitätsmedizin Berlin, Germany*
[b]*Department of Civil and Industrial Engineering, University of Pisa, Italy*

During level walking, arm swing plays a key role in improving dynamic body stability. *In vivo* investigations with a telemeterized vertebral body replacement showed that spinal loads can be affected by differences in arm positions during sitting and standing [1, 2]. However, little is known about how arm motion and consequently thorax rotation could influence the lumbar spine and hip joint forces and motions during walking. The present study aims therefore to provide a better understanding of the contribution of the upper limbs to human gait, investigating ranges of motion (ROM) and joint reaction forces (JRFs).

Forty-seven reflective markers were placed on six healthy males (age 29±3 years). A three-dimensional motion analysis was carried out via a Vicon Motion Capturing System with ten cameras, operating at 150 Hz. Two AMTI force plates recorded in synchrony the ground reaction forces (GRFs) at a frame rate of 900 Hz. Each subject performed five gait tasks, including walking with a small, normal, and large arm swing (SAM, NAM, LAM), walking with arms bound to the body (BAM) and walking with arms folded across the chest (CAM). Each task was repeated six times. The filtered motion data were imported into the Anybody Modelling System v. 6 for the kinematic and inverse dynamics investigation. All statistical analyses were performed using R Software. For validation of the model, three subjects with hip instrumented implants were measured.

Thorax ROM was significantly associated with arm position during gait in the transversal plane. Post-hoc pairwise multiple comparison tests demonstrated significant differences ($p<0.001$) between walking with a normal or large arm motion (NAM, LAM) and walking with a suppressed or small arm swing (CAM, BAM, SAM). No significant differences in sagittal and frontal ROM were found. Hip abduction and adduction ROM varied significantly both for dominant and non-dominant leg. The median ROM was about 20% higher during LAM than during BAM, CAM and SAM. Only for non-dominant limb, we found a statistical difference in hip external and internal rotation ROM when we compared LAM to NAM, BAM, CAM and SAM. Predicted peak spinal loads (figure) in L5-S1 and T12-L1 showed significant differences between SAM and CAM and between SAM and LAM. Changes in arm swing patterns and amplitude did not significantly affect hip joint reaction forces (Fig. 1).

Therefore, although arm swing has a relevant effect in kinematics, spinal and hip loads are not strongly influenced by changes in arm motion and position during walking.

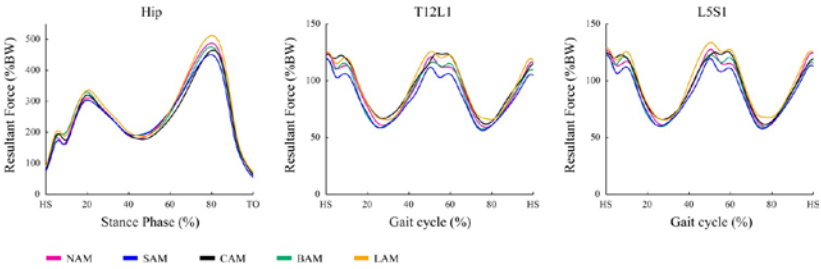

Fig. 1: Averaged reaction forces at hip joint, upper lumbar spine (T12L1) and lower lumbar spine (L5S1).

[1] Zander T, Dreischarf M, Schmidt H, Bergmann G, Rohlmann A, Spinal loads as influenced by external loads: A combined in vivo and in silico investigation, *Journal of biomechanics*, *48(4)*, 2015, 578-84

[2] Dreischarf M, Bergmann G, Wilke HJ, Rohlmann A, Different arm positions and the shape of the thoracic spine can explain contradictory results in the literature about spinal loads for sitting and standing, *Spine (Phila Pa 1976), 35(22),* 2010, 2015-21.

Functional In Vitro Testing of Pedicle Screw Anchorage

Schmoelz W, Keiler A, Heinrichs C

Medical University of Innsbruck, Dept. of Trauma Surgery, Innsbruck, Austria

For in vitro comparisons of various pedicle screw designs or augmentation techniques axial pullout tests are frequently used and published by some authors. Pullout tests are relatively easy and quick to perform. However, their clinical relevance is limited because in vivo investigations with instrumented implants pointed out that pedicle screws are mainly loaded in cranio-caudal direction with a superimposed bending moment and only with a very small component of axial pullout force. Therefore, a test setup applying an increasing cyclic load in cranio-caudal direction superimposed with a small bending moment was developed. In the course of several experiments the load protocol was refined to investigate pedicle screw anchorage with varying augmentation techniques and materials in vertebral bodies with reduced bone quality. The failure load magnitudes of the non-augmented and augmented pedicle screws were compared to in vivo measurements of an internal fixator instrumented with telemetric load sensors.

Several in vitro experiments to investigate pedicle screw loosening have been conducted. The design of all experiments was a left right pedicle screw comparison of different augmentation techniques and materials to improve screw anchorage. Overall a total of 128 pedicle screws implanted in 64 vertebral bodies were cyclically loaded until failure in a servohydraulic material testing machine. The vertebral body was fixed on an x-y bearing table to allow motion in one plane and the loading was applied with a lever arm of 15mm to the screw head and free rotation. The relative motion of the pedicle screw in the vertebral body was recorded with a motion analysis system attached to the screw head and the fixation of the vertebral body. In initial experiments the load was applied in force control with a continuously increasing load magnitude in compression. Further experiments were conducted in displacement controlled load application with stepwise increasing force limits in compression and a constant force limit in tension.

In vertebral bodies pedicle screws implanted in a standard non augmented technique (n=51) showed a mean failure load around 230N with some screws implanted in vertebrae with reduced bone quality loosening already at 140N. Pedicle screws augmented with different techniques and cements (n=77) all reached a mean failure load above 400N in all techniques with some screws implanted in vertebrae with reduced bone quality becoming loose at 250N.

For non-augmented screws the main failure mode was a cut out of the screw through the cranial endplate. Both, the force and displacement controlled load application showed comparable failure loads for augmented and non-augmented pedicle screws. However, in the force controlled loading the load application rate increased with increasing screw motion, while the displacement controlled load had a constant loading rate and allowed to evaluate the loosening mechanism due

to loading in compression and tension. Comparing the failure loads with in vivio measurements with an internal fixator showed, that reported peak forces for everyday activities (200-250N) can be higher than the failure loads found for non-augmented screws, while with all augmentation techniques and materials the failure loads for pedicle screws was higher than reported loads during everyday activities.

An Under-Sized Pedicle Screw Reaches a Similar Biomechanical Performance as an Over-Sized Screw after Fatigue Loading – an In-Vitro Human Cadaveric Study

Wang JL[a], Shih YT[a], Chen YH[b], Lai DM[b], Chien A[c]

[a]*Institute of Biomedical Engineering, National Taiwan University, Taipei, Taiwan*
[b]*Department of Surgery, National Taiwan University Hospital, Taipei, Taiwan*
[c]*Department of Physical Therapy, China Medical University, Taichung, Taiwan*

Screw-rod type of spinal instrumentation is widely used in the treatment of spinal disorders. Despite the advances in medical technology innovations, screw looseness remains one of the most frequent failures with this type of implantation system. The selection of screw size plays a crucial role in the success of spinal instrumentation as larger sized screws increase the risk of pedicle failure during insertion but small-sized screws are thought to compromise the stability of the instrumentation. By investigating the relationship between screw diameter and the pullout strength of pedicle screw after fatigue loading, this study seeks to find quantitative biomechanical data to assist surgeon in the selection of the appropriate screw. Two hypotheses were proposed for this research: 1) the fixation strength of larger screw will be higher than that of smaller screws immediately after implantation. 2) After fatigue loading, while the fixation strength will decrease for all screw sizes, larger screws will more effectively retain their fixation strength.

27 human cadaveric thoracic spine vertebrae (T3-T8) were harvested from 5 human cadavers (2 males & 3 females, ranged: 52-83 years). The mean BMD of the specimens was 0.645 g/cm^2 (ranged: 0.353-0.848 g/cm^2), which is indicative of severe osteoporosis. Two sizes of poly-axial screws (4.35mm x35 and 5.0mm x35, Depuy Synthes Spine Inc., West Chester, PA) were randomly chosen and implanted into each of the two pedicles of each vertebrae by an experienced surgeon and specimens were randomly distributed into control group (n=9), fatigue group of 5,000 cycles (n=9) and fatigue group of 10,000 cycles (n=9). The fatigue test was conducted with peak-to-peak loadings of 10-100N at 1 Hz for 5,000 and10,000 cycles. Each specimen was then embedded into the epoxy resin mold with rib before being placed in the custom jig for performing the axial pullout tests at a constant pullout rate of 5 mm/min. The ultimate pullout strength (N) were obtained for analysis. A paired t-test was conducted to determine the differences of pullout strength between the different screw sizes.

The BMD was of no significant different between each group (p=0.492). In the 5.0 mm group and the 4.35 mm group, the averaged pullout strength were 363.3(138.3)N and 259.0(159.3)N in the control group, 332.5(165.2)N and 316.1(106.0)N in the 5,000 cycles fatigue group, 208.0(90.1)N and 229.3(99.9)N in the 10,000 cycles fatigue group (Fig. 1).The difference of pullout strength among the three groups were not significant (p=0.089, 0.405). In the control and two fatigue groups, there were no significant differences between the two sizes of screws (p=0.071, 0.716, 0.639). The pullout strength of the larger screws was

higher than that of the smaller screws in the control group but in the fatigue groups, pullout strength was closer to each other.

In terms of the pullout strength, even though no significant difference was found in each group, our results indicated two tendencies. First, The pullout strength of the larger screws was higher than that of the smaller screws in the control group but in the fatigue groups, pullout strength were closer to each other. Second, for the larger-sized screw (5 mm) the pullout strength decreased with the number of fatigue cycles. However, the pullout strength of smaller-sized screw (4.35 mm) seems to be invariant with fatigue cycles. The stiffness data indicated almost the same tendency as the pullout strength. Overall, we proved the first hypothesis, but failed the second one. Two main findings were concluded in this research: First, the pullout strength of the larger-sized screw was higher than that of the smaller-sized screw right after the implantation. Second, both sizes of screws exhibited similar pullout strengths after fatigue loading. The pullout strength of larger-sized screws is not higher than that of smaller-sized screws. This indicates that the smaller-sized screws may be chosen for less risk of pedicle breakage without sacrificing fixation strength.

This study provided a quantitative biomechanical insight for the selection of size of pedicle screws. It indicated the under-sized screws should be considered since its biomechanical performance was similar to the over-sized screws, but at the lower risk of breaking the pedicle cortex.

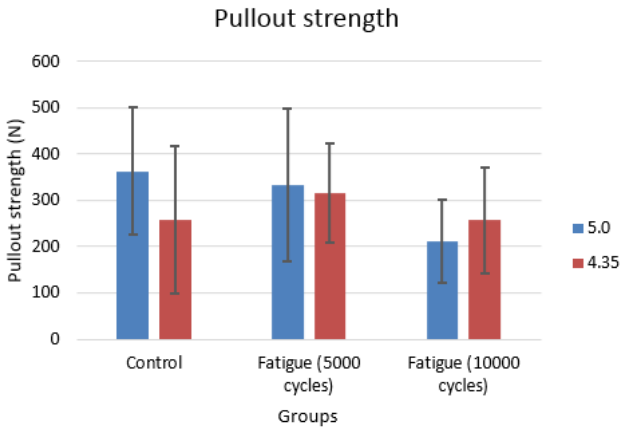

Fig. 1 The pullout strength between two different sizes of pedicle screws (5.0 mm vs. 4.35 mm) in three group.

Development and Validation of a µFEA Model for the Investigation of the Pedicle-Screw-Bone-Interface Under Different Loading Conditions

Chevalier Y[a], Fertmann-Matsuura M[a], Krüger S[b], Fleege C[c], Rauschmann M[c], Schilling C[b]

[a]*Ludwig Maximilians University Munich, Department of Orthopaedic Surgery, Physical Medicine & Rehabilitation, Campus Grosshadern, Munich, Germany*
[b]*Aesculap AG, Research & Development, Tuttlingen, Germany*
[c]*Orthopädische Universitätsklinik Friedrichsheim gGmbH, Wirbelsäulenorthopädie, Frankfurt a.M., Germany*

The state-of-the-art implants in clinical practice are typically developed based on empirical findings rather than on comprehensive understanding of the spinal environment involving postural loads and deformation during daily activities. This may partly explain the clinical occurrence of screw or rod fracture, screw loosening, loss of correction or adjacent segment disease. While pedicle screw rod instrumentation is still the gold standard for the treatment of a diverse range of spinal degenerative disorders, anchorage in the elderly spine with poor bone quality remains challenging. Yet, there are no models available to assess the specific influence of screw design parameters at the pedicle-screw-bone-interface. In our study, we aimed to develop numerical micro finite element (µFE) models based on µCT scans to investigate the screw bone interface on a micro scale level.

24 vertebrae extracted from 5 fresh frozen human lumbar spines were divided into two groups based on CT-based bone mineral density (BMD) (group A: high BMD, n=12, uncemented fixation; group B: low BMD, n=12, cemented fixation). Two screw types were implanted in the left (Aesculap Ennovate pedicle screw, Pentacore® design) and right pedicles (Aesculap S^4 pedicle screw, conical screw design) of each vertebra to ensure an autologous left/right comparison. All vertebrae were then scanned with a µCT (v|tome|x s 240, General Electrics) at an isometric resolution of 56 µm, and images converted to µFE models (Chevalier, 2015) of sub-regions around each screw with a mean of 6 million nodes. These µFE models were assigned linear isotropic materials and solved under static 0.1mm displacement simulating axial screw pull-out. The predicted pull-out stiffness was then calculated as a ratio of reaction force to applied displacement. In parallel, physical tests were performed regarding pullout and torsion strength on sub groups of group A and B (n=6). Correlations were then established between the experimental strength, the predicted pull-out stiffness, and the local BV/TV calculated from the µCT scans.

Experimental pull-out and torsional strengths were moderately to strongly correlated to BV/TV around the implanted screw for both screw type (pull-out, R^2>0.81; torsion, R^2>0.65). Numerical predictions of pull-out stiffness also correlated well with experimental pull-out and torsional strengths (R^2>0.73 and R^2>0.69), with stronger correlations for the Pentacore screw design (R^2>0.87). Ratio

of left and right screw predicted stiffness were not significantly different with the experimental ratios in both loading modes ($p>0.482$), showing similarities in structural effects of screw design for the experimental and µFE models. These predictions also showed differences in bone tissue stresses around the two types of screws depending on local bone density and proximity to the cortical bone (Fig. 1).

This study proposed the use µFE models to evaluate some of the several biomechanical factors that might affect pedicle screw anchorage. These refined µFE models include a detailed geometrical representation of bone microstructure and interfaces, and allowed structural predictions that correlated well with experimental measurements. They showed how fixation stiffness and bone tissue stresses are influenced not only by bone quality but loading and implant design. This approach will be extended to simulate torsional loads and other physiological loads such as compression bending as well as variations in cementing techniques, and how these could potentially minimize the risks of anchorage failures.

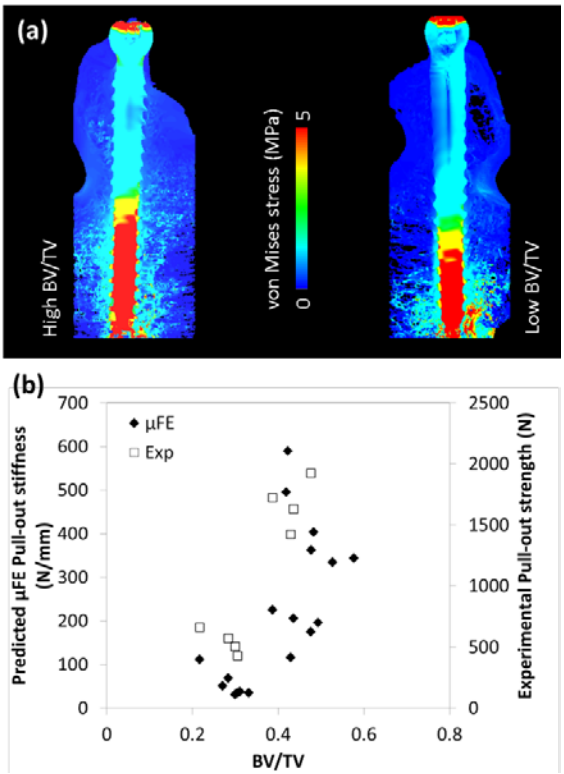

Fig. 1: a) Local µFE-based von Mises stress prediction for pedicle screws in high and low density bone
b) relationships between predicted and measured structural properties with local BV/TV around the screw.

Chevalier Y, J.Biomech.Eng 2015

On the Clinical Relevance of International Standards for Preclinical Evaluation of Posterior Stabilization Devices

La Barbera L[a,b], Galbusera F[b], Villa T[a,b]

[a]*LaBS, Department of Chemistry, Materials and Chemical Engineering "G.Natta", Politecnico di Milano, Milano, Italy*

[b]*IRCCS Istituto Ortopedico Galeazzi, Milano, Italy*

The clearing process established for posterior spine stabilization implants by the notified bodies (e.g. Food and Drug Administration), is based on precise and repeatable test methods which implement the essential loading and boundary conditions met during clinical use [ASTM F1717-2015, ISO 12189-2008]. However, standards describe specific assumptions, which complicate the interpretation of the results and the drawing of any correlation to clinical practice. Issues arise also when implants with different clinical indications (i.e. rigid fixation vs. semi-rigid stabilization) have to be compared using alternative standard constructs (i.e. corpectomy vs. low-stiffness springs vs. high-stiffness springs).

This study draws a parallelism between the current standards and the clinical practice, with the final aim to increase user awareness and to translate the results of standard evaluation to the clinics.

The FE (finite elements) models of ASTM F1717 and ISO 12189 standards, reproducing respectively a corpectomy scenario and a 2-FSUs (functional-spine-units) synthetic construct based on calibrated springs, were instrumented with pedicle screws/spinal rods (Figure). Standard models were loaded with a simple vertical load up to 2 kN.

The FE model of an already validated L2-L4 spine segment was modified to represent a variety of scenarios requiring posterior instrumentations, as often met during clinical practice: a full corpectomy, a 2-FSU instrumented scenario and a vertebral body replacement (Fig. 1).

Standing (500N) and upper body flexion (1150N+7.5Nm) were considered as simple everyday life activities. Models reproducing clinical scenarios were validated with *in vitro* and *in vivo* measurements obtained by Rohlmann, Wilke and colleagues using instrumented posterior fixation devices.

We investigated the influence of anterior support stiffness, K_A (i.e. spring stiffness in standards construct) and posterior implant stiffness, K_P (rod elastic modulus: 210, 110, 45, 10 GPa representative of steel alloys, titanium alloys, Ostapek and PEEK) on specific clinical outputs often met in clinical studies. The range of motion (ROM) and load-sharing on the hardware (both the axial load and bending moment in flexion) were compared and discussed.

Standards generally catch the trends observed in the output variables in clinical scenarios. However, a peculiar kinematic behaviour, affected both by spring stiffness and rod material, was noticed. Despite the range covered by output variables during standard tests does not always correspond to meaningful values, careful selection of input parameters and load values allows to reproduce specific clinically-relevant conditions.

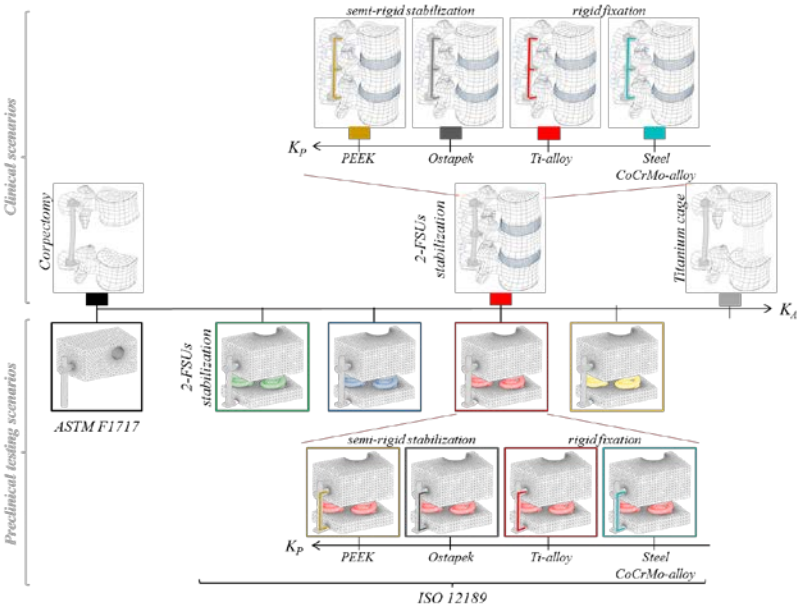

Fig. 1: Preclinical testing scenarios according to the current international standards (given its symmetries, we modelled only ¼ of each construct) and its corresponding clinical scenario (sagittal symmetry was assumed). K_A denotes the anterior support stiffness; K_P denotes the stiffness of the posterior hardware.

Superimposed Eccentric Sudden Trunk Loading: Effect on Trunk Peak Torque and Muscle Activity

Mueller S, Engel T, Mueller J, Mayer F

University of Potsdam, Outpatient Clinic, Potsdam, Germany

Trunk stability is considered essential to counteract overloading and therefore reduce injury risk. Especially in recreational and elite athletes, compensation of sudden loading is regarded as important factor in achieving stability and performance of the trunk during training and competition. In this context, reduced trunk extensor strength is discussed as highly relevant.

Therefore, the purpose was to develop a feasible and valid sudden eccentric trunk extensor loading task for active persons.

Sixty-seven active female and male participants without back pain (32f/35m, 23.8±10.6yrs, 176±9cm, 72±12kg, Training: 821±638min/week; back pain VAS: 0.1±0.2) were included in the study. Maximum strength in trunk extension (ROM: 55°) was tested on an isokinetic dynamometer in isometric (MVC), concentric (30°/s; PT_{con}) and eccentric (30°/s; PT_{ecc}) mode. Furthermore, sudden trunk loading was assessed by eccentric (30°/s) mode with superimposed customized dynamometer-based perturbation ($PT_{ecc+pert}$). Furthermore, neuromuscular trunk activity was assessed with a 12-lead EMG (trunk: 6 ventral, 6 dorsal muscles) in all conditions. Back pain intensity was assessed pre and post testing by a visual analog scale (VAS: 0-10cm). Peak torque [Nm] and EMG amplitudes (RMS normalized to MVC [%]) were calculated. Data is presented with mean±SD and perturbation effects were analyzed by ANOVA (α=0.05). Sub analysis were applied for gender and age (<18yrs/≥18yrs).

The superimposed trunk perturbation did not cause any back pain. Trunk peak torque was lowest for concentric and highest for perturbation testing (PT_{con}: 201±63, PT_{ecc}: 264±82, $PT_{ecc+pert}$: 339±97; $p<0.05$). EMG amplitudes were statistically significant higher in concentric condition ($p<0.05$), but not different between eccentric and perturbation ($p>0.05$). This pattern was also visible for subgroups (gender, age), but on different absolute levels.

The superimposed trunk loading induced higher peak torque values and it´s use is therefore valid as a sudden perturbation task. Especially for athletes, this challenging test might give further insight into trunk compensation strategies. Validation for back pain patients still needs to be accomplished.

Supported by BISp (IIA1-080102A/11-14; IIA 1-080126/09-13)

MiSpEx – the National Research Network for Medicine in Spine Exercise

Effect of High-Intensity Perturbations During Core-Specific Sensorimotor Exercises on Trunk Muscle Activation Pattern

Mueller J, Mugele H, Hadzic M, Stoll J, Mueller S, Mayer F

University Outpatient Clinic, Sports Medicine & Sports Orthopaedics, University of Potsdam, Germany

Core-specific sensorimotor exercises are evident to enhance neuromuscular activity of the trunk muscles (TM). However, it is unclear if unexpected, high intensity perturbations lead to altered neuromuscular activation pattern and therefore enhances training efficacy.

Sixteen participants (8m/8f; 29±2yrs; 175±8cm; 69±13kg) were prepared with a 12-lead bilateral trunk EMG (Mm. rectus abdominis, external obliquus, internal obliquus, latissimus dorsi, thoracic and lumbar erector spinae). Warm-up on an isokinetic dynamometer was followed by maximum voluntary isometric contraction measurement (MVC). Next, participants performed four conditions (10 repetition each) for a (left-sided) one-leg stance with hip abduction on a stable surface (HA), on an unstable surface (HA_U), with perturbation (HA+P) and on an unstable surface with perturbation (HA_U+P) in randomized order. Afterwards, bird dog (BD) was performed under the same 4 conditions (BD, BD_UP, BD+P, BD_U+P). A soft pad under the left foot (HA) or the right knee (BD) was used as an unstable surface. Exercises were conducted on a moveable platform (split-belt treadmill) and perturbations (100ms duration; 10rep.) were applied randomly in anterior-posterior direction. Root mean square (RMS) normalized to MVC (%) was always calculated for the whole movement cycle. Muscles were grouped to ventral right;left (VR;VL), and dorsal right;left (DR;DL). Ventral-Dorsal (V:D) and Right/ Left ratio (S_R;S_L) were calculated (repeated-measures ANOVA;α=0.05).

Average amplitudes of all muscle groups and conditions in bird dog were higher compared to hip abduction ($p \leq 0.0001$; Range: BD: 14±3% (BD; VR) to 58±3% (BD_U+P; DR); HA 7±2% (HA; VR) to 24±4% (HA_U+P; DR)). EMG-RMS showed significant differences ($p<0.001$) between conditions for all muscle groups. No significant differences were present in EMG-ratios (V:D; S_R:S_L) for any condition ($p<0.05$).

The use of additional high-intensity perturbations during core-specific sensorimotor exercises lead to enhance trunk neuromuscular activity and should be implemented into core exercise. In addition, BD exercise is more suitable to adress trunk muscles.

Supported by BISp (ZMVI1-080102A/11-18)

Systems Identification of Trunk Stabilization suggest Acceleration Sensitivity of Muscle Spindle Feedback

van Dieën JH

Dept. of Human Movement Sciences, Research institute MOVE, Vrije Universiteit Amsterdam, Amsterdam, The Netherlands

Trunk stabilization can be defined as maintaining control over trunk posture and movement, in spite of the disturbing effects of gravity and external and internal perturbations. Trunk stabilization is required to control posture and movement during daily activities and it has been hypothesized that inadequate stabilization could contribute to low-back pain. However, the processes underlying trunk stabilization are incompletely understood at present.

To assess trunk stabilization, we used a recently developed method in 35 healthy subjects. In short, upper-body sway was evoked by continuous unpredictable, multi-sine force-controlled perturbations to the trunk in the anterior direction, resulting in small fluctuations around a fixed working point. Subjects were instructed to either 'maximally resist the perturbation' (resists task) or to 'relax but remain upright' (natural balance task). Frequency response functions (FRFs) of the admittance (the amount of movement per unit of force applied) and reflexes (the increase in EMG amplitude per unit of trunk displacement) were obtained. To these FRFs, we fitted a physiological model, to estimate intrinsic stiffness and damping, as well as feedback gains and delays. Different model versions were compared to assess which feedback loops contribute significantly to trunk stabilization.

Intrinsic stiffness and damping and muscle spindle (short-delay) feedback alone were sufficient to accurately describe trunk stabilization. Adding Golgi tendon organ, vestibular and visual feedback did not improve model fit. However, a model with feedback based on trunk movement and velocity alone yielded unrealistically low reflex delays. Addition of acceleration feedback yielded realistic delays and improved model fit. This result is in line with previous studies on whole-body balance control which suggest that muscle spindle feedback encodes acceleration in addition to velocity and muscle length, leading to improved stabilization.

Muscle Strength and Neuromuscular Control in Low Back Pain: Elite Athletes vs. General Population

Moreno Catalá M, Schroll A, Laube G, Arampatzis A

Department of Training and Movement Sciences, Humboldt-Universität zu Berlin, Germany

Chronic low back pain (LBP) is a worldwide-recognized problem with dramatic consequences for the quality of life of the affected patients. There is evidence that LBP patients show deficits in the neuromuscular control of the spine stability compared to healthy controls [1, 2]. However, there is a lack of studies taking into account the specificity of LBP in competitive sports. Our purpose was to investigate the athletic-based specificity of neuromuscular differences between healthy and LBP individuals and to identify appropriate markers for the characterization and evaluation of LBP.

Two groups of athletes with (n=15) and without LBP (n=15) and two groups of non-athletes with (n=15) and without LBP (n=14) participated in the study. Muscle strength of the trunk was assessed during maximal isometric and isokinetic contractions using dynamometry. To quantify the neuromuscular control of trunk stability we examined trunk stiffness and damping as well as muscle response patterns using Quick Release experiments. Furthermore, we investigated the local dynamic stability of the spine using the maximum finite-time Lyapunov exponent (λ_{max}) under static and dynamic conditions. For the statistical analysis a two-way ANOVA was performed.

The maximum isometric trunk extension moments were significantly lower in the LBP participants compared to healthy controls in both athletes and non-athletes. The analysis of interaction between condition and groups showed that trunk stiffness was lower only in the non-athlete LBP participants. Trunk damping and muscle reaction times were significantly higher for the LBP participants. No significant differences were found in λ_{max} between groups and conditions.

Isometric muscle strength decrease of the trunk extensors is a LBP specific characteristic in athletes as well as in non-athletes. This provides evidence that this parameter is a suitable marker for the evaluation of LBP. Trunk stiffness is not sensitive enough to distinguish LBP participants from healthy controls in elite athletes, indicating an athletic-based specificity in the neuromuscular control of spine stability.

[1] Graham R.B. et al, *J. Biomech, 47(6):*1459–64, 2014.

[2] Hodges P. et al, *J. Biomech, 42(1):*61–66, 2009.

Generating Desired Optimal Trajectory of Trunk for Rhythmic and Discrete Sagittal Movement by Central Pattern Generators

Abedi M[a], Vossughi GR[a], Parnianpour M[a], Khalaf K[b]

[a]*Department of Mechanical Engineering, Sharif University of Technologies, Tehran, Iran*
[b]*Department of Biomedical Eng. Khalifa University of Science and Research, Abu Dhabi, UAE*

The biomechanical simulation of trunk motion has become an essential tool in exploring spinal loading during recreational, work and daily activities. Optimization-based Inverse dynamics is used to estimate required muscular forces and moments at each joint which are subsequently compared with muscle activities and joint loading measures such as intra-discal pressure and instrumented fixators' data. *In silico* modeling, encounters with multiple degrees of freedom (i.e. kinematic and kinetic redundancy) and inter joint coordination patterns during healthy and low back pain conditions. The purpose of this study is to illustrate the feasibility of using central pattern generators (CPGs) to simulate optimal trajectories for repetitive and point to point movement while coordinating the motion by coupling the modified Hopf oscillators.

Central pattern generators (CPGs) have been used to generate trajectories of joints for rhythmic and discrete movements in human spine flexion-extension. To design CPGs, optimal trajectories of joints have been used for both rhythmic and discrete movements. These trajectories have been obtained for 65 degrees flexion-extension from upright position, for π second and $\pi/2$ second period of movement for rhythmic and discrete movements, respectively. For rhythmic movements, some changes are applied on the formulation of Hopf oscillator so to enable the CPGs producing these optimal trajectories. This new oscillators are able to produce any desired trajectory. Also for discrete movements, CPGs are designed with aid of dynamical systems with point attractors at the end of movement. Certain parameters in the formulation are tuned to adjust the amplitude and velocity of movements and by creating connections between CPGs the relative phases between degrees of degrees of freedoms are determined. Numerical simulations are made for sagittal motion of seven links: pelvic, L1 to L5 vertebrae, and thorax.

Optimal trajectories have been calculated in our previous study, by minimizing an objective function which is combination of energy, torque rate and jerk. Figures 1-3 show the optimal trajectories of joints during flexion-extension rhythmic movement and flexion, extension discrete movements, respectively. The algorithm showed the relative errors between desired optimal and simulated motion by CPGs to be less than 3.9%, 0.3%, 0.3% for angular acceleration, velocity and position trajectories, respectively.

The following model allows simulation trajectories that are stable can be linked to commercial software such as ANYBODY or SIMMS to explore personalized motions in the spine and the relative coordination amongst its degrees of freedom for healthy and low back pain patients. In future, we need to control the spine muscle actuators with feedback and feedforward sensory and motor signals to achieve these rhythmic and discrete movement to learn more about inaction of the motor control and biomechanics of spine.

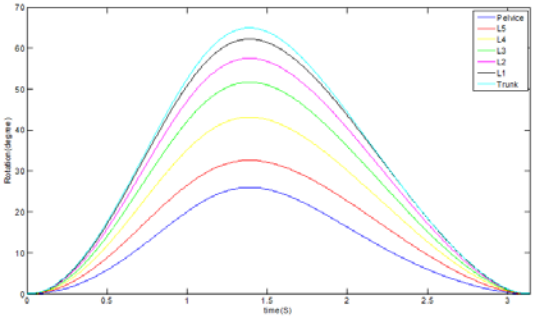

Fig. 1: Optimal trajectory for rhythmic flexion-extension movement

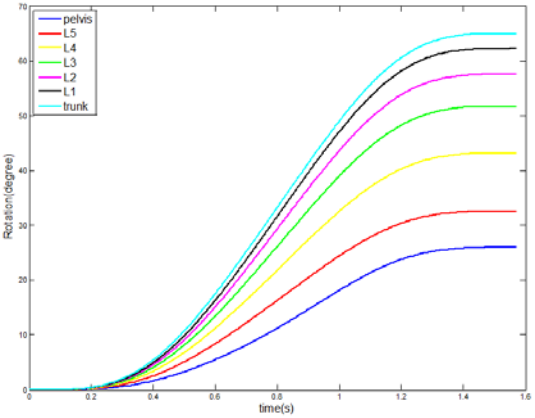

Fig. 2: Optimal trajectory for discrete flexion movement

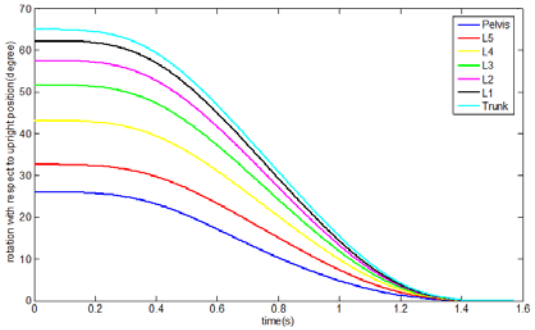

Fig. 3: Optimal trajectory for discrete extension movement

Subject Specific Proprioceptive Control Model for Spine Disorders Analysis

Amabile C[a], Van Den Abbeele M[a], Pillet H[a], Moal B[a], Lafage V[b], Carlier R[c], Skalli W[a]

[a]*Institut de Biomécanique Humaine Georges Charpak, Arts et Métiers ParisTech, Paris, France*
[b]*Hospital for Special Surgery, New York, NY, USA*
[c]*Raymond Poincaré Hospital, Garches, France*

Spine surgery has known tremendous changes since the eighties, with various concepts of implants aiming at fusion of a vertebral segment or at motion preservation. Yet in 2016 the rate of mechanical complications is still high, particularly for spine deformities with global alignment issues. Finite element models provide better understanding of instrumented spine behavior, however understanding relationship between malalignment and spine loads is essential, which require subject specific muscle modelling. Based on the proprioceptive model proposed in Pomero et al [1], a methodology is proposed to get subject specific input data, then investigate spine and muscle loads in 20 asymptomatic volunteers and patients with spinal disorders.

Using a free body diagram at L3 level, the model is based on the assumption that muscles act “to protect the spine”, i.e. to maintain spine load components below at an acceptable threshold. Based on each muscle’s location, orientation, and cross sectional area (CSA), weights are attributed to each muscle according to its ability to regulate each load component, then a spine load regulation control loop is set. Antagonist muscle activation is taken into account using the law proposed in [2]. Biplanar X-Rays (BPXR) were used to reconstruct spine and external envelope [3], and a density model was used to assess the net reaction force. After MRI muscle 3D reconstruction, data fusion between BPXR and MRI data was performed as described in [4], thus yielding subject specific input for the muscle model. Muscle maximum force was set from CSA and could be reduced in case of fat infiltration. The model was built for 12 asymptomatic subject (one 28 yrs old and 12 from 52 to 71 yrs) and 8 preoperative patients with spine deformities (54 to 70 yrs). Matlab Simulink software was used.

For asymptomatic subjects muscle regulation always succeeded in preserving spine loads below thresholds, with resulting spine and muscle loads consistent with literature findings. For some of the patients, malalignment yielded a high bending moment which regulation yielded much higher spine compression and muscle forces, and regulation failed when simulating decrease of maximum muscle force.

Although still preliminary, such model could help in better understanding the possible vicious circle in which spine malalignment yield spine overloading. It better explains the role of each muscle in spine load regulation, and may be a first step in subject specific spine loading in finite element models for surgery planning.

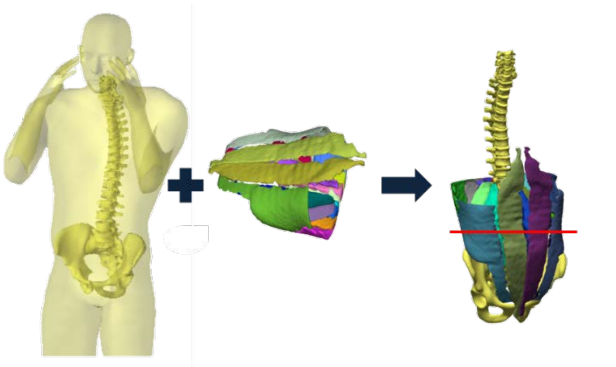

Fig. 1: Data fusion between BPXR and MRY to build subject specific musculoskeletal model.

[1] Pomero V, Lavaste F, Imbert G, Skalli W. Comput Methods Biomech Biomed Engin. 2004 7(6):331-8

[2] Zhou BH, Baratta RV, Solomonow M, Olivier LJ, Nguyen GT, D'Ambrosia R.D, IEEE Trans. Biomed. Eng. 1996 43, 150–160

[3] Nérot A, Choisne J, Amabile C, Travert C, Pillet H, Wang X, Skalli W. J Biomech. 2015 Dec 16;48(16):4322-6

[4] Hausselle, J., Assi, A., El Helou, A., Jolivet, E., Pillet, H., Dion, E., Bonneau, D., Skalli, W., Comput. Methods Biomech. Biomed. Engin. 2012 17, 480–487.

Acknowledgements: To the ParisTech BiomecAM Chair program on subject specific musculoskeletal modeling.

Does Multifidus Muscle Disruption Cause Intervertebral Discs Degeneration in the Lumbar Spine of Rat?

Maas H[a], Noort W[a], Hodges P[b], van Dieën J[a]

[a]*Department of Human Movement Sciences, MOVE research institute, Vrije Universiteit Amsterdam, The Netherlands*

[b]*The University of Queensland, NHMRC Centre of Clinical Research Excellence in Spinal Pain, Injury and Health, School of Health & Rehabilitation Sciences, Brisbane, Australia*

Low back pain has been hypothesized to be caused by mechanical dysfunction of the spine, i.e. segmental instability, which may be the result of intervertebral disc (IVD) degeneration. Patients with low back pain often also show localized atrophy of the deep, paravertebral multifidus (MF) muscle, which plays an important role in stabilization of the spine. Thus, stability of spinal segments could be impaired by both IVD degeneration and MF atrophy. Each might cause the other, but the order of events is unknown. The aim of the present study was to investigate whether elimination of MF causes IVD degeneration. Changes in IVD structure were compared to an IVD lesion model, known to result in IVD degeneration, as well as to a control group.

Data were obtained from 36 male Wistar rats, which were randomly assigned to one of three groups: (i) Lumbar IVD lesion, in which the L4/L5 disc was stabbed; (ii) Lumbar MF resection, in which all MF tissue between L3 and L6 was excised bilaterally; (iii) Control, in which no intervention was applied. 7, 14, and 28 days post-intervention (n=4 in each group and time point), L4/L5 discs, as well as left and right MF fascicles (L3-L6, L4-S1; in disc stab and control groups) and longissimus (LO) were harvested, weighed, and frozen for histological analysis. Sections were stained with Alcian Blue & Picrosirius Red to assess the area of the nucleus pulposus (NP) and that of the whole IVD.

ANOVA indicated significant group differences in relative NP area, as well as significant interaction between group and post-op days. At 14 days post-op exclusively, post-hoc analysis revealed significant differences between control/MF and stab (Figure). Relative NP area of the stab group was only 20%% of that of the control group. No significant effects were found for whole IVD area. For MF normalized to body mass, group differences and significant interaction between group and post-op days were found. At 7 days post-op, normalized MF mass was significantly lower (20%) in the stab group. No differences in MF mass were found 14 and 28 days post-op. For normalized LO mass, significant differences between post-op days and significant interaction between group and post-op days were found. At 28 days post-op, normalized LO mass was significantly lower (16%) in the stab group. No differences in LO mass were found 7 and 14 days post-op.

These results indicate that MF disruption does not cause degeneration of the IVD in the rat lumbar spine within the period measured. A lesion in the IVD results in a rather rapid decrease in the size of the NP as well as in atrophy of MF and LO muscles. To assess whether MF disruption enhances IVD degeneration and/or adequate MF function is required for the recovery process, effects of simultaneous disc stab and MF disruption should be investigated.

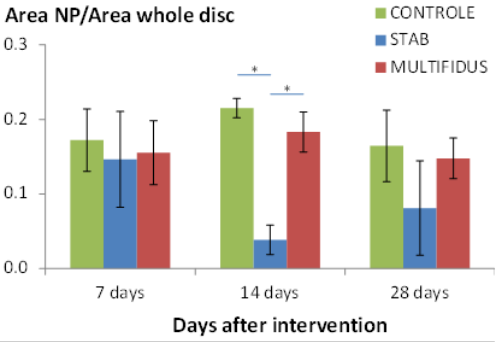

Fig. 1: Relative Nucleus pulposus (NP) area measured at different post-op days.

Ambulatory Hand Force Estimation during Manual Lifting using an Inertial Sensor Suit and Instrumented Force Shoes

Faber GS[a,b,c], Chang CC[c,d], Kingma I[a], Dennerlein JT[b,e], van Dieën JH[a]

[a]*Department of Human Movement Sciences, Faculty of Behavioural and Movement Sciences, Vrije Universiteit Amsterdam, MOVE Research Institute Amsterdam, The Netherlands*
[b]*Department of Environmental Health, Harvard T.H. Chan School of Public Health, Boston, MA, USA*
[c]*Liberty Mutual Research Institute for Safety, Hopkinton, MA, USA*
[d]*Department of Industrial Engineering & Engineering Management National Tsing Hua University, Taiwan, ROC*
[e]*Department of Physical Therapy, Movement, and Rehabilitation Sciences, Northeastern University, Boston, MA, USA*

Hand forces (HFs) are often measured during biomechanical assessment of manual materials handling. In most field studies it is not possible to directly measure HFs without affecting the natural motion pattern. Therefore, in a previous study we proposed a HF estimation method based on ground reaction forces (GRFs) and body segment accelerations. As a proof-of-principle this method was tested with laboratory equipment: GFRs were measured with force plates (FPs) and segment acceleration were measured using an optical motion capture (OMC) system [1].

In the current study, we evaluated this HF estimation method but now based on an ambulatory measurement system, consisting of inertial motion capture (IMC) system and instrumented force shoes (FSs).

Sixteen participants lifted a 10-kg box from ground level while 3D full-body kinematics were measured using an OMC and an IMC system, and 3D GRFs were measured using a FPs and FSs. 3D HFs were estimated three times based on different data sources: 1)FP+OMC, 2)FP+IMC and 3)FS+IMC. The estimated HFs were compared (RMSerror) to reference HFs that were calculated based on box kinematics and the GRFs of a FP that the box was lifted from.

Averaged over subjects and 3D force directions, the HF RMSerror was 8N when using the laboratory equipment (FP+OMC). When using the IMC instead of OMC data (FP+IMC), RMSerror increased to 11N. Finally, when replacing the FP data with the FS (FS+IMC), RMSerror increased to 14N.

Whether this error is acceptable depends on application of the method. For example, for the assessment of low back loading during manual lifting, this error seems acceptable. Assuming a moment arm of 0.5m from the low back to the hands this error would result in about 7.5Nm error in low-back moment estimates, which is small relative to peak low-back moments of 200-300 Nm during manual lifting .

Hand forces (HFs) are often measured during biomechanical assessment of manual materials handling. In most field studies it is not possible to directly measure HFs without affecting the natural motion pattern. Therefore, in a previous study we proposed a HF estimation method based on ground reaction forces (GRFs) and body segment accelerations. As a proof-of-principle this method was tested with

laboratory equipment: GFRs were measured with force plates (FPs) and segment acceleration were measured using an optical motion capture (OMC) system [1].

In the current study, we evaluated this HF estimation method but now based on an ambulatory measurement system, consisting of inertial motion capture (IMC) system and instrumented force shoes (FSs).

Sixteen participants lifted a 10-kg box from ground level while 3D full-body kinematics were measured using an OMC and an IMC system, and 3D GRFs were measured using a FPs and FSs. 3D HFs were estimated three times based on different data sources: 1)FP+OMC, 2)FP+IMC and 3)FS+IMC. The estimated HFs were compared (RMSerror) to reference HFs that were calculated based on box kinematics and the GRFs of a FP that the box was lifted from.

Averaged over subjects and 3D force directions, the HF RMSerror was 8N when using the laboratory equipment (FP+OMC). When using the IMC instead of OMC data (FP+IMC), RMSerror increased to 11N. Finally, when replacing the FP data with the FS (FS+IMC), RMSerror increased to 14N.

Whether this error is acceptable depends on application of the method. For example, for the assessment of low back loading during manual lifting, this error seems acceptable. Assuming a moment arm of 0.5m from the low back to the hands this error would result in about 7.5Nm error in low-back moment estimates, which is small relative to peak low-back moments of 200-300 Nm during manual lifting.

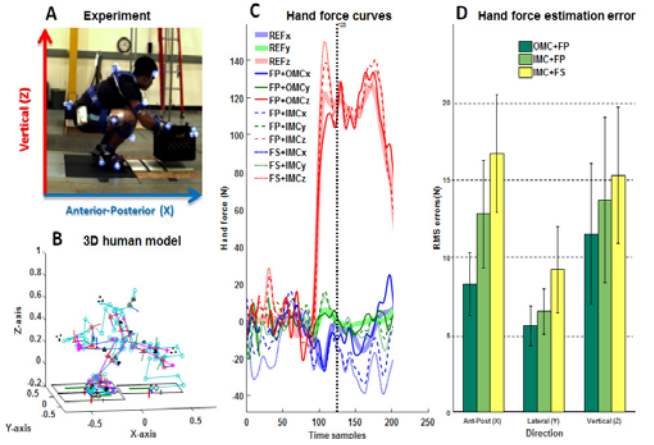

Fig. 1:

A: Photo of subject during experiment.

B: Matlab visualization of 3D model.

C: Typical example of the 3D curves of the reference hand forces (REF) and the estimated hand forces.

D: Hand force RMS errors, averaged over 16 subjects, for each direction and method.

[1] Faber GS, Chang CC, Kingma I, Dennerlein JT, 2013. Estimating dynamic external hand forces during manual materials handling based on ground reaction forces and body segment accelerations. Journal of Biomechanics, 46, 2736–2740.

JULIUS WOLFF INSTITUT

CHARITÉ
UNIVERSITÄTSMEDIZIN BERLIN

Estimating the L5S1 Moment Using a Simplified Ambulatory Measurement Setup

Koopman AS, Kingma I, Faber G, van Dieën JH

MOVE Research Institute, Department of Human Movement Sciences, Vrije Universiteit Amsterdam, The Netherlands

Peak mechanical loading (PML) of the spine has been shown to be an important risk factor for the development of low-back pain. Knowledge about the PML in realistic working conditions can help in reducing the back load. To allow for selecting the optimal number of sensors in an ambulatory system, the objective of this study was to investigate the effect of using several simplified ambulatory measurement setups on estimates of PML.

Nine healthy male subjects lifted a box (10kg) from the floor. Hand forces, ground reaction forces (GRF) and full-body kinematics (Optotrak) were measured using a golden standard (GS) laboratory setup. In the ambulatory setup, hand forces were estimated based on the GRF and full body kinematics were measured using an inertial motion capturing (IMC) system (Xsens). Using top-down inverse dynamics, 3D L5S1 moments were calculated with the GS system and with several combinations of IMC sensors.

Estimation errors of IMC setup's (Figure 1) were quantified as root-mean-square differences and absolute peak of extension moments relative to the GS setup. Averaged over subjects (mean (SD)), L5S1 extension moment RMSerrors (Nm) were lowest with the highest number of IS's (A) (Feet, Shanks, Thighs, Pelvis, Thorax, Head, shoulders, Upper arms, Forearms and Hands) 15.66 (6.3) and increased to 23.5 (8.3), 35.8 (8.4) and 28.2 (9.2), for the setup in which only 8 (B) (Shanks, Pelvis, Thorax Upper arms and Forearms), 6 (C) (Pelvis, Thorax Upper arms and Forearms) and 6 (D) IS's (Shanks, Pelvis, Thorax and Upper arms) were used. Peak moment (Nm) absolute differences relative to GS varied from 18.3 (13.1) to 25.2 (18.5), 33.7 (20.8), and 42.5 (18.9), for IMC setup's A, B, C and D, respectively.

While reasonable PML estimates can be obtained with IS, omitting the shank IS led to unacceptable errors. Furthermore, omitting the forearm sensor led to an underestimation of the PML because of the unknown hand position.

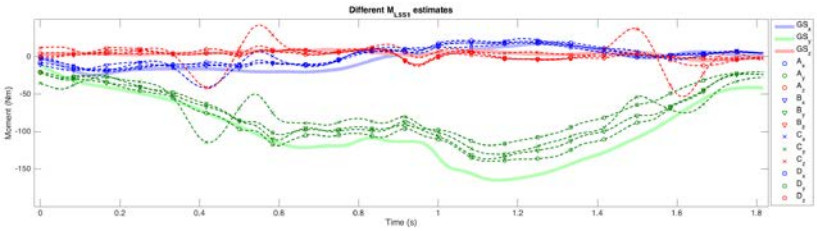

Fig. 1: Typical example of moment time series for different measurement setups. X-axis is lateral bending, y-axis is flexion/extension, z-axis is twisting. For codes of measurement setups see text.

Mechanical Demands of a Lowering and Lifting Task on the Lower Back of Patients with Acute Low Back Pain

Shojaei I, Hooker Q, Salt EG, Bazrgari B

University of Kentucky, Lexington, KY, USA

Despite extensive research related to the lower back biomechanics in patients with chronic low back pain (LBP), less attention has been paid to those with acute LBP. Understanding changes in the lower back biomechanics with progression from an acute episode to chronic and/or recurrent LBP can inform early management before transition to a disabling disorder. The objective of this study was set to investigate differences in mechanical demand of lowering and lifting a load in the sagittal plane on the lower back between individuals with and without acute LBP.

Participants included a group of 19 females (aged 40-70 years) with health-care provider diagnosed acute LBP (<3 months) and an age-matched group of 19 asymptomatic female controls. Kinematics and kinetics data were respectively collected using accelerometers and a force platform during a task involving lowering a 4.5 kg load from upright standing posture to the knee height and then lifting back to the initial upright posture. Mechanical demands of the task on the lower back (i.e., net external moment and reaction forces) were estimated using measured kinematics and kinetics along with an inverse dynamic procedure involving a rigid multi-segment model of the lower extremities and pelvis [1]. Estimated forces and moments were normalized to body mass and stature*body mass respectively.

Peak values of thoracic rotation, lumbar flexion, velocity, acceleration, and deceleration were all smaller (F>6.82, p<0.015) in patients compared to controls. However, there was no difference in max and mean values of the mechanical demands of the task on the lower back (F<2.96, p>0.097) between the groups (Table 1). Similar mechanical demands for both groups suggest a comparable total internal tissue responses for offsetting the task demand. However, smaller lumbar flexion in patients suggests a smaller passive contribution to the task demand which should be compensated by larger active control. Such a conclusion is consistent with the reports of larger active control in LBP patients vs. asymptomatic controls [2]. Estimation of muscle forces and spinal loads in patients with acute LBP requires detailed modeling.

Table 1: Mean (SD) of the outcome measures for patients vs. controls during the lowering and lifting task. TMM shearing/compression denotes the shearing/compression demand at the time of max moment (TMM). Boldface indicates a significant difference.

	Thoracic Rotation	Pelvic Rotation	Lumbar Flexion	Velocity	Acceleration	Deceleration
Patients	**75.2 (10.3)**	42.6 (10.2)	**32.6 (11.0)**	**32.8 (15.7)**	**58.0 (31.9)**	**59.7 (31.3)**
Controls	**85.4 (11.3)**	34.0 (11.9)	**51.4 (13.4)**	**49.2 (14.1)**	**85.7 (36.9)**	**90.3 (46.8)**
	Max Moment	TMM Shearing	TMM Compression	Mean Moment	Mean Shearing	Mean Compression
Patients	79. 1 (17.1)	463.4 (33.0)	30.2 (78.9)	40.1 (10.6)	373.3 (24.9)	193.6 (39.6)
Controls	81.5 (25.0)	451.9 (40.3)	97.2 (90.8)	39.7 (17.9)	362.2 (26.0)	219.3 (48.0)

[1] Shojaei et al. 2016 Journal of Biomechanics. 49 (6), 896-903

[2] Colloca and Hinrichs. 2005 J. Manip. & Phys. Therap. 28 (8), 623-631

Acknowledgment: This work was supported in part by the National Center for Research Resources and the National Center for Advancing Translational Sciences [UL1TR000117]. The content of this manuscript is solely the responsibility of the authors and does not necessarily represent the official views of the NIH.

Faster Walking Speeds Differentially Alter Spinal Loads in Persons with Traumatic Lower Limb Amputations

Hendershot BD[a,b], Shojaei I[c], Bazrgari B[c]

[a]DOD-VA Extremity Trauma and Amputation Center of Excellence, Bethesda, MD, USA
[b]Walter Reed National Military Medical Center, Bethesda, MD, USA
[c]University of Kentucky, Lexington, KY, USA

Persons with lower limb amputation (LLA) commonly report low back pain and perceive altered trunk motions/postures during activities of daily living as primary contributors [1]. When walking at a self-selected pace, our prior work has demonstrated altered trunk motions among persons with vs. without LLA are associated with 26-60% increases in spinal loads [2]. Here, we expand these efforts by presenting preliminary data of a much larger sample* regarding the influence of walking speed on spinal loads in this population. Trunk and pelvic kinematics, collected during level-ground walking at 3 controlled speeds (~1.0, 1.3, and 1.6 m/s), were extracted for 1 male servicemember with unilateral transfemoral amputation (35 yr, 173.0 cm, 106.8 kg) and 1 male servicemember without amputation (27 yr, 179.0 cm, 72.0 kg). These kinematic data were input to a kinematics-driven, non-linear finite element model of the lower back to estimate the resultant compressive and lateral/anteroposterior shear loads at L5/S1 using an optimization-based iterative procedure [3]. Peak compressive, lateral, and anteroposterior shear loads generally increased with increasing walking speed. However, increases in compression and lateral shear with increasing walking speed were larger among the person with vs. without LLA, particularly in lateral shear at the fastest speed (Fig. 1A-B). In contrast, peak anteroposterior shear decreased with increasing walking speed among the person with LLA (Fig. 1C). Although walking is generally not a mechanically demanding task for the low back (i.e., loads are well below reported injury thresholds), walking faster for persons with LLA appear to differentially alter external demands on the lower back and internal loads among tissues within the spine. Thus, over time, repeated exposures to faster walking speeds may contribute to the elevated risk for low back pain after LLA, due to fatigue failure of spinal tissues, though further work to more completely characterize spinal loads during activities of daily living is warranted.

* Final results from n ≥ 20 in each group (with additional speeds and levels of amputation) will be presented at the workshop

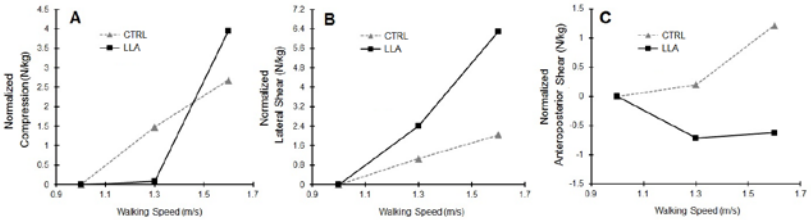

Fig. 1: Normalized changes in (A) compression, (B) lateral shear, and (C) anteroposterior shear with increasing walking speed, for an individual with lower limb amputation (LLA) and an uninjured control (CTRL). To highlight the influences of walking speed, changes in spinal loads are shown with respect to values obtained in the 1.0 m/s walking speed and are normalized by body mass.

[1] Devan, H., Carman, A. B., Hendrick, P. A., Ribeiro, D. C., & Hale, L. A. (2015). Perceptions of low back pain in people with lower limb amputation: a focus group study. *Disability and Rehabilitation*, *37*(10), 873-883.

[2] Shojaei, I., Hendershot, B. D., Wolf, E. J., & Bazrgari, B. (2016). Persons with unilateral transfemoral amputation experience larger spinal loads during level-ground walking compared to able-bodied individuals. *Clinical Biomechanics*, *32*, 157-163.

[3] Bazrgari, B., Shirazi-Adl, A., & Arjmand, N. (2007). Analysis of squat and stoop dynamic liftings: muscle forces and internal spinal loads. *European Spine Journal*, *16*(5), 687-699.

Acknowledgements: This work was supported, in part, by an award (5R03HD086512-02) from the National Center for Medical Rehabilitation Research (NIH-NICHD) and the Office of the Assistant Secretary of Defense for Health Affairs, through the Peer Reviewed Orthopaedic Research Program (award #W81XWH-14-2-0144). The views expressed in this abstract are those of the authors, and do not necessarily reflect the official policy or position of the U.S. Departments of the Army, Navy, Defense, nor the U.S. government.

The Rib Cage Affects Intervertebral Disc Pressures in Dynamic Tests of Cadaveric Thoracic Spines

Anderson DE[a,b], Mannen EM[c], Tromp R[a], Wong BM[c], Sis HL[c], Cadel ES[c], Friis EA[c], Bouxsein ML[a,b]

[a]*Beth Israel Deaconess Medical Center, Boston, MA, USA*
[b]*Harvard Medical School, Boston, MA, USA*
[c]*The University of Kansas, Lawrence, KS, USA*

While the rib cage is thought to provide stability or "load sharing" for the thoracic spine, in reality the effects of the rib cage on thoracic spine loading are not well studied. Intervertebral disc pressures are frequently measured in cadaveric spine tests to provide insight into spinal loading. Applied pure moments increase intradiscal pressures in lumbar spine specimens [1], but such measurements are lacking in the thoracic region. Thus, our objective was to examine thoracic intradiscal pressures under applied pure moments, and to determine the effect of the rib cage on these pressures.

Eight fresh-frozen human cadaveric thoracic spines (T1-T12) with the rib cage intact were obtained (4 female, 4 male, age range 61-71). Specimens were positioned upright in a testing machine (Applied Test Systems, Butler, PA) with a compressive follower load of 400 N applied. Dynamic pure moments (0 to ±5 N·m) were applied in axial rotation, flexion/extension, and lateral bending. Disc pressures were measured at T4-T5 and T8-T9 using needle-mounted pressure transducers (Gaeltec, Isle of Skye, Scotland), first with the rib cage intact, and again after the rib cage was removed. Pressure measurements were normalized to pressure at 0 N·m, then the slopes of pressure vs. increasing moment were calculated via linear regressions. The effect of rib cage on pressure-moment slope was examined with a mixed effects model for each spinal level and direction of applied moment, adjusting for specimen as a random variable (Stata/IC 13.1, StataCorp LP, College Station, TX).

The pressure-moment slopes differed between Flexion and Extension ($p < 0.05$), so these were analyzed separately, while left and right directions were combined for axial rotation and lateral bending analyses. Slopes were significant (>0) in AR and LB, in Flexion at T4-T5, and in Flexion at T8-T9 with no rib cage ($p < 0.05$, Table 1). The pressure-moment slope was higher with no rib cage at T4-T5 for all loading directions and at T8-T9 for AR only ($p < 0.05$, Table 1).

Overall, removing the rib cage increased the pressure-moment slope in most conditions, and more at T4-T5 than T8-T9. Removal of the rib cage had the largest impact in Axial Rotation, increasing the slope about three-fold. While pressure increased with applied moment in other directions, slopes were not significant in Extension, perhaps due to a shift of loading from the disc to the posterior elements as the spine moves into extension [2]. Analysis of the same specimens under compressive follower loads alone found unclear and likely minimal effects of the ribcage on disc pressure [3]. This combined with the current findings suggests that the rib cage helps the thoracic spine to resist moments or angular motion rather

than compressive loading.

Table 1: Pressure-moment slopes (95% confidence intervals, units of % pressure increase per N·m) with and without the rib cage present. Significant slopes (>0) are in bold. *Different than Intact ($p < 0.05$).

Moment	Level	Rib Cage Intact	Rib Cage Removed
Axial Rotation	T4-T5	**3.80 (0.60 – 7.00)**	**12.83 (9.63 – 16.02) ***
	T8-T9	**3.79 (1.27 – 6.33)**	**9.87 (7.33 – 12.41) ***
Flexion	T4-T5	**6.34 (2.84 – 9.83)**	**9.44 (5.88 – 13.00) ***
	T8-T9	4.39 (-0.44 – 9.22)	**6.65 (1.82 – 11.48)**
Extension	T4-T5	0.71 (-3.56 – 4.97)	3.60 (-0.72 – 7.92) *
	T8-T9	-2.65 (-6.64 – 1.34)	-1.49 (-5.49 – 2.50)
Lateral Bending	T4-T5	**2.33 (1.33 – 3.33)**	**4.43 (3.37 – 5.50) ***
	T8-T9	**2.30 (0.14 – 4.46)**	**2.50 (0.34 – 4.66)**

[1] Rohlmann A, et al., *Spine,* 26(24): E557-E561, 2001.

[2] Adams MA, et al., *Clin Biomech (Bristol, Avon)*, 9(1): 5-14, 1994.

[3] Anderson DE, et al., *Journal of Biomechanics*, 49(7): 1078-1084, 2016.

Acknowledgements: This study was supported by the National Institute on Aging (K99AG042458) and by a Mentored Career Development Award from the American Society for Bone and Mineral Research.

The Contribution of the Ribcage to Thoracolumbar Spine Biomechanics in a Sheep Model: Progress Towards a Validated Computational Representation of Ribcage Biomechanics

Newell N, Grant CA, Adam CJ, Little JP

Paediatric Spine Research Group, CCHR at IHBI, Queensland University of Technology, Brisbane, Australia

The sternum and ribs play a significant role in providing stiffness to the thoracolumbar spine, however, the relative contribution of the ribs and intercostal soft tissue connections has not been individually isolated in experimental studies. This pilot study sought to investigate the contribution of the sternum, ribs and intercostal soft tissues in influencing spinal stiffness, using both biomechanical testing methods and an experimentally validated FE model of the thoracolumbar spine with ribcage.

Biomechanical Testing: An osseoligamentous thoracolumbar spine was harvested from a merino sheep immediately following euthanasia (Fig. 1). A six-degree-of-freedom robotic arm applied rotational loading to simulate physiological motion (Flexion = 29^{o}, Right axial rotation=27^{o}). The lowermost vertebral body was potted in dental acrylic and rotational motion applied to the uppermost thoracic vertebrae via the tool point of the arm. The spine was tested in four stages of dissection – i) *Intact*, ii) intercostals severed bilaterally (*NoInterC*), iii) sternum fractured (*NoStern*), and iv) ribcage resected leaving 50mm rib head (*NoRibs*). Reaction forces and moments were recorded at the base of the specimen (JR3, Woodland, USA) and the rotational stiffness of the spine was calculated at each stage of dissection. Following spinal testing, ligament and annulus fibrosus samples were harvested from select thoracic and lumbar motion segments. Ligament samples were loaded in uniaxial tension (Precycle: 5 cycles to 10%, 0.5Hz; Loading: maximum strain 400% at 0.1/sec) and annulus fibrosus samples were loaded in unconfined compression (Precycle: 5 cycles to 5% strain, 0.4Hz; Loading: maximum strain 50% at 0.01/sec) to obtain force-displacement data.

FE Modelling: Using custom image processing and FE pre-processing software, a geometrically and materially individualised FE model of the sheep thoracolumbar spine was developed (Fig. 1). Using mechanical testing data for ligament and annulus fibrosus samples from the ovine spinal joints, material parameters describing these soft tissues were derived and included in the FE model. The remaining material parameters were derived from prior studies of human spinal tissues. Loading conditions simulating the experimental testing conditions were applied – L6 was fixed in all directions and rotational loading replicating physiological ranges of flexion and axial rotation were applied at T1. The FE predicted spinal stiffness at each of the four stages of dissection were compared with the experimental data and the ability of the FE model to predict specimen-specific mechanics assessed.

The experimental moment-rotation response was nonlinear and the peak rotational stiffness (85-100% rotational displacement) decreased between each stage of dissection for both motions. The peak stiffness relative to the *Intact* condition for the *NoInterC*, *NoStern* and *NoRibs* conditions decreased to; 60%, 38% and 17% during axial rotation; and 94%, 87% and 53% during flexion. Overall, the experimental results indicated that the intercostal connections, sternum and osseous ribs all play key biomechanical roles during rotation of the spine.

The peak rotational stiffness for the *Intact* FEM showed good agreement with experimental results for flexion (Experimental: 0.22Nmm/^{o}; and FE: 0.20Nmm/^{o}) and axial rotation (Experimental: 0.18Nmm/^{o}; and FE: 0.16Nmm/^{o}). Similarly, the peak predicted stiffness for the *NoRibs* FEM was in reasonable agreement with the experimental results for flexion (Experimental: 0.13Nmm/^{o}; and FE: 0.17Nmm/^{o}) and axial rotation (Experimental: 0.03Nmm/^{o}; and FE: 0.05Nmm/^{o}). However, the relative decrease in predicted FEM stiffness with successive removal of the linear elastic intercostal connector elements (*NoInterC* FEM) and after fracture of the sternum (*NoStern* FEM) was not in agreement with the experimental findings. This suggested that while the overall mechanics of the simulated thoracolumbar spine was comparable to the physical specimen, accurately simulating the load-sharing behaviour of the ribcage cannot be achieved by replicating only the anatomical structures but requires a more detailed representation of the intercostal connections in order to appropriately calibrate the FE predicted behaviour.

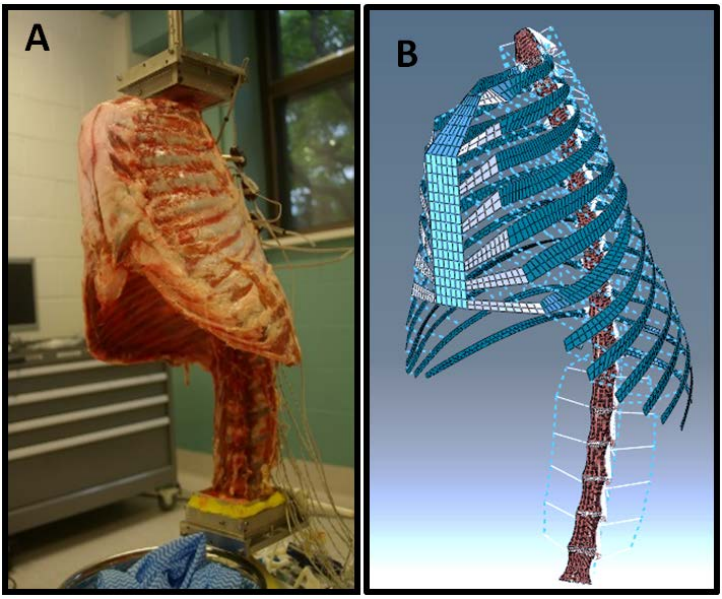

Fig. 1: Sheep spine. A Testing sample. B. FEM

The Julius Wolff Institute is located at the Charité Campus Virchow-Klinikum.

Arriving by plane

Airport Berlin-Tegel:
Take the bus TXL and get off at “Turmstraße”. Change to the subway station U9 (direction “Osloer Straße”) and leave the train at “Amrumer Straße”.

Airport Berlin-Schönefeld:
Take the S-Bahn-Line S9 from Berlin-Schönefeld (direction “Pankow”) and get off at “Ostkreuz”. Change at “Ostkreuz” to the S-Bahn S42 (Ringbahn) and leave the train at “Westhafen”. Walk across the Putlitzbrücke to the Föhrer Straße.

Arriving by train

Take the train to one of the DB stations - preferably “Zoologischer Garten”. Change at “Zoologischer Garten” to the subway U9 (direction “Osloer Straße”) and get off at “Amrumer Straße”.

Alternatively, you can take from central station (“Hauptbahnhof”) the bus 142 (direction “Leopoldplatz”) and get off at “Amrumer Straße”.

Arriving by car

From the freeway A 100 take the exit Seestraße. Ample parking is available in the public parking garage at Seestraße 4. The garage is always open and costs 1 € for every full/partial hour or maximum 10 € per calendar day. The first 29 minutes are free. Guests who stay at the Virchow-Gästehaus have free parking included here.

On the campus the first 59 minutes are free and every hour afterwards costs 2 €. Disabled parking is available on the campus on Mittelallee.

General Information

Registration
Registration for the workshop is required. Please contact Friedmar Graichen at: friedmar.graichen@charite.de

Registration fee for participants without oral presentation is required
Participation in the workshop, coffee breaks, lunch breaks, happy hour and dinner

Payment and confirmation of payment
An invoice and confirmation of payment will be sent via electronic mail.

Workshop language
The workshop language is English.

WIFI access
Will be provided.

General Guidelines for Authors and Presenters

Submitting your presentation / technical information
Please prepare your presentation in PowerPoint 4:3 aspect ratio. A presentation notebook with a PDF reader and an MS Office PowerPoint 2010 will be provided. The use of personal notebooks will not be accepted, it may interrupt the flow of the program in the lecture hall. A laser pointer will be available at the speaker's podium in the lecture hall. A technical supervisor will help you.

Speaker's preparation
Please hand in your presentation on USB flash drive to our technical staff available in the room where the talk is scheduled, no later than 90 minutes before the beginning of the session. You may view and/or edit your presentation before.

Hotels

Virchow Gästehaus der Charité
Seestraße 4-5, D-13353 Berlin, Germany
Phone: +49 30 450 578 062
E-Mail: gaestehaus@charite.de
http://gaestehaus.charite.de

Gästehaus Axel Springer
Föhrer Straße 14, 13353 Berlin, Germany
Phone: +49 30 450 060
E-Mail: gaestehaus@dhzb.de
http://www.dhzb.de

Supported by

We would like to thank everybody who helped us to make this **2nd International Workshop on Spine Loading and Deformation** happen.

Our special thanks to all our supporters:

SCHM 2572/6-1

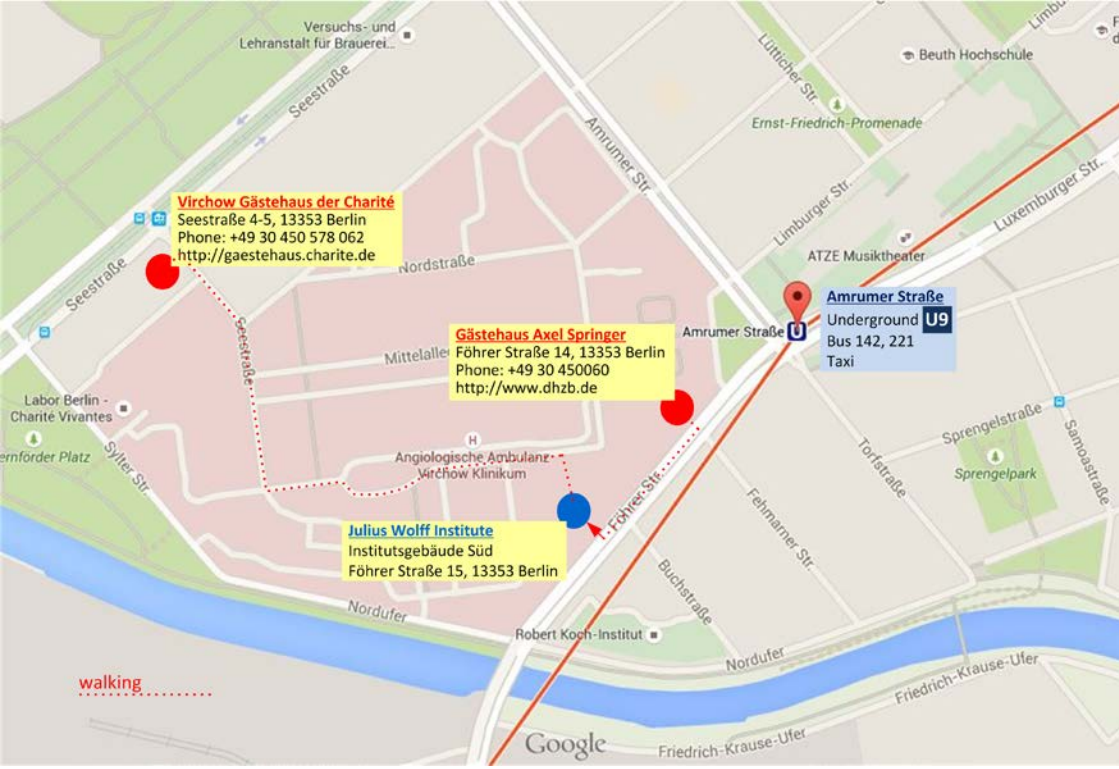

Institutsgebäude Süd

Julius Wolff Institute

Ground Floor

1. Registration Desk (only May 18th 10am-1pm)
2. Lecture Hall
3. Coffee Break, Lunch Break, Happy Hour